Understanding the Formation of CO_2 and Its Degassing Behaviours in Coffee

by

Xiuju Wang

A Thesis
presented to
The University of Guelph

In partial fulfilment of requirements
for the degree of
Doctor of Philosophy
in
Food Science

Guelph, Ontario, Canada

© Xiuju Wang, May, 2014

ABSTRACT

UNDERSTANDING THE FORMATION OF CO_2 AND ITS DEGASSING BEHAVIOURS IN COFFEE

Xiuju Wang
University of Guelph, 2014

Advisor:
Professor Loong-Tak Lim

In the present study, the effect of roasting temperature-time conditions on residual CO_2 content and its degassing behaviours in roasted coffee was investigated. The results show that the residual CO_2 content in the roasted coffee beans was only dependent on the degree of roast and independent on the roasting temperature applied. However, CO_2 degassing was shown significantly faster ($p<0.05$) in roasted coffee processed with high-temperature-short-time (HTST) than those roasted with low-temperature-long-time (LTLT) process. Moreover, the CO_2 degassing rate increased with the degree of roast. CO_2 degassing in ground coffee was significantly faster than in whole beans with the rate highly dependent on the grind size and roasting temperature, but less dependent on the degree of roast. CO_2 degassing rate increased with the increasing of environmental temperature and relative humidity.

Although CO_2 degassing has been a challenging problem in the coffee industry for decades, there is still no clear understanding of precursors of CO_2. In the present study, the hypothesis of "chlorogenic acid (CGA) is the principal precursor of CO_2" was tested. Although strong negative linear correlation ($R^2>0.9$) between total CGA and residual CO_2 content during coffee roasting was detected, and vanishing of IR bands of the C=O group in caffeic acid and quinic acid moieties during heating of pure CGA at coffee roasting temperature was observed, the quantification analysis of CO_2 generation from pure CGA heating indicated only ~ 8% yields at 230°C, which led us to conclude that

CGA was one of the CO_2 precursors but not the principal one. Accordingly, an alternate idea was put forward, hypothesizing that Maillard reaction could account for the CO_2 formed. Roasting studies of glycine-sucrose simple models showed that large amount of CO_2 was formed from Maillard reaction under coffee roasting conditions, confirming the importance of Maillard reaction in CO_2 formation in roasted coffee. The isolation and roasting studies of green coffee fractions showed that CO_2 was generated from various green coffee components, including water insoluble proteins and polysaccharides. Around 50% of CO_2 was formed from lower molecular weight compounds with this fraction representing ~25% of green coffee by weight.

Acknowledgements

Firstly I would like to express my profound gratitude to my advisor, Dr. Loong-Tak Lim for giving me the opportunity to conduct this project. Besides, I also appreciate his encouragements, patience, guidance, and support during the entire project. My appreciation goes to all my advisory committee members - Drs. Amar Mohanty, Lisa Duizer, Massimo Marcone, Robert Lencki, and Yukio Kakuda for providing their sound advice, constructive comments on my research, and continuous support.

This research could not been conducted without the assistance of all the staff and researchers in food science department. Thanks all the staff in the Main office for all their help in various aspects. Many thanks to Dr. Sandy Smith for her friendly support and help during the entire research. I also want to express my appreciation to Drs. John Craven and Robert Lencki for letting me use the GC in their lab, and Dr. Yukio Kakuda for the help with HPLC works.

I convey my special thanks to my entire lab family members in the packaging and biomaterial group: Ana Cristina Vega Lugo, Ruyan Dai, Solmaz Alborzi, Suramya Minhindukulasuriya, Roc Chan, Khalid Moomand, Alex Jenson, Niya Wang, and Yucheng Fu for giving me the support in various aspects and making the whole study process a sweet memory. Moreover, I would like to express my deepest gratefulness to my parents and my husband for their infinite love, care and support.

Last but not least, financial support provided by NSERC and Mother Parkers Tea & Coffee Inc. is also greatly appreciated.

Table of Contents

Acknowledgements....iv
Table of Contents....v
List of Tables....viii
List of Figures....x
List of Abbreviation....xv
Nomenclature....xvii
CHAPTER 1 : LITERATURE REVIEW....1
1.1 Coffee....1
1.1.1 Coffee plant....1
1.1.2 Green coffee bean processing....3
1.1.3 Chemical composition of green coffee beans....7
1.2 Coffee roasting....15
1.2.1 Main aspects of roasting process....15
1.2.2 Physiochemical changes during roasting....17
1.2.3 Roasters....25
1.2.4 Degree of roast....28
1.2.5 Maillard reaction....31
1.2.6 Volatile aroma compounds in roasted coffee....33
1.3 Mass transfer mechanism in porous media....36
1.3.1 Molecular diffusion....37
1.3.2 Knudsen diffusion....38
1.3.3 Surface diffusion....39
1.3.4 Convective flow of gases due to gas pressure....40
CHAPTER 2 : RESEARCH OBJECTIVES....42
CHAPTER 3 : EFFECT OF ROASTING TEMPERATURE-TIME CONDITIONS ON CO_2 FORMATION AND PHYSIO-CHEMICAL PROPERTIES OF ROASTED COFFEE BEANS-A KINETICS STUDY....45
3.1 Introduction....45
3.2 Material and Methods....47
3.2.1 Roasting procedure and sample preparation....48
3.2.2 Color measurement....49
3.2.3 Roast loss....50
3.2.4 Residual CO_2 content....50
3.2.5 Volatile compounds analysis....51
3.2.6 Model fitting....52

3.3 Results and Discussion 53
3.3.1 Kinetics of color changes 53
3.3.2 Kinetics of roast loss 60
3.3.3 Changes in residual CO_2 content 64
3.3.4 Evolution of volatile compounds 67
3.4 Conclusions 72
CHAPTER 4 : EFFECT OF ROASTING TEMPERATURE-TIME CONDITIONS ON CO_2 DEGASSING BEHAVIOUR IN ROASTED COFFEE 73
4.1 Introduction 73
4.2 Materials and Methods 75
4.2.1 Roasting procedure and sample preparation 75
4.2.2 Determination of residual CO_2 content 78
4.2.3 CO_2 degassing behaviour test 78
4.2.4 CO_2 degassing modeling 80
4.2.5 Attenuated Total Reflectance (ATR)-FTIR analysis of roasted coffee power 81
4.2.6 Moisture, oil content and density 81
4.2.7 Cell wall porosity test by mercury intrusion porosimetry 82
4.2.8 Moisture isotherm of roasted coffee bean 83
4.2.9 Statistical analysis 84
4.3 Results and Discussion 84
4.3.1 Effect of roasting conditions on the residual CO_2 content in roasted coffee 84
4.3.2 Effect of roasting conditions on CO_2 degassing behaviour 88
4.3.3 Effect of roasting conditions on chemical compositions of roasted coffee 94
4.3.4 Effect of roasting conditions on the cell wall porosity of roasted coffee 97
4.3.5 Effect of temperature on CO_2 degassing in roasted coffee beans 100
4.3.6 Effect of RH on CO_2 degassing in roasted coffee beans 103
4.4 Conclusion 106
CHAPTER 5 : INVESTIGATION OF CHLOROGENIC ACIDS AS THE PRINCIPAL CO_2 PRECURSOR IN COFFEE 108
5.1 Introduction 108
5.2 Materials and Method 110
5.2.1 Coffee roasting 110
5.2.2 Determination of residual CO_2 content 111
5.2.3 Volume of roasted coffee beans 111
5.2.4 Analysis of CGA and total polyphenol 112
5.2.5 Heating of pure CGA 114
5.2.6 ATR - FTIR analysis of CGA and CGA char 114

5.2.7 CGA spiking of green coffee beans 115
5.2.8 Determination of evolved CO_2 during roasting of coffee and pure CGA 115
5.3 Results and Discussion 117
5.3.1 Degradation of CGA and formation of CO_2 during coffee roasting 117
5.3.2 Thermal degradation of pure CGA under coffee roasting temperatures 120
5.3.3 Quantitative analysis of CO_2 formation from CGA, caffeic and quinic acid degradation 126
5.3.4 CO_2 formation from CGA spiked green coffee beans 128
5.4 Conclusion 131
CHAPTER 6 : COMPOSITION OF GREEN COFFEE FRACTIONS AND THEIR CONTRIBUTION TO CO_2 FORMATION DURING ROASTING 132
6.1 Introduction 132
6.2 Materials and methods 133
6.2.1 Coffee roasting and kinetics of CO_2 formation 133
6.2.2 Amino acid-sugar roasting reaction model 134
6.2.3 Isolation of green coffee fractions 134
6.2.4 Roasting of isolated fractions 135
6.3 Results and discussion 136
6.3.1 CO_2 formation kinetics during coffee roasting 136
6.3.2 CO_2 formation from heating of amino acid or sugar under coffee roasting conditions 138
6.3.3 CO_2 formation from roasting of amino acid-sucrose mixture under coffee roasting conditions 139
6.3.4 Effect of addition of CGA on CO_2 formation in glycine-sucrose model system 140
6.3.5 Fragmentation of green coffee components and their contribution to CO_2 formation 141
6.4 Conclusion 143
CHAPTER 7 : CONCLUSION AND RECOMMENDATIONS 145
CHAPTER 8 : REFERENCES 148
CHAPTER 9 : APPENDIX 159

List of Tables

Table 1.1- Comparison between Arabica and Robusta coffee plant 2

Table 1.2- Composition of green Arabica and Robusta coffee[a] 8

Table 1.3- Composition of lipid fraction of green coffee beans. 11

Table 1.4- Type of roasters based on various principles of roasting systems 25

Table 1.5- Basic mechanical principles of some commercial coffee roasters 27

Table 1.6- Potent odorants in roasted coffee 35

Table 3.1- Estimated equation parameters, coefficient of detemination (R^2) and mean square errors (MSEs) obtained by fitting Eq. 3.2, 3.3 and 3.4 to L^* values... 57

Table 3.2- Estimated equation parameters, coefficient of determination (R^2) and mean square errors (MSEs) obtained by fitting Eq. 3.5, 3.6 and 3.7 to RL values.. 63

Table 3.3- Peak identification of 33 volatile compounds in Figure 3.13 71

Table 4.1- Roasting temperature-time conditions used to obtain roasted coffee samples. 76

Table 4.2- Saturated salt solution used in the moisture isotherm determination of the roasted coffee bean HTST-D at 25 °C 83

Table 4.3- Residual CO_2 content of roasted coffee beans at various temperature-time roasting conditions 86

Table 4.4- Effect of grinding on residual CO_2 content in ground coffee samples..... 87

Table 4.5- Derived Weibull distribution model parameters (α, β, C_∞), D_{cacl} (calculated diffusion coefficients), coefficient of determination (R^2), and RMSE (root mean square error). 93

Table 4.6- Some physiochemical properties of roasted coffee 95

Table 4.7- Derived Weibull distribution model parameters (α, β, C_∞), D_{cacl} (calculated diffusion coefficients), coefficient of determination (R^2), and RMSE (root mean square error) from CO_2 degassing experiments at temperature of 4, 15, 25 and 40°C. 102

Table 4.8- Derived Weibull distribution model parameters (α, β, C_∞), D_{cacl} (calculated diffusion coefficients), coefficient of determination (R^2), and RMSE (root mean square error) from CO_2 degassing at RH of 0, 33, 58 and 81%. 105

Table 5.1- Physiochemical properties, residual CO_2, total CGA and total polyphenol contents of roasted Ethiopian and Columbian coffee beans 119

Table 6.1- low moisture glycine-sucrose roasting reaction model 134

Table 6.2- Roast loss and *L**, *a**, *b** value of roasted coffee samples (Figure 6.2), indicating the degree of roast. 137

List of Figures

Figure 1.1- Transverse (A) and longitudinal (B) section of coffee berry (fruit). Adapted from Wintgens (2004b). 3

Figure 1.2- Dry and wet processing of green coffee beans. 5

Figure 1.3- Structure of CGA precursors-quinic, caffeic (CA), and ferulic acids (FA). ... 13

Figure 1.4- Structure of characteristic aroma compounds of green coffee, 3-isobutyl-2-methyoxypyrazine and 2-methoxy-3-isopropylpyrazine. 15

Figure 1.5- Main events that take place during the roasting of green coffee beans, showing a combined heat and mass transport superposed by endothermic and exothermic reactions. 16

Figure 1.6- The possible degradation path and products of trigonelline during coffee roasting. 20

Figure 1.7- Chlorogenic acid contents at different degrees of roasting adapted from Belitz et al. (2009). 21

Figure 1.8- Structures of green coffee and roasted coffee (a) longitudinal cut view of green coffee beans; (b) cell structure of green coffee under SEM; (c) longitudinal cut view of roasted coffee beans; (d) cell structure of roasted coffee under SEM. Photos are from Illy and Viani (2005). 23

Figure 1.9- Schematic diagram showing the porous structure of roasted coffee beans. ... 24

Figure 1.10- Maillard reaction scheme compiled from Martins et al (2001) 32

Figure 1.11- Strecker degradation and possible formation mechanism of pyrazine from amino ketones, compiled from Berger (2007). 33

Figure 1.12- The effect of pore size on the changes of basic transport mechanism. The pore size drops from the top of the figure to the bottom. The selectivity is often larger for smaller pores. Compiled from Cussler (2009) 41

Figure 3.1- Modified commercial fluidized bed roaster showing various components and positions of thermocouple. 48

Figure 3.2- Air and bean core temperatures at 240°C roasting temperature set point, showing the effective control of the apparatus in Figure 3.1 on roasting temperature. 49

Figure 3.3- Apparatus for measuring the residual CO_2 content in roasted coffee beans and ground coffee. 51

Figure 3.4- Kinetics of L^* value changes of coffee beans roasted at temperature of 220, 230, 240 and 250°C. Within each figure, the top, middle and bottom horizontal dotted lines indicate lightness values corresponded to light, medium and dark roast degrees, respectively. The roast degrees were determined by visually comparing the color of coffee grounds with industy standard disks established by Specialty Coffee Association of America (SCAA). Predicted plots are derived from first-order kinetics model (Eq. 3.3). 56

Figure 3.5- Arrhenius plots of rate constant for L^* evolution, showing different activation energies for first and second stage roasting processes.....58

Figure 3.6- Kinetics of a^* and b^* value changes of coffee beans roasted at temperature of 220, 230, 240 and 250°C. 59

Figure 3.7- Color development of coffee beans roasted at 220, 230, 240 and 250°C for different roast times. 60

Figure 3.8- Kinetics of the roast loss for coffee beans roasted at 220, 230, 240 and 250°C. The horizontal lines indicate when the coffee beans attained the medium roast degree. Predicted plots are derived from zero-order kinetic model (Eq.3.5)..62

Figure 3.9- Arrhenius plots of rate constant of roast loss evolution, showing different activation energies for first and second stage roasting processes. 64

Figure 3.10- Residual CO_2 content at different roasting temperature-time conditions (a) and the plots between residual CO_2 with L^* value (b) (L: light roast; M: medium roast; D: dark roast). 66

Figure 3.11- Arrhenius plots of rate constants, determined from zero-order kinetic models, for changes of residual carbon dioxide content during the initial phase of roasting.....67

Figure 3.12- Changes of total peak area of coffee volatiles chromatogram with roasting time at roasting temperatures of 220, 230, 240 and 250°C. 69

Figure 3.13- Volatile profiles, as indicated by chromatographic peak areas from SPME analysis, for light, medium and dark roasted coffee beans processed at different roasting temperatures (■: 220°C, ■: 230°C, ■: 240°C, ■: 250°C). Horizontal axis indicates 33 chromatographic peaks following the sequence of elution. 70

Figure 4.1- Averaged particle size (in radius) distribution of coarse, medium and fine ground coffee. 77

Figure 4.2- Schematic diagram of CO_2 degassing test apparatus (a) and typical FTIR spectrum of headspace air, showing the strong absorbance at 2341 cm^{-1} due to CO_2 (b).....79

Figure 4.3- Representative CO_2 degassing data (symbols) at 25 °C for coffee beans roasted using different temperature-time conditions. Solid line represents the best fit curves of Weibull distribution model, showing its goodness of fit to the experimental data. HTST: high-temperature-short-time; LTLT: low-temperature-long-time; D: dark roast degree; M: medium roast degree. 91

Figure 4.4- Representative CO_2 degassing data (symbols) at 25 °C for coffee samples ground to different sizes (coarse, medium and fine). Solid lines represent the best fit curves of Weibull distribution model to the experimental data. HTST: high-temperature-short-time; LTLT: low-temperature-long-time; D: dark roast degree; M: medium roast degree.....92

Figure 4.5- (a) Representative FTIR spectra of ground LTLT-M, LTLT-D, HTST-M, and HTST-D samples; (b) two factor score plots of PCA analysis of FTIR data; (c) loading plot of first principle component. HTST: high-temperature-short-time; LTLT: low-temperature-long-time; D: dark roast degree; M: medium roast degree.....97

Figure 4.6- Representative porosimetric curves of finely ground coffee LTLT-M, LTLT-D, HTST-M, and HTHT-D samples, showing mesopores (2-50 nm) present in the cell walls. The inset summarizes the averaged particle size (in diameter) distribution of coffee samples subjected to the mercury porosimetry analysis, indicating that the particles were less than 30 μm. HTST: high-temperature-short-time; LTLT: low-temperature-long-time; D: dark roast degree; M: medium roast degree.....100

Figure 4.7- Representative CO_2 degassing data (symbols) at different degassing temperatures. Solid line represents the best fit curves of Weibull distribution model, showing its goodness of fit to the experimental data.....102

Figure 4.8- Arrhenius plot of D_{cal} of CO_2 degassing, showing activation energy of 29.73 KJ/mol.....103

Figure 4.9- Representative CO_2 degassing data (symbols) at 25°C with different relative humidity control. Solid line represents the best fit curves of Weibull distribution model, showing its goodness of fit to the experimental data. Insert shows the CO_2 degassing kinetic at RH 81%. 104

Figure 4.10- Representative moisture sorption isotherm of roasted coffee beans at 25° C. The dotted line represents the best fit curves of GAB equation, showing its goodness of fit to the experimental data (symbols). 106

Figure 5.1- Apparatus for determining evolved CO_2 during coffee and pure CGA roasting 116

Figure 5.2- Plot of residual CO_2 and total CGA content in roasted coffee, showing strong negative linear correlation. 120

Figure 5.3- Semi-log plot of weight loss kinetics data of CGA in roasting temperature of 210, 230, 250, and 270°C, with the data fitted with logarithmic equation. W_t: weight at roasting time t; W_0: initial weight. 122

Figure 5.4- Arrhenius plot of weight loss kinetics of CGA heating under coffee roasting temperatures. 122

Figure 5.5- CGA degradation ratio under heating temperature of 210, 230, 250, and 270 °C. (a) plot of CGA degradation ratio with roasting time; (b) plot of CGA degradation ratio with roast weight loss. 123

Figure 5.6- FTIR spectra of CGA, caffeic acid and quinic acid, showing wavenumbers of C=O stretching in quinic acid moiety (1681 cm^{-1}) and caffeic acid moiety (1639 cm^{-1}).....125

Figure 5.7- FTIR spectra of CGA chars after heating at temperature of 230°C for various times, showing the vanishing of C=O stretching in both quinic acid and caffeic acid moiety. 125

Figure 5.8- The possible CGA degradation mechanism during coffee roasting, taking 5-CQA as an example. 126

Figure 5.9- Amountof CO_2 formed from CGA heating at 230 °C (a); and the effect of temperature on the obtained CO_2 amount (heating of 1.5 g CGA)(b). 128

Figure 5.10- Residual CO_2 content and amount of CO_2 evolved during roasting of untreated green coffee, control and 6% CGA spiked coffee at 230 °C for 20 min. Same letter on top of the bar shows there is no significant difference in the total CO_2 formation during roasting. 130

Figure 6.1- Fraction isolation process from green coffee.....135

Figure 6.2- CO_2 formation (residual + evolved) and the ratio of evolved to residual CO_2 amount during coffee roasting under roasting temperature of 230 °C by using the apparatus as shown in Figure 5.1. 137

Figure 6.3- Amount of CO_2 formed from heating of sugar or amino acid (glycine) under coffee roasting temperature of 230°C for 20 min. 139

Figure 6.4- Amount of CO_2 formed from roasting of sugar and amino acid (glycine) mixture under coffee roasting temperature of 230 °C for 20 min. 140

Figure 6.5- Effect of addition of CGA on CO_2 formation in sucrose-glycine Maillard model reaction system. 141

Figure 6.6- Weight distribution of each coffee fraction (a) and their contribution to the amount of CO_2 formation (b).....143

Figure 9.1- The residual CO_2 content in roasted coffee beans from various roasting temperature-time combinations and their headspace CO_2 and O_2 concentration after packaging. The packing condition is 5 grams of roasted coffee beans was packaged in 12 ml glass amber vial with septum containing lid. The headspace CO_2 and O_2 concentration was determined by a headspace gas analyzer (Gaspace Advance Micro, Illinois Instruments, IL USA) after one week storage. The residual CO_2 content and headspace O_2 and CO_2 consternation was plotted with both roasting time and L^* value of the tested coffee beans. The green, red and blue lines represents the residual CO_2 content, headspace CO_2 concentration and headspace O_2 concentration, respectively. 160

Figure 9.2- Changes of volatile chromatograms (in section 3.3.4) with roasting time at different roasting temperature of 220, 230, 240 and 250 °C, showing the formation of volatiles is superimposed by an accelerated decay of some aroma compounds during the final roasting stage. 164

Figure 9.3- Changes of 33 volatile compounds in Table 3.3 during coffee roasting at roasting temperature of 220, 230, 240 and 250 °C. X-axis is the lightness value (L^*) and y-axis is the peak area. Blue, red, green and purple lines represent 220, 230, 240 and 250 °C roasting temperature, respectively. 166

Figure 9.4- FTIR spectra of ECGA and CGA standard.....167

Figure 9.5- HPLC chromatograms of SCGA and ECGA.....167

Figure 9.6- Original, control and 6% CGA spiked green coffee beans in Chapter 5 168

Figure 9.7- (A) Ground coffee for isolation; (B) exhausted ground coffee (Fraction D); (C) roasted coffee from A at 250 °C for 25 min; (D) roasted coffee from B at 250 °C for 25 min. 169

List of Abbreviation

HTST	High temperature short time
LTLT	Low temperature long time
CGA	Chlorogenic acid
CGAs	Total chlorogenic acids
3-CQA	3-caffeoylquinic acid
4-CQA	4-caffeoylquinic acid
5-CQA	5-caffeoylquinic acid
3, 4-diCQA	3, 4-dicaffeoylquinic acid
3,5-diCQA	3,5-dicaffeoylquinic acid
4,5-diCQA	4,5-dicaffeoylquinic acid
5-FQA	5-feruloylquinic acid
3-FQA	3-feruloylquinic
4-FQA	4-feruloylquinic acid
SCAA	Specialty Coffee Association of America
16-OMC	16-O-methylcafestol
ATR	Attenuated total reflectance
FTIR	Fourier transform infrared
HS-SPME	Headspace phase microextraction
GC	Gas chromatography
MS	Mass spectroscopy
RH	Relative humidity
IR	Infrared

RL	Roast loss
FID	Flame ionization detector
GAB equation	Guggenheim-Andersen-de Boer equation
ECGA	Experimental chlorogenic acid
HPLC	High performance liquid Chromatography
IUPAC	International Union of Pure and Applied Chemistry

Nomenclature

ϕ	Porosity
DAA*	Self-diffusion coefficient
u	Molar-average velocity
λ	Mean free path
N	Avogadro's number
T	Absolute temperature
k	Boltzmann constant
σ	Jones diameter of the spherical molecules
J	Mass flux from diffusion
β	Porous media factor
D	Molecular diffusivity in bulk
D_P	Molecular diffusivity of the gas in porous medium
τ	Tortuosity factor
D_{KA}	Knudsen diffusivity of diffusing species A
d_{pore}	Diameter of pore
F_g	Mass flux from convection
E_a	Activation energy
k_0	The pre-exponential factor of Arrhenius plot
R	The universal gas constant (8.314 $J \cdot mol^{-1} \cdot K^{-1}$)
MSE	Mean square error

R^2	Coefficient of determination
D_{calc}	Calculated diffusion coefficient
α	Scale parameter in Weibull model
β	Shape parameter in Weibull model
γ	Surface tension of the mercury (480 mN/m);
θ	Contact angle between solids and mercury (140°);

CHAPTER 1 : LITERATURE REVIEW

1.1 Coffee

Coffee, a water infusion of ground roasted coffee, is one of the mostly widely consumed beverages and is the most traded commodity after oil. It is greatly appreciated for its delightful odour and flavour, as well as for the stimulating effects of caffeine (Grosch 1998; Buffo and Cardelli-Freire 2004; Illy and Viani 2005). Although Canada does not grow coffee, it is one of the major coffee consumers in the world, at 6.4 kg per capita in 2010 (Anon).

1.1.1 Coffee plant

The genus *Coffea* belongs to the botanical family of *Rubiaceae* (a family of flowering plants) (Davis et al. 2006) and comprises more than 70 different species. However, only three species *Coffea. arabica* L., *Coffea. canephora* Pierre ex Froehner, and *Coffea. liberica* Bull ex Hiern are of commercial importance, of which Liberica coffee only contributes to less than 1% of the world coffee production (Illy and Viani 2005). The most widespread varieties of *C. arabica* are 'Typica' and 'Bourbon' and from these different strains and cultivars have been developed. The best known variety for *C. canephora* is 'Robusta'. Therefore, *C. canephora* is often simply referred as Robusta. Some hybrids of *C. arabica* and *C. canephora* have also been developed, aiming to improve disease resistance of Arabica coffees and improve the cup quality of Robusta.

The coffee plant is an evergreen shrub or small tree, which can grow up to 10 meters in height depending on the varieties and growth conditions. But the height is usually managed for easy harvesting. Robusta plant has a shallow root system and it flowers irregularly, taking about 10-11 months for cherry to ripen, producing oval-shaped beans. The Robusta plant has a greater crop yield than that of *C. arabica*, as it is less

susceptible to pests and diseases. Thus Robusta trees need much lesser amounts of herbicide and pesticide than the Arabica counterpart. Approximately 40% of the coffee produced in the world is Robusta. It is mostly grown in Vietnam, followed by Western and Central Africa, and Brazil. Arabica coffee is genetically different from other coffee species, having four set of chromosomes rather than two. Arabica coffee is grown throughout Latin America, and Central and East Africa (Wintgens 2004a; Illy and Viani 2005). Further detailed differences between Arabica and Robusta coffee are summarized in Table 1.1.

Table 1.1- Comparison between Arabica and Robusta coffee plant

	Arabica	Robusta
Chromosomes (2n)	Tetraploid (2n=44)	Diploid (2n=22)
Time from flower to ripe cherry	8-9 months	10-11 months
Flowering	after rain	irregular
Ripe cherries	fall	stay
Yield (kg beans/ha)	1500-3000	2300-4000
Root system	deep	shallow
Optimum temperature (°C)	18-22	20-25
Optimal rainfall (mm)	1500-1800	1500-3000
Optimum altitude (m)	900-1800	200-900
Coffee leaf rust	susceptible	tolerant to resistant
Hemileia vastatrix	susceptible	resistant
Koleroga	susceptible	tolerant
Nematodes	susceptible	resistant
Tracheomycosis	resistant	susceptible
Coffee berry disease	susceptible	resistant

Compiled from Wintgens (2004a)

The coffee fruit is a 2-seeded drupe fruit, commonly called berry or cherry. Sometimes the fruit contains only one round seed called peaberry. The ripe coffee berry

consists of a red skin layer which is called the exocarp or the epicarp, a pulp layer which is thick, sweet gelatinous-pectic mesocarp and coffee seeds. Each seed is wrapped in a thin silverskin (rudimentary integument) and protected by a parchment hull (fibrous endocarp) (Wintgens 2004b; Illy and Viani 2005). *C. arabica* varieties generally produce an oval convex seed with an S-shaped longitudinal slit (the central cut) on the flat side, while *C.canephora* seeds are more round with a straight central cut. The coffee seeds mostly consist of endosperm with a small embryo at the base of the seed. Figure 1.1 shows the schematic transverse and longitudinal section of coffee cherry.

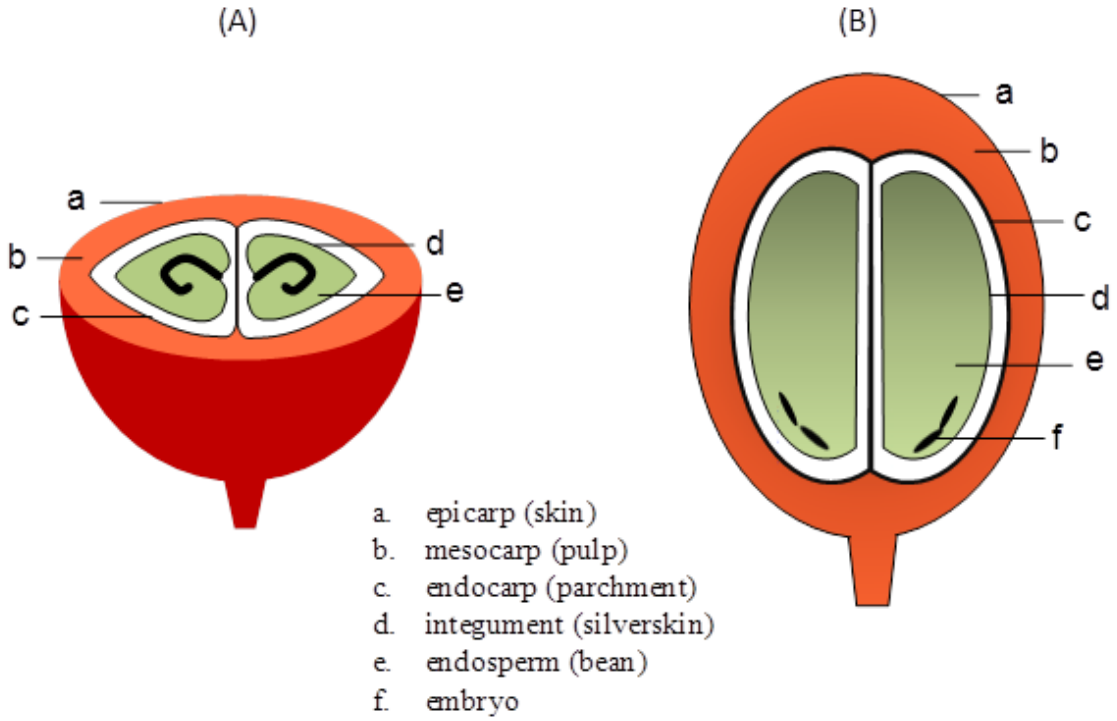

Figure 1.1- Transverse (A) and longitudinal (B) section of coffee berry (fruit). Adapted from Wintgens (2004b).

1.1.2 Green coffee bean processing

Currently, there are mainly two methods being used for processing coffee cherries to yield the green coffee beans. The dry processing, also known as “natural process”,

produces dried cherry coffee by drying the whole berries immediately after harvest on patios, racks under the sun, or in mechanical dryers. This method is simple and less demanding with respect to harvesting. In contrast, wet processing, also known as “washed process”, use only ripe berries that have been selectively picked manually or are mechanically separated, since unripe cherries or cherries that have partially dried on the tree cannot be handled by the pulping machines. Various stages for these two processes are illustrated in Figure 1.2 (Clarke and Macrae 1987).

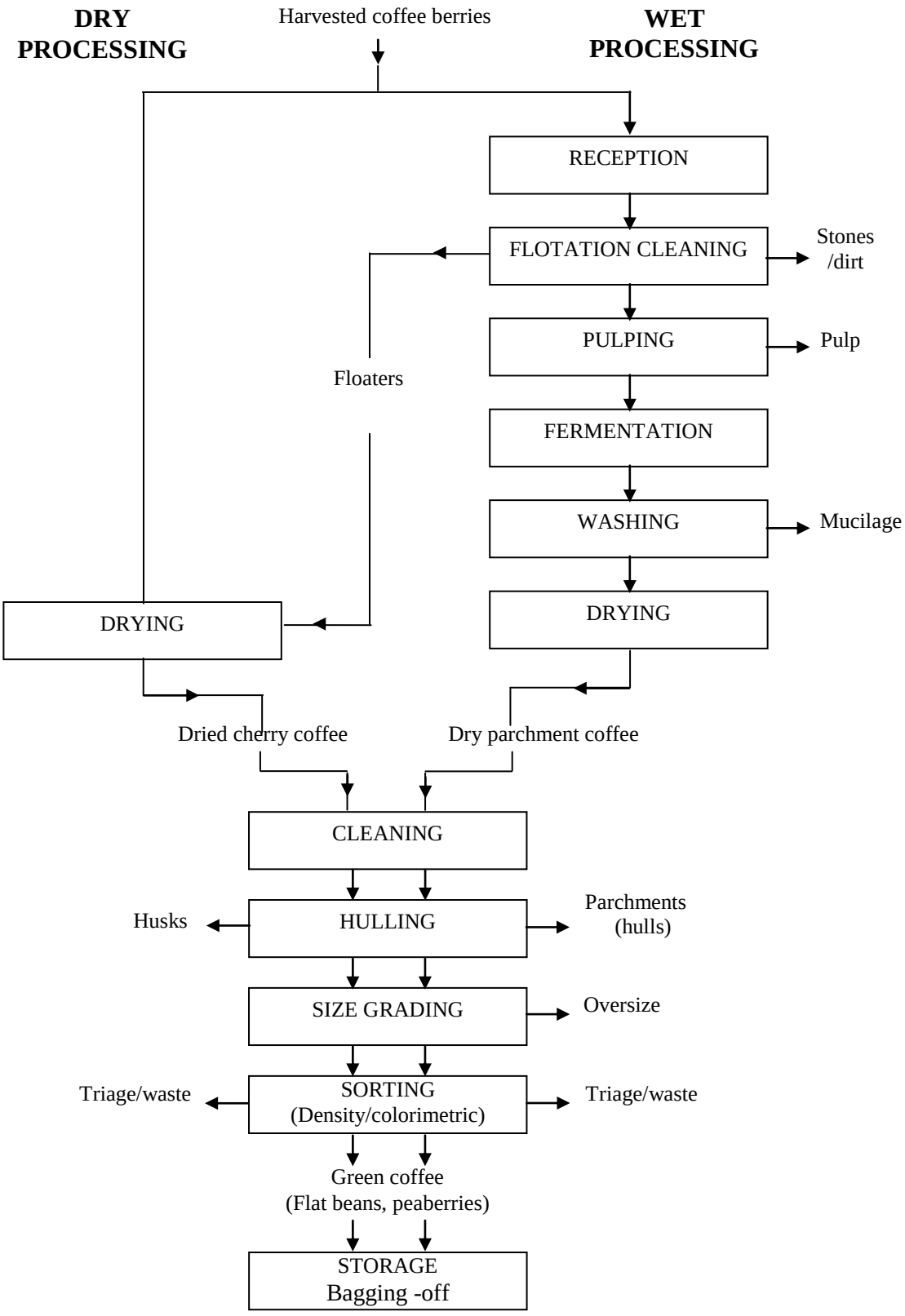

Figure 1.2- Dry and wet processing of green coffee beans.

The green coffee beans resulting from the wet and dry methods yield coffee brews of different sensorial characteristics. This difference is in part due to the fact that coffee beans derived from the dry processing are dried while they are in contact with the sweet mucilage, and hence the resulting coffee brew tends to be heavy in body, sweet, smooth, and complex in sensory properties. On the other hand, wet processing provides much consistent and higher quality green coffee beans that have cleaner and brighter brew characteristics.

Other green coffee beans processing methods have also been used, although they are less common. One of these processes is known as “pulped natural process”, which involves pulping of the coffee cherry to remove the skin as in the wet process, and drying. So, the fermentation stage commonly used in wet processing to remove mucilage is omitted in pulped natural process. This results in a brew that has a combined characteristic of both a dry- and wet-processed coffee beans. Another type of coffee that has emerged on the market is called “re-passed or raisins” beans. These coffees are removed from the rest of the floater (Figure 1.2) and then pulped. They can then be processed as the wet process or used as pulped naturals. It is found much sweeter than the traditional dry- and wet-processed coffee beans, since cherry floaters have been dried on the tree before being collected, allowing the bean to interact with mucilage for a longer time. Another variant of coffee that has gained considerable attention is the “Kopi Luwak”, the Indonesian words for “civet coffee”, which is famous for the unique green beans processing methodology involved. Unlike the typical wet- and dry-processing approaches, Kopi Luwak is processed in the digestive system of the indigenous palm civet. During this process, the fresh component of the cherry is digested by the civet but the beans are excreted in their feces. The gastrointestinal fermentation and enzymatic digestion reactions impart a unique flavour to the beans which has been described as

earthy, musty, syrupy, smooth, and rich with both jungle and chocolate undertones (Marcone 2004).

1.1.3 Chemical composition of green coffee beans

The green coffee beans of *C. arabica* (Arabica coffee) and *C. canephora* (Robusta coffee) show considerable differences in their chemical compositions. Compared to Robusta green coffee beans, Arabica beans contain substantially higher lipids, sucrose, and trigonelline contents, but lower caffeine and chlorogenic acids (CGAs) contents (Table 1.2). Minor constituents specific to one species have also been identified, such as 16-O-methylcafestol which is only detected in the Robusta coffee.

Table 1.2- Composition of green Arabica and Robusta coffee[a]

Constituent	Arabica	Robusta	Components
Soluble carbohydrates	9-12.5	6-11.5	
Monosaccharide	0.2-0.5		*Fructose, glucose, galactose, arabinose (traces)
Oligosaccharides	6-9	3-7	*Sucrose (>90%), raffinose (0-0.9%), stachyose (0-0.13%)
Polysaccharides	3-4		* Polymers of galactose(55-65%), mannose (10-20%), arabinose (20-35%), glucose(0-2%)
Insoluble carbohydrates	46-53	34-44	
Hemicelluloses	5-10	3-4	*Polymers of galactose (65-75%), arabinose (25-30%), mannose (0-10%)
Cellulose, β (1-4) Mannan	41-43	32-40	
Acids and phenols			
Volatile acids	0.1		
Nonvolatile aliphatic Acids	2-2.9	1.3-2.2	*Citric acid, malic acid, quinic acid
Chlorogenic acid	6.7-9.2	7.1-12.1	*Mono-, dicaffeoyl- and feruloylquinic acid
Lignin	1-3		
Lipids	15-18	8-12	
Wax	0.2-0.3		
Oil	7.7-17.7		*Main fatty acids: 16:0 and 18:2 (9,12)
N Compounds	11-15		
Free amino acids	0.2-0.8		*Main amino acids: Glu, Asp, Asp-NH_2
Proteins	8.5-12		
Caffeine	0.8-1.4	1.7-4.0	*Traces of theobromine and theophylline
Trigonelline	0.6-1.2	0.3-0.9	
Minerals	3-5.4		

Compiled from Wintgens (2004a), Illy and Viani (2005), and Belitz et al. (2009).
[a] values in %, dry basis

Moisture content

Water content is one of the most critical quality parameters of green coffee beans, which influences their water activity and stability during storage. Elevated water content may cause fermentation and mould growth, which could lead to either the development of off-flavoured brews and/or the formation of health hazardous mycotoxins (Illy and Viani 2005; Reh et al. 2006). Generally, a water content ranging between 8.0 and 12.5% is considered to be adequate to avoid the above unwanted deterioration.

Three official standard ISO methods currently exist for the determination of moisture content in green coffee beans, namely ISO 1446, ISO 1447, and ISO 6673. ISO 1446 involves the desiccation of about 3-4 g of ground green coffee in phosphorus pentoxide containing container at 48°C ± 2°C until weight constancy. ISO 1447 allows approximately 5 g of whole beans drying at 130°C. ISO 6673 measures the mass loss of whole beans (about 10 g) at 105°C with forced air ventilation. ISO 1446 exclusively measures water but might leave some residual water difficult to extract. Thus the measured value from this method could be lower than the actual moisture content in green coffee beans. For the oven based methods -ISO 1447 and ISO 6673, the degradation reactions at high drying temperature could lead to bias in the weight loss, resulting in a higher measured value.

The monolayer moisture value is an important parameter to evaluate the dry food stability. When the moisture content is below the monolayer moisture value, the rate of quality loss is negligible, since water is strongly bound to the food and is not involved in any deteriorative reaction. A wide range of monolayer moisture values of green coffee beans has been reported in the literature. Pittia *et al*. (2007) and Rocculi *et al.* (2011) calculated relatively lower values of 4.34 and 5.28 g/100 g of solids respectively at 20°C by fitting the Guggenheim-Anderson-de Boer (GAB) equation to the moisture sorption

isotherms, while at the same temperature, values of 7.09 and 7.60 g/100 g of solids was reported by other researchers (Samaniego-Esguerra, Boag, and Robertson 1991; Goneli et al. 2013). The different monolayer moisture contents observed may be due to different coffee beans tested.

Lipids

Coffee beans contain 8 to 18 % (dry basis) of lipid depending on the varieties and species. Green Robusta beans generally have lower lipids content than the Arabica beans (Table 1.2). Around 75% of coffee oil is in triglyceride form, with linoleic and palmitic acids being the main fatty acids. The remaining fraction is made up of the unsaponifiable components, which are mainly composed of ~19% total free and esterified diterpene alcohols, ~5% total free and esterified sterol, and a small amount of tocopherols (Table 1.3). The diterpene compounds, either free or esterified, have drawn considerable attention recently due to their serum cholesterol raising effect (Higdon and Frei 2006). Cafestol, kahweol, and 16-O-methylcafestol (16-OMC) are the three main diterpenes. Arabica green coffee beans contain cafestol and kahweol, while Robusta coffees contain cafestol, small amount of kahweol, and 16-OMC. It has been suggested that 16-OMC can be used as a reliable indicator compound for Robusta coffee (e.g., adulteration detection of the presence of Robusta in coffee blend), since this compound is present only in the Robustas (~10-50 mg/kg) but not in the Arabicas (Kolling-Speer, Strohschneider, and Speer 1999; Speer and Kölling-Speer 2006).

Table 1.3- Composition of lipid fraction of green coffee beans.

Compounds	% dry matter
Triacylglycerols	75.2
Esterified diterpene	18.5
Free diterpene	0.4
Esterified sterols	3.2
Free sterols	2.2
Tocopherols	0.04-0.06
Phosphatides	0.1-0.5
Tryptamine derivatives	0.6-1.0

Compiled from Speer and Kölling-Speer (2006)

Nitrogen-containing compounds

Caffeine is probably the most important nitrogen-containing compound in coffee, with its content in green coffee largely influenced by the coffee species. Robusta coffees tend to have higher caffeine content than the Arabica counterparts. Moreover, the *C. arabica* is highly homozygotic and caffeine contents in most cultivars are reported to be highly similar, while the *C. canephora* var. Robusta coffees have a larger caffeine content variation (Mazzafera and Silvarolla 2010).

Besides caffeine, other nitrogenous fractions in coffee include proteins, free amino acids, and trigonelline. Proteins make up ~8.5-12% (dry basis) of green coffee beans (Montavon, Mauron, and Duruz 2003). Green coffee proteins are mainly 11S storage protein and contain approximately equal amount of water-soluble and water-insoluble fractions. The water-soluble proteins are mainly consisted of globulins (85%) and albumin (15%). A nitrogen-to-protein factor of 5.5 could be used to calculate the protein content in coffee from the total nitrogen content (Bekedam 2008). During roasting, ~21%

of the proteins are lost, indicating their involvement in Maillard browning reactions, such as coffee melanoidin formation (Bekedam 2008).

Free amino acids in green beans are mainly glutamic acid, proline, alanine, asparagine and aspartic acid. These free amino acids are unstable under roasting conditions. As a result, negligible amount of free amino acids remains in the beans after roasting (Clarke and Vitztbum 2001; Illy and Viani 2005). Amino acids are involved in the formation of flavour and color compounds in coffee brew; both quantity and types of amino acids affect the intensity and quality of aroma.

Chlorogenic acid (CGA)

Green coffee beans possess one of the largest amounts of chlorogenic acid (CGA) among plants, at approximately 3-12% (dry basis) (Clifford and Kazi 1987; Ky et al. 2001; Farah et al. 2005; Perrone et al. 2008). CGA is the phenolic ester of quinic acid with trans-cinnamic acids. In coffee, the nine main isomers are 3-caffeoylquinic acid (3-CQA), 4-caffeoylquinic acid (4-CQA), 5-caffeoylquinic acid (5-CQA), 3,4-dicaffeoylquinic acid (3,4-diCQA), 3,5-dicaffeoylquinic acid (3,5-diCQA), 4,5-dicaffeoylquinic acid (4,5-diCQA), 5-feruloylquinic acid (5-FQA), 3-feruloylquinic acid (3-FQA) and 4-feruloylquinic acid (4-FQA) (Ky et al. 2001; Farah et al. 2005; Perrone et al. 2008). Among the isomers, 5-CQA is the most abundant CGA fraction, representing about 56-62% of the total CGA present in green coffee beans (Farah and Donangelo 2006). Figure 1.3 shows the structures of quinic, caffeic, and ferulic acids (Perrone et al. 2008).

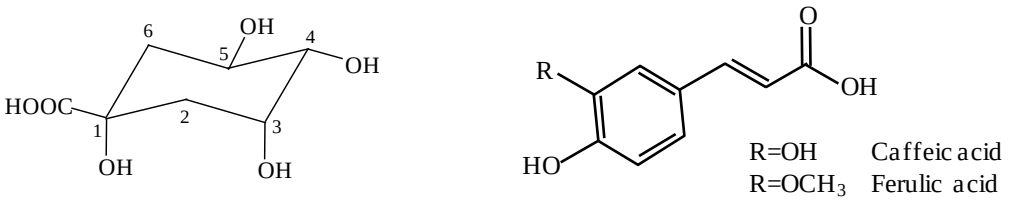

(-)-Quinic acid *trans* cinnamic acid

Figure 1.3- Structure of CGA precursors-quinic, caffeic (CA), and ferulic acids (FA).

CGA has been implicated in their health promoting effects, including antioxidant properties, cancer-protective effects, body weight reduction, and modulation of glucose metabolism in human (Higdon and Frei 2006; Thom 2007). In plants, CGA is one of the secondary metabolites that provide cellular defences (e.g., antioxidant, free radical-scavenging, UV light-absorbing). Moreover, they are antimicrobial agents that protect the plants against the proliferation of bacteria, fungi, and viruses (Farah and Donangelo 2006; Sahoo, Kasera, and Mohammed 2012). In general, CGA contents in green Robusta beans tend to be higher than in Arabica beans. Moreover, researchers have shown that positive correlations exist between caffeine and CGA contents in many coffee species, which may be related to the presence of caffeine-chlorogenate complexes (Campa et al. 2005; D'Amelio et al. 2009). The caffeine-chlorogenate complex might be described as 1:1 hydrophobically bound π-molecular complex. In particular, it was proposed that the plane of the caffeine molecule is parallel to the plane of the aromatic ring of the caffeoyl ester group and that the five and six-membered rings of the nitrogen heterocycle are equally involved in complex formation. The caffeine-chlorogenate complexation has been indicated as a crucial mechanism to explain the compartmentation of caffeine in *Coffea* plants and the qualitative relationship between caffeine and chlorogenic acid content among wild *Coffea* species.

Polysaccharides

Polysaccharides make up ~50% of the green beans' dry weight and are the principal structure building material of the cell walls. There are three major polysaccharides present in green beans, namely (galacto)-mannans, arabinogalactan-proteins (AGPs) and cellulose.

The galactomannans are the predominant components in the coffee bean cell wall accounting for ~50% of the polysaccharides (Redgwell and Fischer 2006; Bekedam 2008). Coffee bean mannan consists for the most part of linear chains of β-1,4-mannosyl residues with single galactose units α-linked at C-6 of a mannosyl residue. A wide range of degree of substitution from 130:1 to 3:1 has been reported (Redgwell and Fischer 2006). The presence of acetyl group, linked at the O-2 and O-3 position of the mannosyl residues, were reported (Oosterveld et al. 2004; Nunes, Domingues, and Coimbra 2005). In addition, arabinosyl residues were contained in the soluble galactomannans as side chains (Nunes, Domingues, and Coimbra 2005). The solubilisation of galactomannans is a critical factor in determining the yield of soluble coffee power during commercial extraction. Besides cellulose, galactomannans are the most resistant polymers to solubilisation. One of the principal determinants of galactomannan solubility is the frequency of substitution of the mannan backbone.

Arabinogalactans are highly water-soluble and have an arabinose:galactose ratio of about 0.4:1, consisting of a backbone of β-(1→3)-linked galactan with galactose and arabinose residues containing short side chains linked at the C-6 position (Fischer et al. 2001; Bekedam 2008). In mature green beans, about one third of the polysaccharides are arabinogalactans, some of which are covalently linked to proteins as arabinogalactan proteins (AGPs). The AGP content in green beans is around 15% and consisted of approximately 12% protein and 85% arabinogalactan. Arabinogalactan content in green

Arabica beans is lower (14%) as compared to the Robusta beans (17%) (Merwe et al. 1990; Fischer et al. 2001).

Volatile compounds

Green coffee beans have a characteristic "green peas" aroma, which is mainly contributed by 3-alkyl-2-methoxypyrazines, of which 3-isobutyl-2-methyoxypyrazine and 2-methoxy-3-isopropylpyrazine are important (Figure 1.4). 2-Methoxy-3,5-dimethylpyrazine is the second important odorant on the basis of odour activity value, which brings the earthy odour to green coffee beans (Clarke and Vitztbum 2001; Belitz, Grosch, and Schieberle 2009). Being very stable compounds, the methoxylpyrazine compounds in green coffee beans are able to survive the roasting process. However, the odour of the methoxylpyrazines is largely suppressed due to the formation of other aroma compounds formed.

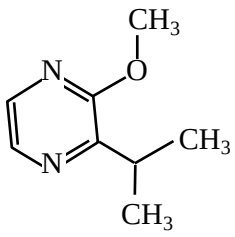

2-methoxy-3-isopropylpyrazine

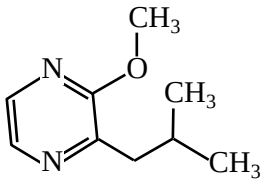

3-isobutyl-2-methyoxypyrazine

Figure 1.4- Structure of characteristic aroma compounds of green coffee, 3-isobutyl-2-methyoxypyrazine and 2-methoxy-3-isopropylpyrazine.

1.2 Coffee roasting

1.2.1 Main aspects of roasting process

Roasting of green coffee beans generally takes place at above 200°C to develop the characteristic flavours, colors and structural properties of roasted coffee. The

physicochemical changes occurred during roasting are complex, involving interactions between materials and process parameters. Some of the main events that take place during coffee roasting are illustrated in Figure 1.5 (Clarke and Vitztbum 2001; Illy and Viani 2005). During roasting, heat from hot gases or hot surfaces is transferred into the green bean. The increase in temperature causes moisture to evaporate in an endothermic process. As heating continues, exothermic reactions start to take place, with concomitant formation of volatiles and CO_2. The resulting increase in internal pressure of the beans causes them to expand and crack. When the desired degree of roast (color, flavour , roast mass loss and so on) is reached, the beans are discharged from the roaster and cooled rapidly by water quenching and/or air cooling (Clarke and Vitztbum 2001).

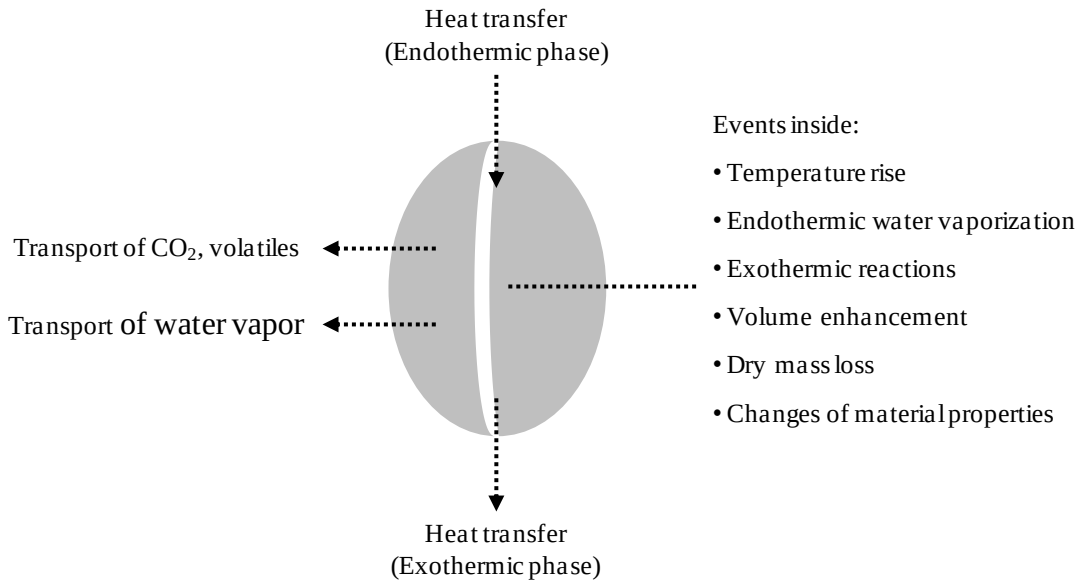

Figure 1.5- Main events that take place during the roasting of green coffee beans, showing a combined heat and mass transport superposed by endothermic and exothermic reactions.

The roasting temperature and roasting time are two important parameters that determine the quantity of heat transferred to the beans (Illy and Viani 1995). High-temperature-short-time (HTST) and low-temperature-long-time (LTLT) roasting profiles

are generally used in the literature to investigate the effect of roasting time and temperature on the physicochemical and sensory properties of the roasted coffee products (Schenker 2000; Schenker et al. 2000; Schenker et al. 2002; Baggenstoss et al. 2008; Franca et al. 2009). Roasting time of less than 4 min is commonly called high yield or fast roasting (Schenker 2000; Clarke and Vitztbum 2001). Coffee beans roasted using the high yield process are larger in size, have a reduced density and greater porosity. Because of these structural differences, the fast roasted beans allow enhanced water penetration and extraction of the coffee soluble compounds, thus higher yield during brewing (Ortola et al. 1998). However, these products have somewhat higher final water content and exhibit greater oil sweating phenomenon than the traditional roasted coffee. Hence, they are more affected by oxidation and staling during storage (Schenker 2000; Clarke and Vitztbum 2001; Illy and Viani 2005).

Rapid cooling of beans after roasting is critical to avoid over roasting. Cooling can be accomplished by drawing cold air rapidly through the roasted beans or by spraying a minimal amount of cold water on to the roasted beans (also known as “quenching”). The air cooling approach uses large quantities of air, cooling the beans mainly by force convection. Water quenching is faster than air cooling since the former relies on latent heat of vaporization to remove the residual heat. However, the water quenched coffees tend to have a reduced shelf-life due to the increased moisture content (Clarke and Vitztbum 2001; Baggenstoss et al. 2007).

1.2.2 Physicochemical changes during roasting

Roasting is a highly complex process, involving a myriad of chemical reactions, and considerable physical changes, all occurring within 10-15 min at a temperature in excess of 200°C. Over the past two decades, although many researchers have investigated

the physiochemical changes of coffee that take place during the roasting process, complete understanding of the fundamentals behind the process is still lacking. Nevertheless, by comparing the chemical compositions of green and roasted coffee beans that are processed using different temperature-time profiles, considerable information has been derived. This section will review the existing literature on the physiochemical changes during roasting.

1.2.2.1 Chemical changes

Carbohydrates

The main low molecular weight carbohydrate in green coffee is sucrose. In general, Arabica green coffees tend to contain about twice as much sucrose as Robusta. During roasting, sucrose is rapidly degraded and its content is minimal in roasted coffee. A small amount of the sucrose is pyrolyzed and caramelized, while a considerable fraction is hydrolyzed into glucose and fructose. As reducing sugar, the glucose and fructose will take part in the Maillard reactions that are important in contributing to the color and flavour of brewed coffee.

As for polysaccharides, the thermal stability of the arabinogalactans, mannan and cellulose are markedly different during the roasting process. Between 12-40% of the polysaccharides are degraded when subjected to different roasting conditions (Redgwell et al. 2002). The arabinogalactans are more susceptible to thermal degradation, particularly the more heat labile arabinose residues. A 10-fold reduction in molecular weight was observed after light roast due to the fission of the galactan backbone and the debranching of the arabinose side chains (Redgwell and Fischer 2006). Up to 60% degradation of arabinogalactans for dark roast coffee has been reported, while for the mannan fraction, a lower level of degradation (36%) has been observed. As a result,

roasting leads to increased solubility of both the arabinogalactans and galactomannans due to their thermal degradation and structural changes in the roasted coffee. On the other hand, cellulose showed minimal degradation during roasting (Schenker 2000; Redgwell et al. 2002).

Nitrogen-containing compounds

The free amino acid content in green coffee beans is around 0.2-0.8 % (Table 1.2). After roasting, a negligible amount of the original free amino acids is present in the beans (Clarke and Vitztbum 2001; Illy and Viani 2005). Part of *L*-amino acids is isomerised to form *D*-amino acids. There is also a change in the amino acid composition before and after roasting, due to the different reactivity of the amino acids. Arginine, aspartic acid, cystine, histidine, lysine, serine, threonine and methionine are thermal labile, while alanine, glutamic acid and leucine are relatively thermal stable (Belitz, Grosch, and Schieberle 2009). Proteins in coffee beans have been reported to be both fragmented and polymerized upon roasting. Moreover, evidence also suggests that the 11S protein can integrate into the polymeric structure of melanodins formed during roasting (Montavon, Mauron, and Duruz 2003).

Trigonelline content in green coffee is 0.6-2.1% (dry weight basis). About 50-80% of trigonelline is degraded upon roasting, the extent of which is proportional to the degree of roast. The major degradation products are nicotinic acid, pyridine, 3-methyl pyridine, nicotinic acid methyl ester (Belitz, Grosch, and Schieberle 2009) (Figure 1.6). Some of the degradation products are important contributors to the characteristic aroma properties of roasted coffee. For example, pyridines are one of the major contributors to the roasty aroma of coffee.

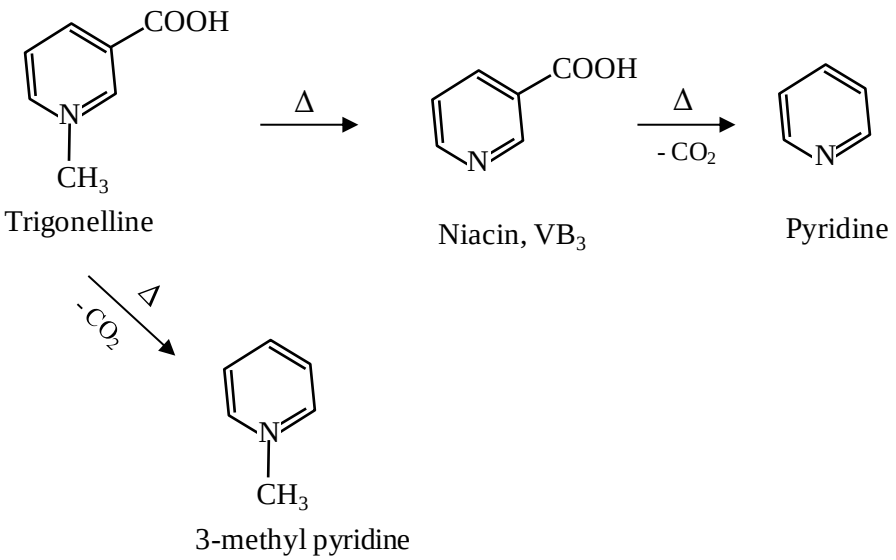

Figure 1.6- The possible degradation path and products of trigonelline during coffee roasting.

Lipids

Overall, there are only slight changes in the lipid fraction upon roasting. The sterols and most of the triglycerides remain unchanged. However, the main diterpenes, i.e., cafestol and kahweol, are decomposed to some extent after roasting. Up to 80% of the initial levels of free diterpenes were lost due to their sensitivity to heat (Kolling-Speer, Strohschneider, and Speer 1999; Speer and Kölling-Speer 2006). Similar to the free form, the contents of cafestol and kahweol esters also decrease during roasting with the extent depending on the roasting temperature, while 16-OMC esters are quite stable. In the roasted coffees, the majority of the cafestol, kahweol and 16-OMC are still esterified.

CGA

Although green coffee beans contain the largest amount of CGA found in plants, ranging from 3 to 12%, its content in roasted coffee is minimal due to the degradation reactions during roasting. When coffee beans are processed to light-medium roasts, approximately 60% of the initial CGA in green beans are degraded. In dark roast coffees,

the majority of the CGA are depleted (Figure 1.7) (Belitz, Grosch, and Schieberle 2009). Besides thermal degradation, it has been suggested that the incorporation of CGA into melanoidins is another pathway that causes the depletion of free CGA in roasted coffee (Perrone, Farah, and Donangelo 2012). Furthermore, up to approximately 30% of the CGA are transformed into their corresponding chlorogenic lactones, by losing a water molecule from the quinic acid moiety (Farah et al. 2005).

During thermal degradation, CGA is probably first hydrolyzed to quinic acid and to the corresponding cinnamic acid. The quinic acid portion can appear as different stereoisomers, as well as quinides (quinic acid lactones), the ratio of which has been observed related to the degree of roast (Clarke and Vitztbum 2001). The cinnamic acid may undergo pyrolysis to form phenolic volatiles, such as 4-vinyguaiacol (Clarke and Vitztbum 2001; Illy and Viani 2005).

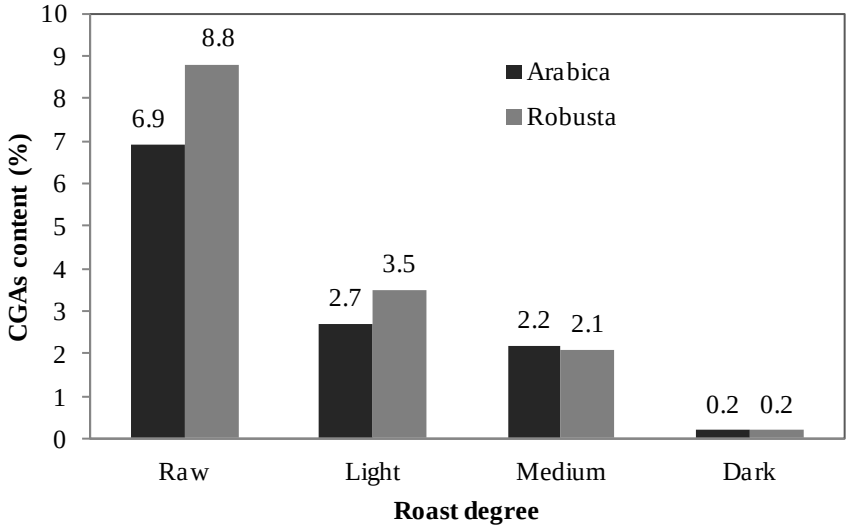

Figure 1.7- Chlorogenic acid contents at different degrees of roasting adapted from Belitz et al. (2009).

1.2.2.2 Physical changes

Roasting of coffee beans causes their color to change progressively from initial greenish-grey to brown, dark brown, and black. The final color of the beans depends on the desired roast degree. Due to the dehydration and pyrolysis reactions, considerable weight loss (14-20% of the initial weight) occurs in coffee beans after roasting (Schenker 2000). Another significant physical change that occurs in coffee beans during roasting is expansion in volume due to the formation of CO_2, moisture vapor, and other volatile compounds. Relative bean volume (volume of roasted beans/volume of green beans) is greater for beans roasted using the HTST process than those processed with the LTLT process. For example, Schenker (2000) reported relative bean volumes of 1.74 and 1.42 for a medium roast coffee, using the HTST and LTLT processes, respectively. As a result of the simultaneous weight loss and volume increase, bean density decreases and a porous structure develops. Typical density of roasted coffee is 0.5-0.8 g/mL as compared to 1.03-1.18 g/mL for the green coffee beans (Alessandrini et al. 2008). Fast roasting generally produces coffee with a lower density due to the larger volume. For example, Schenker (2000) reported density values of 0.622 and 0.747 g/mL for medium roast coffee from HTST (260°C) and LTLT (230°C) process, respectively. Water content also has a major impact on beans density. Pre-drying of the green beans can produce roasted beans of lower-density, implying that the initial moisture present is another determinant for the roasted coffee structure (Clarke and Vitztbum 2001).

1.2.2.3 Micro-structural changes

Coffee beans undergo drastic micro-structural changes during roasting. As shown in Figures 1.8a and 1.8b, the green coffee beans consist of lots of parenchymatous storage cells, the cytoplasm of which contains the essential coffee flavour precursors (e.g., lipids,

proteins, carbohydrates, caffeine, chlorogenic acids, and minerals). At the typical roasting temperatures, the coffee bean is heated above its glass transition temperature and become rubbery (Anderson et al. 2003). Concomitantly, intensive chemical reactions take place within the cell matrices, producing a large amount of gases and volatile compounds. The resulting increased pressure causes the cells to expand considerably. The dehydration, exhausting of green coffee compounds, and swelling of the cell that occurred during roasting result in bean matrices consisting of evacuated cells, with cell walls that form a framework (Figure 1.8d). The evacuated cells have diameters ranging from 34 to 40 µm, which are the main contributor of the roasted coffee bean's porosity. Porosity value of roasted coffee beans varies from 0.474 to 0.738 depending on the roasting conditions and measurement technique used (Schenker et al. 2000).

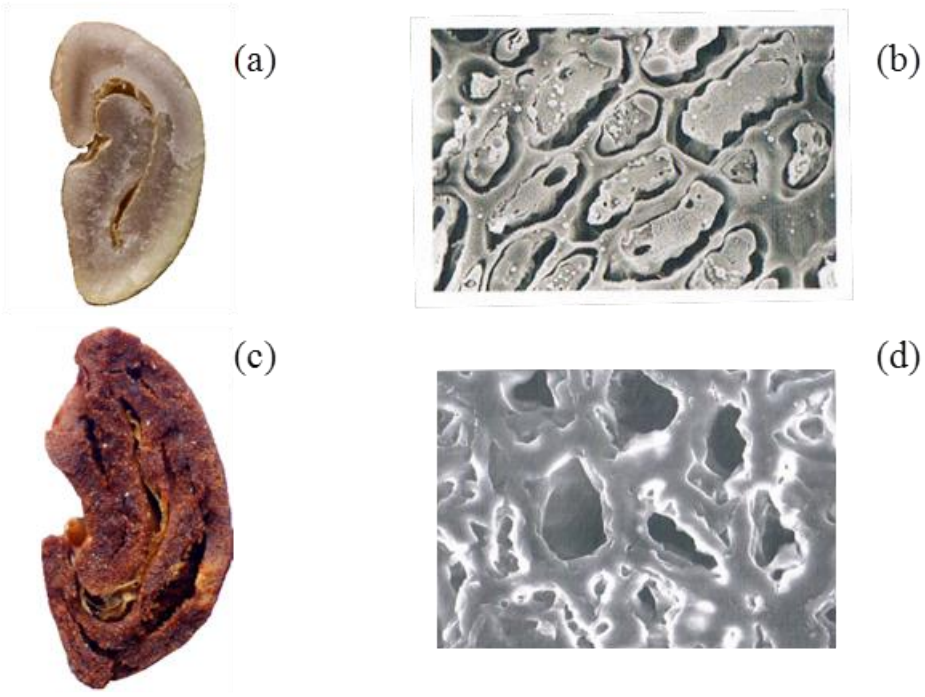

Figure 1.8- Structures of green coffee and roasted coffee (a) longitudinal cut view of green coffee beans; (b) cell structure of green coffee under SEM; (c) longitudinal cut view of roasted coffee beans; (d) cell structure of roasted coffee under SEM. Photos are from Illy and Viani (2005).

In addition, a number of authors assumed the roasting process could alter the porosity of the cell wall. Typical pore size of cell wall is in the range of 10-50 nm, as determined by using mercury porosimetry (Schenker et al. 2000). In addition, bean roasted at higher temperature results in larger size of cell wall pores than those processed at lower temperature (Schenker et al. 2000). Saleeb reported that the majority of the CO_2 was held in pores that were between 1.7 and 3.3 nm, indicating the existence of even smaller pores (Saleeb 1975). On the basis of IUPAC's definition of porous material, the porosity of roasted coffee can be attributed to macropores made up of evacuated cell (>50 nm), as well as mesopores (2-50 nm), and micropores (<2 nm) that appears in the cell walls (Rouquerol et al. 1994). A schematic diagram of this pore hierarchy is presented in Figure 1.9. The pore structure of roasted coffee determines the mass transfer phenomena during coffee storage, such as CO_2 degassing, aroma releasing, and oil migration (Illy and Viani 1995; Schenker 2000). As for the coffee brewing, the higher porosity of coffee will facilitate the extraction of water soluble compounds, as well as leaching of lipid.

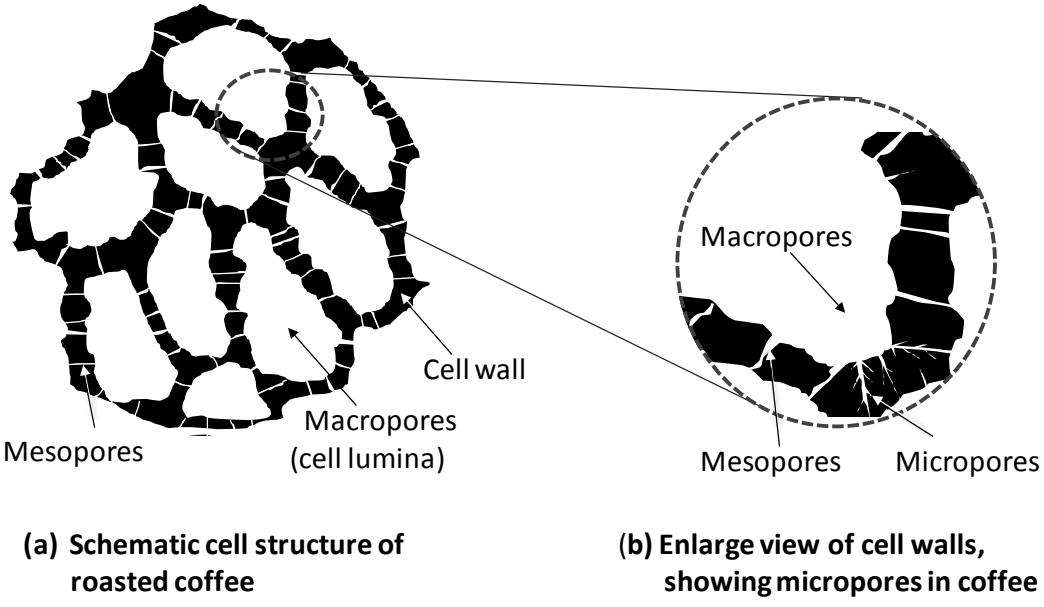

Figure 1.9- Schematic diagram showing the porous structure of roasted coffee beans.

1.2.3 Roasters

A roaster is designed to allow the beans and hot gases to come into contact to achieve the roasting process. The roasters could vary in their way of heating and mixing beans, but all currently successful process technologies require three basic components: (1) a containment chamber; (2) a mixing device to assure homogenous heat exposure; and (3) control of the heat transfer (Clarke and Vitztbum 2001; Illy and Viani 2005). Table 1.4 summarizes the types of roasters based on various principles of roasting system.

Table 1.4- Types of roasters based on various principles of roasting systems

Principle	Roaster type	Descriptions
Product flow	• Batch size • Continuous	Batch roasters provide more flexibility on process layout and control. The demand for large continuous roasters is decreasing because of the tendency for larger coffee product varieties.
Mechanical principle	• Horizontal drum • Vertical fixed drum (with paddles for mixing) • Vertical rotating bowl • Fluidized bed • Spouting bed • Packed bed	The main task of mechanical mixing is to achieve homogenous roasting and to prevent scorching of the beans. The motion of the beans is either produced by mechanical rotation or by the flow of roasting gases.
Heat transfer	• Conduction • Convection • Radiation	Roasters generally contain all three types of heat transfer, but their relative contribution to the overall heat transfer may greatly differ depending on the roaster. Convection is dominant in current roasting technologies in industry.
Air to bean ratio	Values can range from 1 in a typical conventional process up to 150 in fully fluidized bed systems.	The ratio is defined as kg hot air per kg green coffee. This ratio is a characteristic parameter in a roasting process and is dependent on degree of roast.

Adapted from (Clarke and Macrae 1987), (Clarke and Vitztbum 2001) and (Illy and Viani 2005).

Among the various roaster systems currently being used in the industry, the drum roaster by far is the most common. The roaster has a horizontal rotating drum that can be solid or perforated. The perforated design allows for more convective heat transfer than the solid drum. Although large scale horizontal drum roaster can operate in a continuous mode, due to increased consumer demand for different coffee product varieties, there is a trend of increasing use of smaller drum roasters for batch roasting of coffee beans. Another driver for this trend can be attributed to the advancement of sophisticated time and temperature control of modern drum roasters that provide very consistent bean roasting.

Roasting of coffee beans in a fluidized bed roaster is exclusively based on convective heat transfer, during which high velocity hot air is directed towards the beans from the bottom of the roasting machine to achieve the fluidization of the beans (Illy and Viani 2005; Baggenstoss et al. 2008). The hot air suspends and heats the beans simultaneously, allowing very efficient and uniform roasting of beans. Besides, the roasting process can be readily manipulated by adjusting the temperature and velocity of the hot air to vary the time-temperature profile (Clarke and Vitztbum 2001).

Another variant of roaster that has been used by the coffee industry is known as the packed bed roaster. Here, a batch of beans is roasted in a conical chamber, in which a high velocity hot air enters the chamber tangentially and passes through a set of louvers, creating an air flow current that whirls the beans in the chamber. As a result, a spinning packed bed of coffee beans is formed. This packed bed, typically at 30-50 mm thick, reportedly is able to achieve a very high rate of heat transfer, shortening the roast cycle, and producing “high yield” beans with reduced loss in volatile aroma compounds (Clarke and Vitztbum 2001).

Table 1.5 summarizes additional information about the basic mechanical principles of some commercial roasters.

Table 1.5- Basic mechanical principles of some commercial coffee roasters

Roster type	Mechanical Principle	Characteristics
Horizontal drum roaster	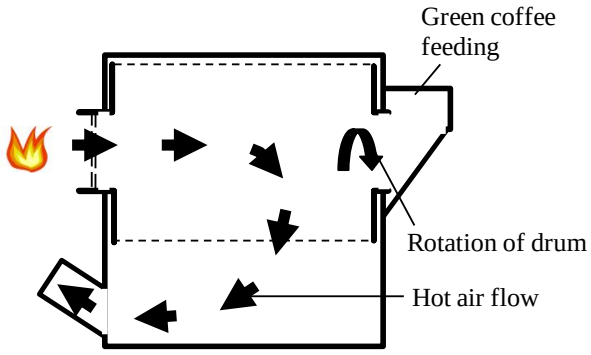	Mixing flights, vanes or paddles are attached to the drum to enhance the tumbling of the beans. Heating is mainly due to direct heating by convective flow of hot air and conductive heating by hot drum walls. Horizontal drum roaster can be batch operated or continuously operated. In the latter, an inner conveyer continuously transports the beans through the roast chamber.
Vertical fixed drum	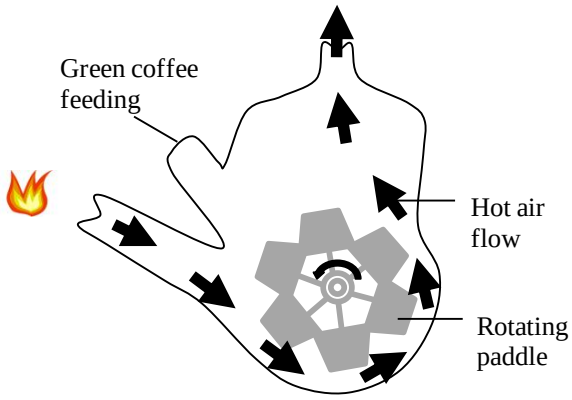	Vertical roasters that are characterized by a static chamber that is equipped with blades or paddles. Heating mode is mainly by convective flow of hot air. Vertical fixed drum roaster is always batch operated.
Rotating bowl	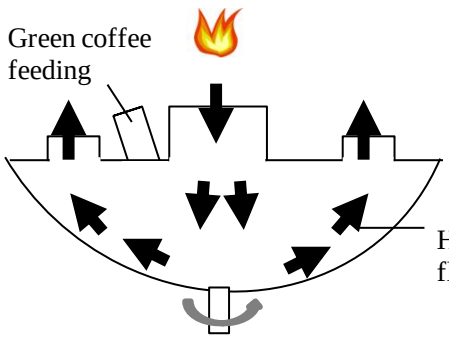	This type of roaster is characterized by centrifugal mixing and roasting with a rotating bowl. Heating is mainly through convective flow of hot air. In the roaster, coffee beans are carried to the periphery of the bowl due to the centrifugal force and air flow. The beans fall back to the centre in spiral motions, creating very efficient mixing. .

Fluidized bed	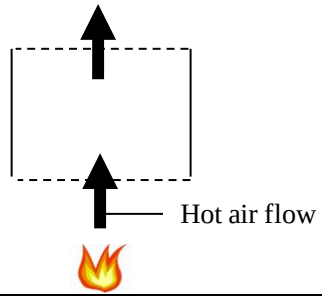	This type of roasters provides direct heating to the beans by hot air. They are batch operated and roasting is fast due to high heat transfer caused by turbulent air current.
Spouted bed	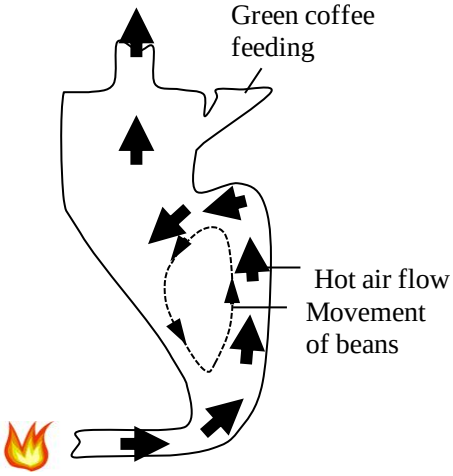	Beans are heated by hot air that moves the beans in a certain flow pattern. Unlike fluidized bed roaster, the spouted bed roaster does not suspend all beans equally in the hot air. The design requires less amount of heated air than fluidized bed roaster. The roaster is batch operated.
Packed bed	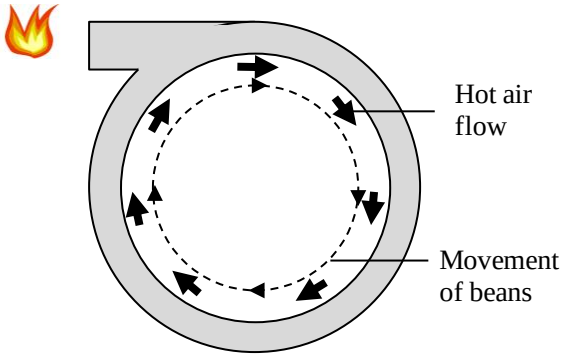	The roaster has a tangential heated hot air inlet, creating flow current that causes spiral upward motion of the beans.

Figures in the table are adapted from Clarke and Macrae (1987), Clarke and Vitztbum (2001), and Schmidt (2006). The first five figures are side view of the roasting chamber, and the last one shows the top view.

1.2.4 Degree of roast

The degree of roast is generally used to describe the extent of roast in coffee beans, which is one of the main criteria for rating the quality of coffee. Various parameters are used to determine the degree of roast for quality control during production and research purposes, including color, roast loss, and organic roast loss (Schenker 2000; Baggenstoss

et al. 2008). Among these properties, bean color is most frequently used. In the industry, especially for small batch roast operations, visual inspection to determine the degree of roast is common. Here, the roastmaster will manually collect bean samples from the roast chamber during various stage of roast to gauge the progress of the roasting and to determine the end point of the process. Besides visual inspection, the degree of roast can be measured using an Agtron® analyzer, which is based on the principle of detecting the reflectance energy from a coffee sample after irradiating it with near infrared (NIR) radiation. The analyzer produces an Agtron number ranging from 0.0 to 100.0; the lower the Agtron number the darker the roast (Anon 2011). The Agtron number can be correlated with some coffee color standards, such as the one developed by the Specialty Coffee Association of America (SCAA; *AGTRON/SCAA Roast Classification Colour Disc System*) to classify coffees into different roast degrees. This system provides trade professionals with an affordable tool to determine the degree of roast and facilitate communication using descriptive terms, such as light, medium, medium-dark, dark, and very dark roasts. In the academia, the lightness value (L^*) is often determined using a spectrophotometer (Ortola et al. 1998; Schenker et al. 2000; Mwithiga and Jindal 2003; Summa et al. 2007; Baggenstoss et al. 2008; Wang, Fu, and Lim 2011). Here, instead of measuring the infrared energy reflected from the samples, electromagnetic radiation in the visible range is determined.

During the roasting process, due to the pyrolysis and other reactions that generate a large amount of volatile gases and vapours, substantial weight loss of the bean is observed. Thus, the overall weight loss and the organic roast loss have also been used as indicators for the degree of roast. In general, coffee beans loose between 14 and 20% of their weight during roasting, depending on the degree of roast, roasting conditions applied, and green coffee bean properties (Schenker 2000). Studies have shown that organic roast loss (ORL)

which measures the extent of loss in organic matters after roasting, is a more reliable indicator than overall roast loss because the former is independent of the moisture content of the green beans (Schenker 2000).

Although the physical indicators discussed above provide convenient means to evaluate the degree of roast of coffee beans, researchers have broadened the list of indicators by carrying out chemical compositional analyses of the beans and the volatile compounds formed and shed light on the complex reaction that take place during the roasting process. For example, Nehring and Maier (1992) reported a correlation between the degree of roast and relative contents of *L*- and *D*- enantiomers of alanine, leucine, phenylalanine and glutamic acid in roasted coffee. This correlation was shown to be independent of the roasting temperature, roasting time, coffee bean varieties, and steam pre-treatment of the green coffee. Another method to indicate the degree of roast is by analysing trigonelline and nicotinic acid content in roasted coffee, because the concentration ratio of trigonelline to nicotinic acid was found to decrease linearly with the increasing of degree of roast (Stennert and Maier 1996). Moreover, the volatile compounds, being a very complex mixture, have been studied to investigate the feasibility of using them as indicators of degree of roast. For example, online determination of roast degree has been investigated through analysing the volatiles evolved during roasting by laser mass spectrometry (Dorfner et al. 2004). Based on the analysis, a multivariate statistical model was created to monitor the degree of roast (Dorfner et al. 2004). In addition to online monitoring, determination of volatile compounds in the roasted coffee was also found to be able to differentiate roasted coffee with different roasting degrees (Franca et al. 2009).

1.2.5 Maillard reaction

The Maillard reaction is of utmost importance for coffee quality, which brings roasted coffee's characteristic brown color and aroma. The Maillard reaction was named after the French chemist Louis Maillard who first reported the phenomenon. However, it was Hodge who first put forward a coherent scheme on the non-enzymatic browning reaction (Hodge 1953). Based on Hodge's scheme, the Maillard reaction is generally divided into three stages. In the initial stage, a condensation reaction takes place between a reducing sugar and an amino group from an amino acid or amino acid residues from a protein, such as the ε-amino group of lysine, and the α-amino groups of terminal amino acids. The condensation reaction results in the formation of an N-substituted glycosylamine (in the case of aldose sugar), which further rearranges to form the Amadori products (or Heyns products if the reducing sugar is a ketose). The intermediate stage starts from the Amadori/Heyns product. This stage features sugar fragmentation products and release of the amino group. The degradation of Amadori products is dependent on the pH of the system. At pH $\leq$ 7, it undergoes mainly 1, 2-enolisation with the formation of furfural when pentose is involved or hydroxylmethylfurfural (HMF) if the sugar is a hexose. At pH>7, the degradation of the Amadori compound mainly involve 2.3-enolisation, where reduction product, such as 4-hydroxyl-5-methyl-2.3-dihydrofuran-3-one and a variety of fission products, including acetol, pyruvaldehyde and diacetyl, are formed. All these compounds are highly reactive and take part in further reactions. For example, carbonyl group can condense with free amino groups, which results in the incorporation of nitrogen into the reaction products. In the final stage, amino groups participate again and lead to the formation of brown nitrogenous polymer, i.e., melanoidins (Figure 1.10) (Martins, Jongen, and Boekel 2001; van Boekel 2006; Bekedam 2008).

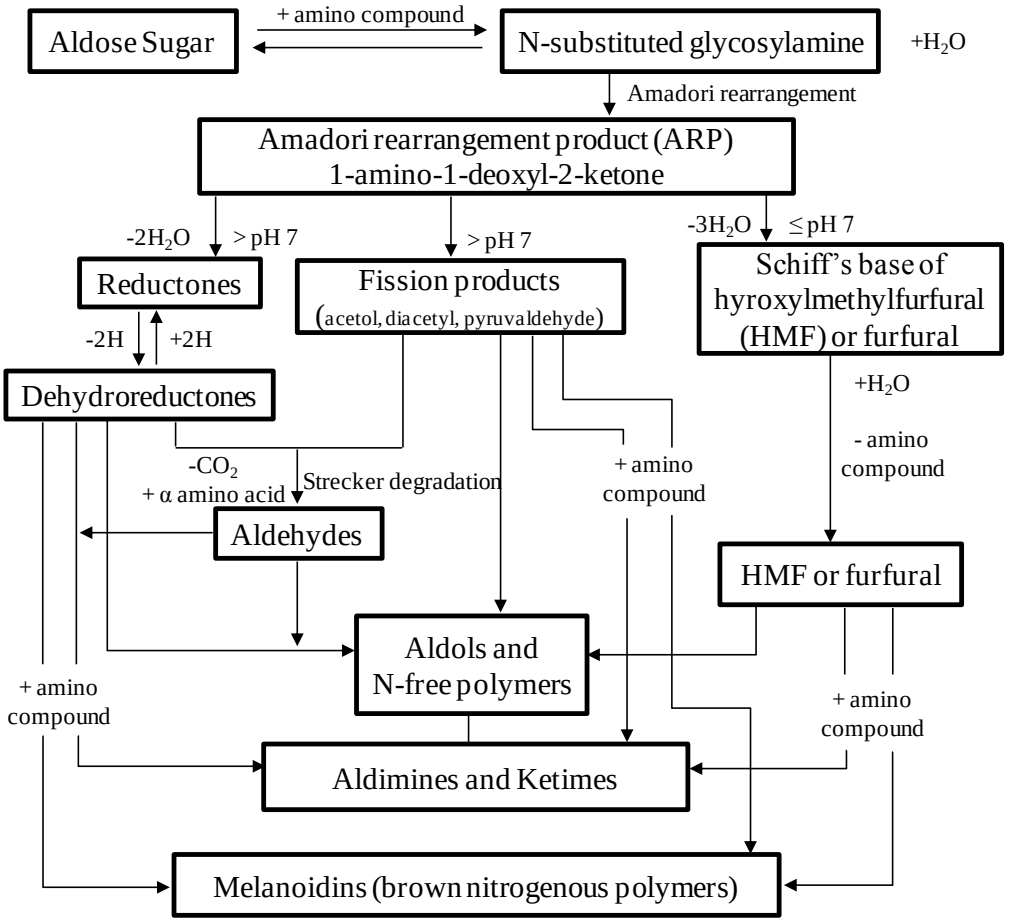

Figure 1.10- Maillard reaction scheme compiled from Martins et al (2001)

The Maillard reaction products can be divided into non-volatile melanoidins and volatile components, referred as Maillard flavours. In relation to the flavour formation, the Strecker degradation is of utmost importance, in which α-dicarbonyl compounds produced from the Maillard reaction react with amino acids, leading to the formation of α-aminoketones and Strecker aldehydes (Figure 1.11). During the initial and intermediate stages of the Maillard reaction, the degradation of sugar is catalyzed by amino compounds. Strecker degradation, on the other hand, can be considered as the degradation of amino acids initiated by carbonyl compounds. Strecker degradation is important not only in the formation of flavour compounds, but also providing reaction routes by which nitrogen and sulphur can be introduced into heterocyclic compounds in the final stage of

the Maillard reaction. The α-aminoketones are the key precursors for heterocyclic compounds, such as pyrazines, oxazoles, and thiazoles. In the case of alkylpyrazines, the most direct and important route for their formation is thought to be via self-condensation of aminoketones or condensation with other aminoketones (Berger 2007). Studies with radioactive carbon have shown that over 80% of the CO_2 liberated in the Maillard reaction originates from the amino acid, somewhat less than 10% coming from uniformly labelled glucose (Stadtman, Chichester, and Mackinney 1952).

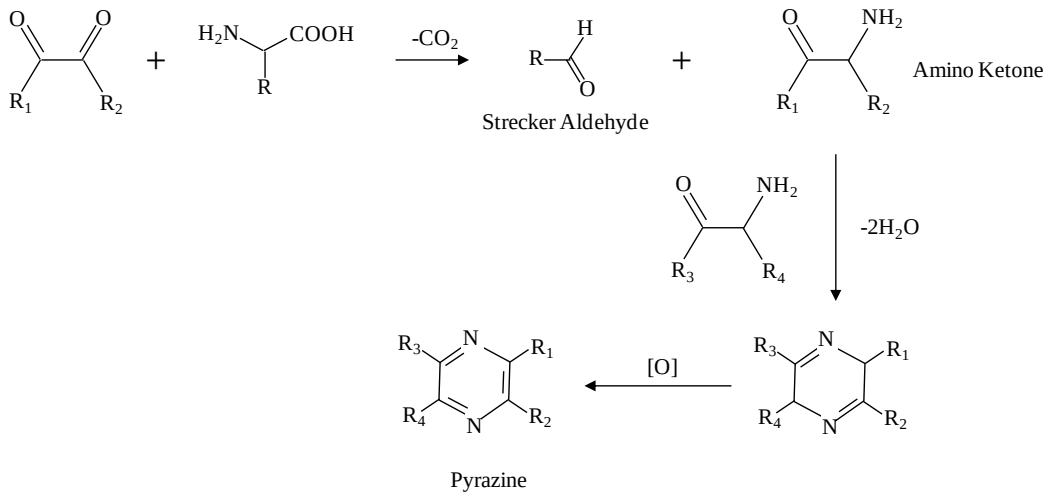

Figure 1.11- Strecker degradation and possible formation mechanism of pyrazine from amino ketones, compiled from Berger (2007).

1.2.6 Volatile aroma compounds in roasted coffee

Besides the stimulatory effect of caffeine, coffee is appreciated for its pleasing aroma. Therefore, numerous investigations have been carried out to identify the volatile compounds. Presently, more than 850 volatile compounds have been identified in roasted coffee, 28 of which have been screened as main odorants that contribute to coffee aroma (Table 1.6) (Semmelroch et al. 1995; Semmelroch and Grosch 1995; Semmelroch and Grosch 1996; Czerny, Mayer, and Grosch 1999; Mayer, Czerny, and Grosch 1999; Mayer, Czerny, and Grosch 2000). In addition, omission sensory experiments reveal that 2-

furfurylthiol, 4-vinylguaiacol, several alkylpyrazines and furanones, acetaldehyde, methylpropanal, 2-methylbutanal and 3- methylbutanal have the greatest impact on the coffee aroma (Czerny, Mayer, and Grosch 1999). Mayer et al. (1999) compared the 28 compounds (Table 1.6) by stable isotope dilution assays in roasted coffee from different origins. They concluded that the origin affected the concentrations of 2,3-butanedione, 2,3-pentanedione, 3-isobutyl-2-methoxy-pyrazine, 4-hydroxy-2,5-dimethyl-3(2H) furanone, 4-vinyl- and 4-ethylguaiacol, 2-furfurylthiol, 3-mercapto-3-methylbutyl-formiate and 3-methyl-2-buten-1-thiol, whereas the roast degree mainly influenced the concentrations of propanal, 5-ethyl-4-hydroxy-2-methyl-3(2H)-furanone, guaiacol, 4-ethylguaiacol, 2-furfurylthiol, 3-methyl-2-butene-1-thiol and methanethiol. Moreover, the aroma profile of Robusta coffee is different with that of Arabica. Robusta coffee contains significantly higher concentrations of alkypyrazines and phenols than the Arabica (Semmelroch et al. 1995; Semmelroch and Grosch 1996). As a consequence, the earthy and smoky/phenolic notes are more intensive in the Robusta coffee. On the other hand, Arabica coffees are usually richer in the odorants of the sweet/caramel group.

Table 1.6- Potent odorants in roasted coffee

No	Group/odorant
	Sweet/caramel-like group
1	Methylpropanal
2	2-Methylbutanal
3	3-Methylbutanal
4	2,3-Butandione
5	2,3-Pentandione
6	4-Hydroxy-2,5-dimethyl-3(2H)-furanone
7	5-Ethyl-4-hydroxy-2-methyl-3(2H)-furanone
8	Vanillin
	Earthy group
9	2-Ethyl-3,5-dimethylpyrazine
10	2-Ethenyl-3,5-dimethylpyrazine
11	2,3-Diethyl-5-methylpyrazine
12	2-Ethenyl-3-ethyl-5-methylpyrazine
13	3-Isobutyl-2-methoxy-pyrazine
	Sulfurous/roasty group
14	2-Furfurylthiol
15	2-Methyl-3-furanthiol
16	Methional
17	3-Mercapto-3-methylbutyl-formiate
18	3-Methyl-2-butene-1-thiol
19	Methanethiol
20	Dimethyltrisulfide
	Smoky/phenolic group
21	Guaiacol
22	4-Ethylguaiacol
23	4-Vinylguaiacol
	Fruity group
24	Acetaldehyde
25	Propanal
26	(E)-β-Damascenone
	Spicy group
27	3-Hydroxy-4,5-dimethyl-3(5H)-furanone
28	5-Ethyl-3-hydroxy-4-methyl-2(5H)-furanone

Adapted from Clarke and Vitzbum (2001) and Belitz et al. (2009)

1.3 Mass transfer mechanism in porous media

A porous medium refers to a solid having void space (pore) that is filled with a gas or liquid. Generally, many of these pores are interconnected so that mass transport is possible through the pores, which is generally a faster transport process than through a solid matrix (Datta 2007). Porosity (ϕ) is an important index of porous medium, which refers to volume fraction of void space which can be defined as the following equation (Tsami and Katsioti 2000):

$$\phi = \frac{V - V_S}{V} = \frac{V_p}{V} = \frac{Pore\ volume}{Total\ bulk\ volume} \tag{1.1}$$

where V is the bulk volume, V_S is the solid volume and V_p is the pore volume.

Porosity cannot give any information concerning pore sizes and their degree of connectivity. Thus, samples of the same porosity can have widely different physical properties. There are many methods for measuring porosity, i.e. direct method, imbibitions method, mercury injection method and gas expansion and gas adsorption methods. The method selection is highly dependent on the nature of the sample. In mercury porosimetry, gas is evacuated from the sample cell, and mercury is then transferred into the sample cell and pressure is applied to force mercury into the sample. At normal pressure, mercury will not enter the pores of sample and thus bulk volume of the sample can be calculated. The pressure on the mercury is then raised in stepwise manner, forcing mercury into the pores. If the pressure is sufficiently high, the mercury will invade all pores. The porosity can then be calculated from the bulk volume and the pore volume. During measurement, applied pressure P and intruded volume of mercury, V, are registered. Beside porosity, parameters describing the pore structure of the sample, such as pore size distribution, the skeletal and apparent density, as well as the specific surface area, can be calculated from the data obtained (Schenker et al. 2000; Datta 2007).

Gas transport in a porous media can be due to different mechanisms. Primarily two mechanisms can be considered - molecular diffusion and convection (pressure driven or Darcy flow). For diffusion in small cylindrical pores, Knudsen diffusion, surface diffusion, capillary condensation, and molecular sieving should be considered. By small it means that the pore diameter is of the same order of magnitude as the molecular size (Cussler 2009).

1.3.1 Molecular diffusion

Gases in the porous media can move by molecular diffusion if the pores are large enough. Mass transfer by diffusion is caused by a random molecular motion which is analogous to heat transfer by conduction. Concentration gradient is the driving force for diffusion mass transfer. Based on kinetic theory of gases, a simplified model for an ideal gas mixture of species A diffusing through its isotope A* yield an equation for the self-diffusion coefficient, defined as (Welty et al. 2008)

$$D_{AA*} = \frac{1}{3}\lambda u \tag{1.2}$$

u is the molar-average velocity of A, and λ is the mean free path, given by

$$u = \sqrt{\frac{8kNT}{\pi M_A}} \tag{1.3}$$

$$\lambda = \frac{kT}{\sqrt{2}\pi\sigma^2 P} \tag{1.4}$$

where M_A is the molecular weight of the diffusing species A, (g/mol); N is Avogadro's number; P is the system pressure; T is the absolute temperature (K); k is the Boltzmann constant; and σ is the Lennard-Jones diameter of the spherical molecules.

As shown in equations 1.2 and 1.4, normally diffusion occurs more intensively at high temperature (high mean molecular velocities) and at low pressures (lower

concentration of molecules, fewer collisions). The molar mass of the molecule also influences the rate of diffusion as light molecules move more rapidly than the heavy ones.

Molecular diffusion of a gas species in clear fluids (no porous media) can be described by Fick's first law

$$J = -D \frac{\partial C_g}{\partial_x} \tag{1.5}$$

where J is the mass flux of gas due to diffusion, D is the molecular diffusivity of the gas, C_g is the concentration and x is the distance. For application to porous media, Fick's first law is often modified by the introduction of a porous media factor β (Webb 2006; Datta 2007)

$$J = -\beta D \frac{\partial C_g}{\partial_x} \tag{1.6}$$

$$D_p = \beta D \tag{1.7}$$

where J is the mass flux of gas due to diffusion in porous medium, D_p is the molecular diffusivity of the gas in porous medium, D is the molecular diffusivity in bulk. The β factor is defined as

$$\beta = \frac{\phi}{\tau} \tag{1.8}$$

ϕ is the porosity, and τ is the tortuosity. Tortuosity can be defined as the ratio between the actual path traveled by a fluid element between two points divided by the straight line path between the same two points. The tortuosity factor is evaluated for diffusion, not advection. For all gas condition, the tortuosity is given (Webb 2006)

$$\tau = \phi^{1/3} \tag{1.9}$$

1.3.2 Knudsen diffusion

Knudsen diffusion takes places in porous system and is dominant compared with molecular diffusion when the mean pore diameter of a porous medium is smaller than the

mean free path of gas molecules (Fen et al. 2011). In many applications involving gas transfer in mesoporous materials, Knudsen diffusion is the predominant transport mechanism. Because of the collision between molecule and wall during Knudsen diffusion, the pore toughness would affect the diffusion.

For Knudsen diffusion, mean free path length is replaced with pore diameter d_{pore}, as species A is more likely to collide with the pore wall as opposed with another molecule. Thus the Knudsen diffusivity of diffusing species A, D_{KA} is (Webb 2006; Welty et al. 2008)

$$D_{KA} = \frac{1}{3} d_{pore}\, u = \frac{1}{3} d_{pore} \sqrt{\frac{8kNT}{\pi M_A}} \tag{1.10}$$

1.3.3 Surface diffusion

The particle migration in the adsorbed state (in the potential field of adsorption) is called surface diffusion. Unlike bulk diffusion, during which there is no interaction between the particles and the inner walls of the pores (except perhaps collisions), particles adsorb on these walls and diffuse on the surface while being adsorbed during surface diffusion. The macroscopic surface diffusion flux J_s is usually related to the gradient of the surface concentration $\frac{\partial C_s}{\partial_x}$

$$J_s = -D_S \frac{\partial C_s}{\partial_x} \tag{1.11}$$

where D_s is surface diffusivity. The D_s is dependent on many parameters, including surface concentration, amount of adsorbent in pores, heterogeneity of the surface and temperature, which make the study of surface diffusion very complicated (Medved and Cerny 2011).

1.3.4 Convective flow of gases due to gas pressure

Transport of gases in a porous material due to pressure can be described by Darcy's law, which simply states that the gas Darcy velocity, u_g, is directly proportional to the gas-phase pressure gradient $\frac{\partial p}{\partial x}$, and the gas-phase permeability, k_g. Darcy's law can be written as (Webb 2006).

$$u_g = - \frac{k_g}{\mu_g} \frac{\partial p}{\partial x} \tag{1.12}$$

where μ_g is gas-phase viscosity. In terms mass flux (F_g), the equation is

$$F_g = - \rho_g \frac{k_g}{\mu_g} \frac{\partial p}{\partial x} \tag{1.13}$$

where ρ_g is the density of the gas. The gas-phase permeability, k_g is a proportionality constant that is usually experimentally determined with unit of square length.

Besides the above-mentioned mechanisms, capillary condensation and molecular sieving could also be involved when the pore size is small enough. Figure 1.12 illustrates the relation between pore size and possible involvement of mass transfer mechanism for the special case of a cylindrical pore (Cussler 2009). In the simplest case, shown at the top of the figure, a pressure drop along the pores causes a convective flow (viscous flow or Darcy's flow). In the second case, where there is no pressure drop but a concentration difference, transport occurs by diffusion. When mesopores (2-50 nm) are present, the mass transport may involve gas diffusion where the gas molecules collide more often with the pore walls than with other gas molecules (Knudsen diffusion). In other cases, gas molecules may absorb on the walls and then diffuse (surface diffusion), or condense within the pores and move as a liquid (capillary condensation). When the pores are of molecular dimensions, one solute may dissolve in solvent held in liquid-filled pores and then diffuse by a "diffusion-solubility mechanism".

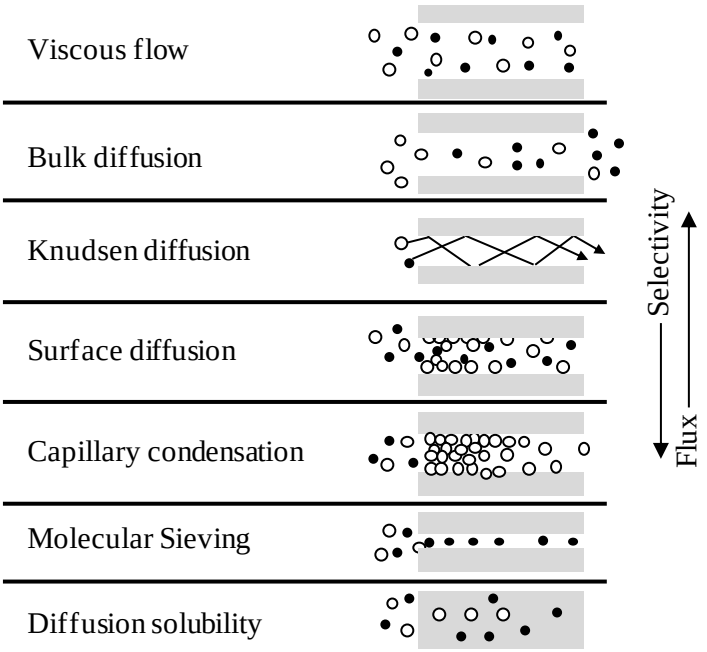

Figure 1.12- The effect of pore size on the changes of basic transport mechanism. The pore size drops from the top of the figure to the bottom. The selectivity is often larger for smaller pores. Compiled from Cussler (2009)

CHAPTER 2 : RESEARCH OBJECTIVES

Staleness in coffee is defined as “a sweet but unpleasant flavour and aroma of roasted coffee” due to oxidation of many pleasant volatiles and the loss of others (Buffo and Cardelli-Freire 2004). Coffee staling takes its origin from the roasting process. As a result of complex reactions that take place during roasting, the coffee beans are transformed into a very unstable system due to the reactive compounds formed and the porous structures created (Schenker 2000; Anderson et al. 2003; Illy and Viani 2005). Therefore, rapid packaging of coffee after roasting is critical to prevent oxidative degradation and loss of aroma compounds.

However, the residual CO_2 present in the beans after roasting must be degassed adequately before packaging, without which the package will swell, straining the seals and potentially compromising the structural integrity. In the worst-case scenario, catastrophic failure may occur. CO_2 degassing from roasted coffee beans is a slow process (Illy and Viani 1995), during which the coffee beans are susceptible to quality deterioration due to the loss of volatile compounds and oxidation. It was reported that approximately 10% loss in shelf-life was resulted for every 24 h coffee holding at room temperature in the air (Cardelli and Labuza 2001). Alternatively, one-way pressure relief valve can be attached to the package, allowing the CO_2 to be released as the interior pressure builds up to a threshold level. However, this approach will add cost to the packaging, and the valve may not function as expected due to sudden perturbation of internal pressure during product handling. Therefore, to maximize the shelf-life and quality of roasted coffee, the CO_2 degassing will need to be optimized, which requires deeper understanding of the generation of CO_2 and its degassing kinetics. This information will also be useful in optimizing the design of pressure relief valve for coffee packaging.

Based on the literature, it is clear that temperature and time are critical determinants of the physiochemical properties of the resulting roasted coffee, including the amount of CO_2 formed and its degassing kinetics. The substantial amount of CO_2 formed during roasting is fundamentally related to the precursor compounds. In the literature, generally it is recognized that CO_2 is formed as a result of Strecker degradation, Maillard reaction, and pyrolysis reactions. Also, it has been implicated that CGA could be the principal CO_2 precursor by a number of researchers (Small and Horrel 1993; Clarke and Vitztbum 2001), on the basis of (1) green coffee beans contain large amounts of CGA found in plants, ranging from 3-12%; (2) substantial loss of CGA during the roasting process of coffee has been previously reported; (3) CGA has a melting point of 207-209 °C which is below the normal coffee roasting temperature; and (4) the existence of carbonyl group in CGA makes it possible to form CO_2 by decarboxylation. However, to date, there is no detail work reported on the origin of CO_2.

The first objective of this research is to understand the effect of roasting temperature-time conditions on the residual CO_2 amount and its degassing behavior in the target product. The second objective is to investigate if CGA is the principal CO_2 precursor in order to elucidate CO_2 formation mechanism in coffee. In order to achieve these objectives, the following studies were undertaken:

(1) To study the effect of roasting temperature-time conditions on residual CO_2 content and some physiochemical properties of roasted coffee.

(2) To investigate the effect of roasting temperature-time conditions on CO_2 degassing behavior in roasted coffee beans and ground coffee.

(3) To study the effect of environmental temperature and relative humidity on CO_2 degassing behavior in roasted coffee beans.

(4) To determine the CGA thermal degradation properties and the formation of CO_2

from CGA thermal degradation under typical coffee roasting conditions.

(5) To study the formation of CO_2 from Maillard reaction by using glycine-sucrose model and to elucidate the contribution of green coffee components to CO_2 formation during roasting.

CHAPTER 3 : EFFECT OF ROASTING TEMPERATURE-TIME CONDITIONS ON CO_2 FORMATION AND PHYSICO-CHEMICAL PROPERTIES OF ROASTED COFFEE BEANS-A KINETICS STUDY

3.1 Introduction

Roasting is an essential process through which the characteristic flavour, color, aroma and structural properties of roasted coffee are developed (Dutra et al. 2001; Schenker et al. 2002; Baggenstoss et al. 2008). Green coffee beans are generally roasted at temperatures above 200°C using different temperature-time profiles to achieve various degrees of roast that are often determined by bean color, roast loss, organic roast loss, water content as well as formation of volatile compounds (Clarke and Vitztbum 2001; Dutra et al. 2001; Baggenstoss et al. 2008).

In general, coffee bean can be categorized into light, medium, and dark roast degrees, depending on the color developed after roasting. The color of roasted coffee is derived mainly from non-enzymatic browning reactions due to sugar caramelization and Maillard reactions. Caramelization involves dehydration of sugar that results in the formation of double bonds or anhydro rings, leading to a complex mixture of unsaturated polymeric compounds (Bemiller and Huber 2008). By contrast, in Maillard reactions, the carbonyl groups of reducing sugars react with free, uncharged amine groups of amino acids or protein to form brown polymers (Ajandouz et al. 2001). Typical sugar contents in Arabica and Robusta green coffees range from 6.2 to 8.4% and 0.9 to 4.8%, respectively (Clarke and Vitztbum 2001), while free amino acid contents range from 0.2 to 0.8%. Glutamic acid, aspartic acid and asparagine are the main amino acids found in green coffee beans (Belitz, Grosch, and Schieberle 2009). Maillard reactions are highly

temperature-dependent with activation energies ranging from 10-160 kJ/mol (Sikorski, Pokorny, and Damodaran 2008). Because Maillard browning reactions are diffusion-controlled, phenomena that alter the mobility of reactant molecules during roasting, such as glass transition, will affect the reaction kinetics (Lievonen, Laaksonen, and Roos 1998). In general, non-enzymatic browning reactions in food system followed zero- or first-order kinetics (Bhattacharya 1996; Özdemir 2000; Maskan 2001; Koca, Burdurlu, and Karadeniz 2007).

Besides inducing the desirable color changes, roasting also results in net losses of matter in coffee beans due to the evolution of water, CO_2, and volatile compounds. CO_2 is generally described as generating from Maillard reaction, Strecker degradation and pyrolysis reactions (Anderson et al. 2003; Buffo and Cardelli-Freire 2004; Geiger et al. 2005). A significant fraction of CO_2 produced during roasting is trapped within the coffee matrix, which gradually releases into the packaging headspace during storage, potentially causing the package to deform or burst (Anderson et al. 2003; Illy and Viani 2005; Baggenstoss et al. 2007). Therefore, it is important to develop a thorough understanding of the relationship between residual CO_2 content and roast degree to predict the degassing requirement of roasted coffee products. Other volatile compounds are also produced during roasting due to Maillard and pyrolysis reactions. Several hundreds of volatile compounds have been identified for different varieties of roasted coffee. The sensory properties of these volatiles have been studied by many researchers (Semmelroch and Grosch 1995; Semmelroch and Grosch 1996; Mayer, Czerny, and Grosch 1999; Mayer, Czerny, and Grosch 2000; Munro et al. 2003; Akiyama et al. 2008).

In order to investigate the effect of roasting temperature-time conditions on CO_2 formation and physiochemical properties of roasted coffee, precise temperature control during roasting is highly required. Fluidized bed roasters, where coffee beans are exposed

to high velocity hot air that simultaneously heats and tumbles individual beans in the roast chamber, are being able to allow an easy and accurate control of the air temperature (Illy and Viani 2005; Baggenstoss et al. 2008).

The physicochemical changes of coffee, especially color, roast loss, CO_2 formation, and volatiles formation are highly complex. Although the effects of roasting on these parameters have been reported in the literature, systematic investigations of these parameters in an integrated study are lacking, especially under different temperature-time roasting conditions. In this section of study, a commercial fluidized bed roaster was modified by adding a temperature controller to allow the control of roasting temperature. The first objective of this section was to investigate the feasibility of the modified roaster on temperature control. Based on the effective control obtained, coffee was roasted under various roasting conditions to investigate the changes of those critical parameters of an Arabica coffee during the isothermal roasting and to elucidate the relationships between them.

3.2 Material and Methods

Brazilian Arabica green coffee beans (Strictly Soft grade) were supplied by Mother Parkers Tea & Coffee Inc. (Mississauga, ON, Canada). Initial moisture content of the beans, determined gravimetrically by the moisture analyzer (IR-50; Denver Instruments, Bohemia, NY, USA), was 7.8% (wet basis). Sodium hydroxide, tri-sodium citrate, sulfuric acid, Drierite desiccant column and Ascarite II NaOH coated silica gel were all purchased from Fisher Scientific International Inc. (Ottawa, ON, Canada). Supelco solid phase microextraction (SPME) fibers (coated with 50/30μm thick divinylbenzene/carbon/polydimethylsiloxane (DVB/CAR/PDMS)) and the manual holder were purchased from Sigma-Aldrich Corp. (St. Louis, MO., U.S.A.).

3.2.1 Roasting procedure and sample preparation

A modified commercial fluidized bed roaster (Fresh Roast SR 500 roaster, Fresh Beans Inc., UT., U.S.A.) was used for roasting coffee beans (Figure 3.1). The hot air temperature was controlled by using a microprocessor temperature process controller (Model CN 7200, Omega Engineering, Inc., Stamford, CT., U.S.A.). The air temperature was measured by a thermocouple (K-type) positioned in the roast chamber. To obtain the bean core temperature, a small hole was drilled into the core of representative green beans, into which fine gauge thermocouples were inserted and affixed with epoxy glue. The beans were placed in the roast chamber, along with the green beans to be roasted such that they tumbled freely with other beans during roasting. Four hot air temperatures (220, 230, 240 and 250°C) were investigated during roasting experiments. Figure 3.2 shows a typical hot air and bean core temperatures at 240°C set point.

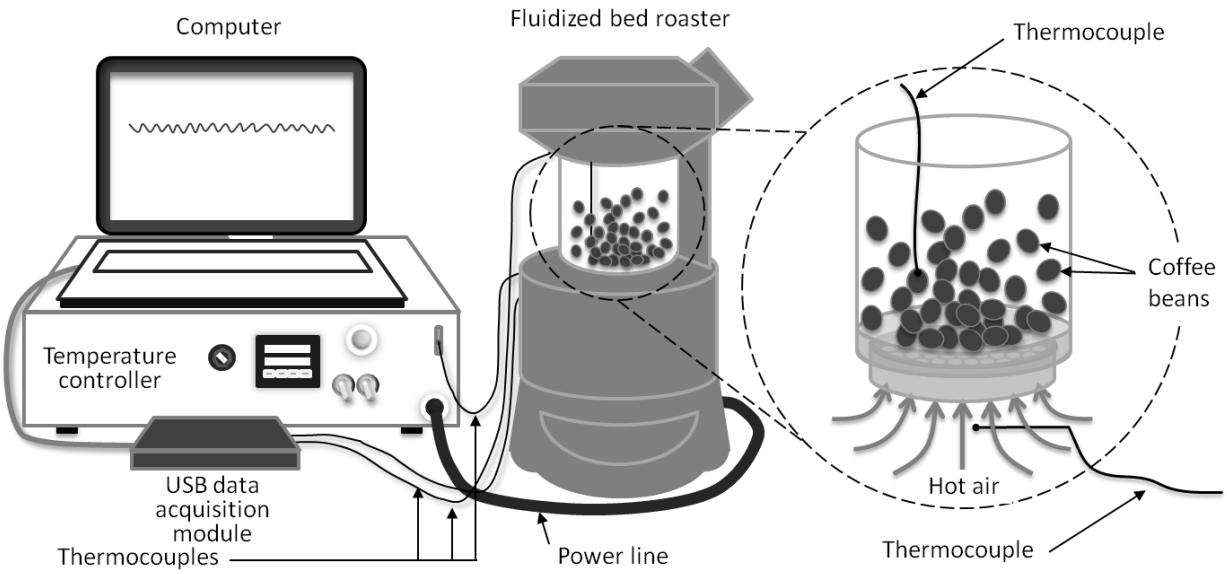

Figure 3.1- Modified commercial fluidized bed roaster showing various components and positions of thermocouple.

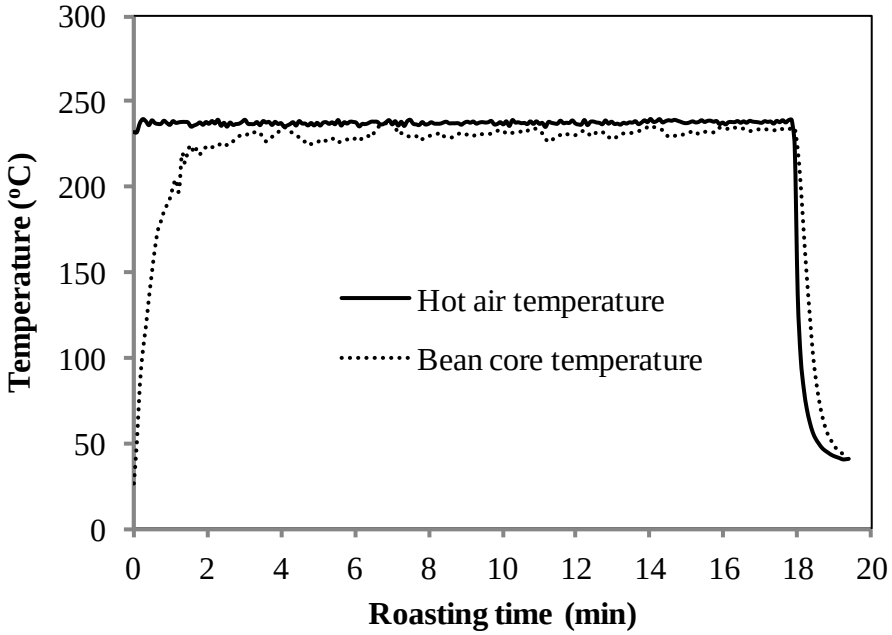

Figure 3.2- Air and bean core temperatures at 240°C roasting temperature set point, showing the effective control of the apparatus in Figure 3.1 on roasting temperature.

To roast the coffee bean, 30 g of green beans were weighed and loaded into the roaster after the hot air reached the target temperature. The beans were roasted for predetermined times to achieve various roast degrees. At the end of roast, coffee beans were cooled quickly by switching off the heater while continuing to fluidize the beans within the roast chamber with cool air. When the air temperature was cooled down to 35°C, the roasted coffee was discharged and the weight was measured. Roasting experiments were carried out with three replicates for each sample. The roasted beans were stored in glass bottles at 4°C until analyzed.

3.2.2 Color measurement

The roasted coffee beans were ground into powders (espresso grind) using a burr grinder (BODUM® Inc., NY, USA) and the lightness values were determined using Konica Minolta CM-3500d spectrophotometer in reflectance mode (Konica Minolta

Sensing, Inc., Osaka, Japan). Before the measurement, the white (L^*=100) and black calibrations (L^*=0) were conducted using the reference standards. The glass Petri dish containing ground coffee was placed under a target mask (30 mm diameter measurement area) and the *CIE* (International Commission on Illumination) L^*, a^*, b^* values were measured. Measurements were repeated four times for each sample by reloading it to the Petri dish. The means were reported.

3.2.3 Roast loss

Weight difference between the green coffee and the corresponding batch of roasted sample from three roasting experiments was measured immediately after cooling. Roast loss (RL) was calculated as follows:

$$RL = \frac{m_{green} - m_{roast}}{m_{green}} \times 100\ (\%) \qquad \text{(Eq. 3.1)}$$

where m_{green} (g) and m_{roast} (g) are weights of green and roasted coffee beans, respectively.

3.2.4 Residual CO_2 content

Residual CO_2 contents retained in coffee beans after roasting were determined gravimetrically by the apparatus in Figure 3.3 (Shimoni and Labuza 2000; Anderson and others 2003). The CO_2 in the coffee was extracted and trapped by mixing the coffee with an alkali tri-sodium citrate solution (50 g/L tri-sodium citrate in 0.25 M NaOH). The solution was then added to a distillation flask connected to a condenser. Sulfuric acid solution (2.5 M) was added to the flask to react with carbonate, thereby releasing the CO_2. A stream of nitrogen was bubbled into the solution to aid the releasing of CO_2. A column of Drierite desiccant was attached to the exit port of the distillation flask to remove moisture. Another column of Ascarite II (NaOH coated silica gel) was connected in series with the Drierite column to trap the dried CO_2. To aid the complete releasing of CO_2, the

flask was heated to 60°C. After one hour, the weight increase of Ascarite II column was recorded and converted to milligram CO_2 per gram roasted coffee beans (mg/g). Triplicate samples were analyzed and average CO_2 content was recorded.

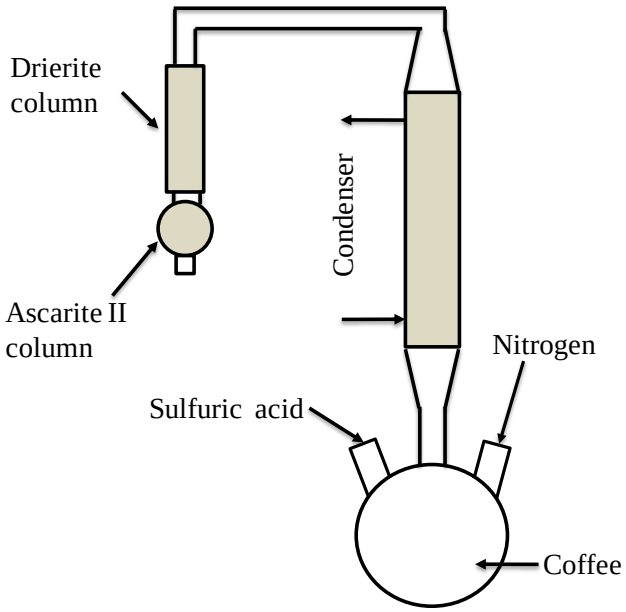

Figure 3.3- Apparatus for measuring the residual CO_2 content in roasted coffee beans and ground coffee.

3.2.5 Volatile compounds analysis

The SPME fiber was conditioned at 270°C for 1 h in the GC injector port before using. Five grams of roasted coffee bean were hermetically sealed in a 25 mL vial and equilibrated at 25°C for 48 h. To sample the headspace volatiles, the fiber was firstly conditioned in the GC injection port at 240°C for 5 min and then withdrawn from the injection port and exposed to the headspace of the vial for 30 min to adsorb the volatile compounds. The analyses were performed on the Angilent-6890 GC-FID system fitted with HP-wax capillary column (30m×0.25mm×0.25μm). The fiber was thermally desorbed for 5 min in the 0.75 mm i.d. liner in a splitless mode. Other chromatographic conditions were as follows: injector temperature, 240°C; FID temperature, 230°C; and H_2

carrier gas flow rate, 1 mL/min. The oven temperature was initially maintained at 35°C for 5 min, then raised to 220°C at 5°C/min ramp, and finally held for 5 min. Chromatogram peaks were integrated using HP Chemstation software (Agilent Technologies). Three measurements were repeated for each sample.

Identification of the compounds obtained from the above GC-FID analysis was performed on a Trace GC Ultra gas chromatographer equipped with a DSQ mass spectrometer (Thermo Electron Corporation, San Jose, CA, USA) fitted with the same column and operated under the same chromatographic conditions as the GC-FID in addition to helium used as the carrier gas. The detector transfer line and ion source temperature were 250 and 200°C, respectively. Electron impact ionization was used at voltage of 70 eV, and the m/z range of 45-300 was collected at 500 amu/s. GC-MS data treatment was carried out using the Xcalibur software (Thermo Electron Corporation) in conjunction with the US national Institute of Standard and Technology mass spectral library. Compounds were matched with FID chromatograms based on chromatogram peak similarities and comparisons with previous studies on the volatile compounds of roasted coffee (Bicchi et al. 1997; Mondello et al. 2004; Ribeiro et al. 2009).

3.2.6 Model fitting

Non-enzymatic browning reactions in food systems generally followed zero-or first-order kinetics. To analyze the kinetics of lightness and roast loss during roasting, the following equations were fitted to the L^* and RL data.

$$L^* = L^* - kt \quad \text{(Eq. 3.2)}$$

$$L^* = L^*_0 \cdot e^{-kt} \quad \text{(Eq. 3.3)}$$

$$L^* = (L^*_0 - L^*_\infty)\, e^{-kt} + L^*_\infty \quad \text{(Eq. 3.4)}$$

$$RL = RL_0 + kt \quad \text{(Eq. 3.5)}$$

$$RL = RL_0 \cdot e^{kt} \quad \text{(Eq. 3.6)}$$

$$RL = RL_\infty - (RL_\infty - RL_0)\, e^{-kt} \quad \text{(Eq. 3.7)}$$

where L^* and RL are the lightness and roast loss of coffee at roasting time t (min); L^*_0 and RL_0 are the lightness and roast loss when t=0, respectively; k is the rate; L^*_∞ and RL_∞ are lightness and roast loss of coffee at infinity roasting time.

Temperature dependence of the rate constant was modeled by Arrhenius equation:

$$k = k_0 \cdot e^{-Ea/RT} \quad \text{(Eq. 3.8)}$$

where E_a is the activation energy (kJ/mol), k_0 is the pre-exponential factor, R is the universal gas constant (8.314 $J \cdot mol^{-1} \cdot K^{-1}$), and T is the absolute temperature (K). The goodness of fit of the model to the data was evaluated by the coefficient of determination (R^2) and mean square error (MSE). The regression analysis was conducted using SPSS Statistics 17.0 (IBM Corporation, Armonk, New York, U.S.A.) and Excel spreadsheet package (Microsoft Corporation, Redmond, Washington, U.S.A.).

3.3 Results and Discussion

3.3.1 Kinetics of color changes

L^* value has been used by researchers to evaluate the degree of roast in coffee (Schenker 2000; Schenker et al. 2002; Sacchetti et al. 2009). Figure 3.4 summarizes the changes in L^* values as a function of roast time, showing that the lightness value of coffee decreased with roasting time. As expected, the higher the temperature, the shorter the time taken to achieve the target degree of roast. For example, to achieve dark roast (L^* = 20), the required process times were approximately 80, 20, 11, and 5 min, when processed at 220, 230, 240 and 250°C, respectively. Reducing the air temperature to 200°C only allowed for the development of light roast but did not produce any darker

beans (data not shown). These findings are consistent with those reported by Schenker (2000).

The kinetic data were initially fitted with first-order equation (Eq. 3.4), which provided a reasonable fit, judging from the high R^2 (>0.98) and low MSE values (0.522 to 2.722). However, closer inspection of the kinetics data revealed that although the equation fitted well with the initial phase of color change, it levelled off quickly to an asymptote instead of following the decreasing *L** trend as time increased (data not shown). From Figure 3.4, it is evident that the changes of *L** value followed a two-stage phenomenon. Therefore, the kinetics data were divided into 1^{st} and 2^{nd} stage regimes, and were fitted separately with the first-order equation (Eq.3.3). The two regimes were well described by the first-order model, with R^2 values ranging from 0.723 to 0.993, and MSE from 0.845 to 6.296 (Table 3.1). The two-stage data were also fitted with the zero-order reaction model (Eq. 3.2), which gives R^2 values ranging from 0.703 to 0.972, and MSE from 0.100 to 16.108 (Table 3.1). Accordingly, the first-order equation (Eq. 3.3) was used for the subsequent analyses.

As temperature increased from 220 to 250°C, the rate constant values increased from 0.159 to 0.372 min^{-1} and from 0.004 to 0.046 min^{-1} for the first and second stages, respectively. From the Arrhenius plot (Figure 3.5), the activation energies for the first and second stage were 59.7 and 170.2 kJ/mol, respectively. These results show that the rate of change in lightness during the later phase of roasting was more sensitive to temperature, than the first stage. The decreased rate of change for *L** value in the second stage was likely due to the decreased moisture content in the beans that slowed down the Maillard reactions. Moreover, as drying proceeded to the second stage, the bean matrices have probably undergone rubbery-to-glassy state transition, thereby slowing down the rate of non-enzymatic browning (Bell 1996; Lievonen, Laaksonen, and Roos 1998; Craig et al.

2001). In addition, low molecular weight carbohydrate (mainly sucrose) degraded quickly into glucose and fructose and entered into browning reactions mainly in the initial stage of roasting. This is consistent with sucrose losses in the literature for light and dark roast coffee, which are about 97% and 99%, respectively (Clarke and Vitztbum 2001). Because of the depletion of low molecular weight carbohydrate, the degradation of polysaccharides becomes the main source of sugar for non-enzymatic browning in the later stage of roasting. Accordingly, the degradation of polysaccharides might have become the rate-limiting step during the second stage, resulting in higher temperature dependence than the initial stage of roasting.

Roast coffee beans were ground and compared to industry standard color disks for roast classification established by Specialty Coffee Association of America (SCAA). It was found that L^* values of 30, 25 and 20 corresponded approximately to light, medium, and dark roast degrees (horizontal dotted lines in Figure 3.4). As shown, the transition from the first to second stage occurred when the coffee samples reached to around the medium roast, indicating that this transition is an important milestone in determining the darkness development during the roasting process.

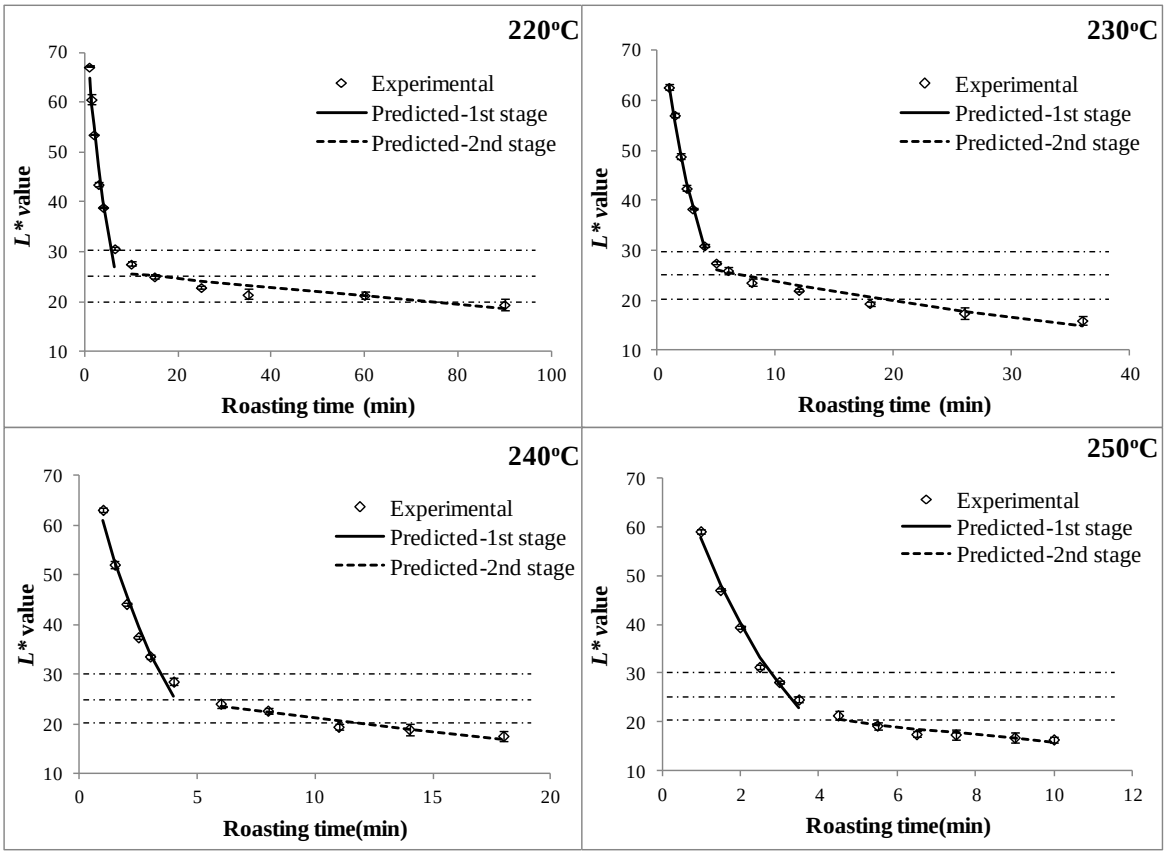

Figure 3.4- Kinetics of L^* value changes of coffee beans roasted at temperature of 220, 230, 240 and 250°C. Within each figure, the top, middle and bottom horizontal dotted lines indicate lightness values corresponded to light, medium and dark roast degrees, respectively. The roast degrees were determined by visually comparing the color of coffee grounds with industy standard disks established by Specialty Coffee Association of America (SCAA). Predicted plots are derived from first-order kinetics model (Eq. 3.3).

Table 3.1- Estimated equation parameters, coefficient of detemination (R^2) and mean square errors (MSEs) obtained by fitting Eq. 3.2, 3.3 and 3.4 to L^* values.

T, °C	Zero-order (Eq. 3.2)								First order (Eq. 3.3)							
	1st stage				2nd stage				1st stage				2nd stage			
	k	L^*_0	R^2	MSE	k	L^*_0	R^2	MSE	k	L^*_0	R^2	MSE	k	L^*_0	R^2	MSE
220	6.456	68.482	0.899	16.018	0.084	26.272	0.722	2.108	0.159	75.864	0.960	6.296	0.004	26.664	0.747	1.912
230	10.838	72.109	0.972	3.311	0.353	27.402	0.880	1.946	0.245	80.669	0.993	0.845	0.018	28.555	0.917	1.358
240	11.328	69.536	0.916	11.494	0.543	26.690	0.840	1.026	0.293	81.831	0.974	3.532	0.028	27.881	0.860	0.890
250	13.559	68.771	0.946	7.717	0.806	23.878	0.703	0.100	0.372	83.914	0.988	1.715	0.046	25.090	0.723	0.930

First order (Eq. 3.4)				
Combined 1st and 2nd stages				
k	L^*_0	L^*_∞	R^2	MSE
0.322	83.178	22.392	0.989	2.722
0.398	85.180	18.952	0.989	2.482
0.467	88.719	19.465	0.980	4.083
0.660	98.792	16.630	0.997	0.522

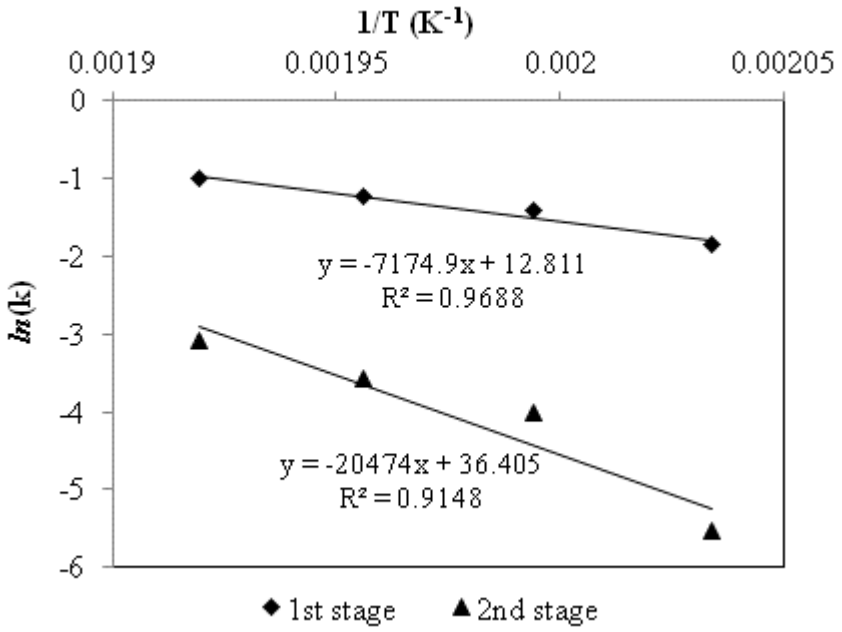

Figure 3.5- Arrhenius plots of rate constant for *L** evolution, showing different activation energies for first and second stage roasting processes.

Besides *L** value, the corresponding changes in *a** and *b** value were also recorded (Figure 3.6). Positive and negative *a** indicates red and green colors, respectively. On the other hand, positive and negative *b** indicates yellow and blue colors. Both *a** and *b** values increased rapidly during early stage of roasting to +15 and +30 maxima, respectively, indicating that there was a concomitant increase in red and yellow colors. The changes in visual color for coffee beans at different roasting temperature-time conditions are presented in Figure 3.7. As shown, yellow color is evident during the early stage of roasting. As the roasting proceeded, both *a** and *b** values decreased asymptotically to about +6, showing that all beans stabilized to the same hue regardless of the four roasting temperatures used.

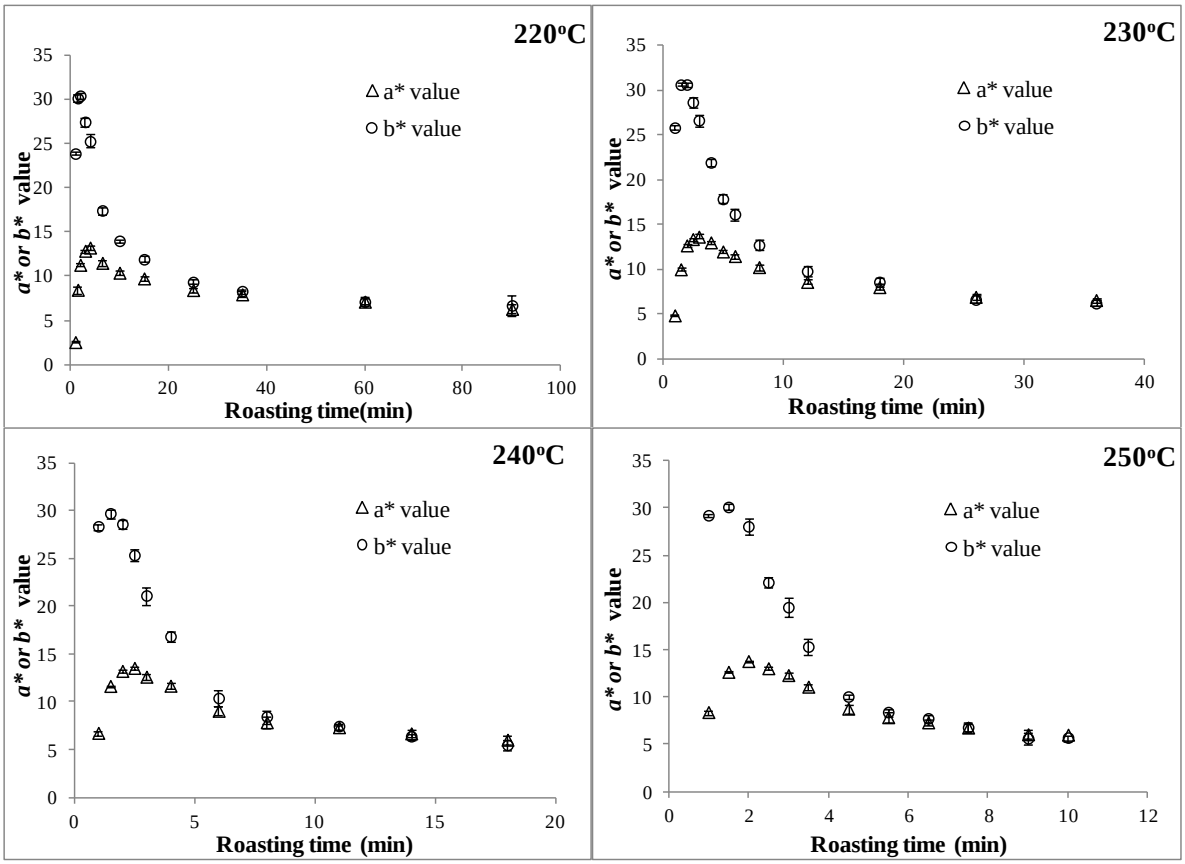

Figure 3.6- Kinetics of *a** and *b** value changes of coffee beans roasted at temperature of 220, 230, 240 and 250°C.

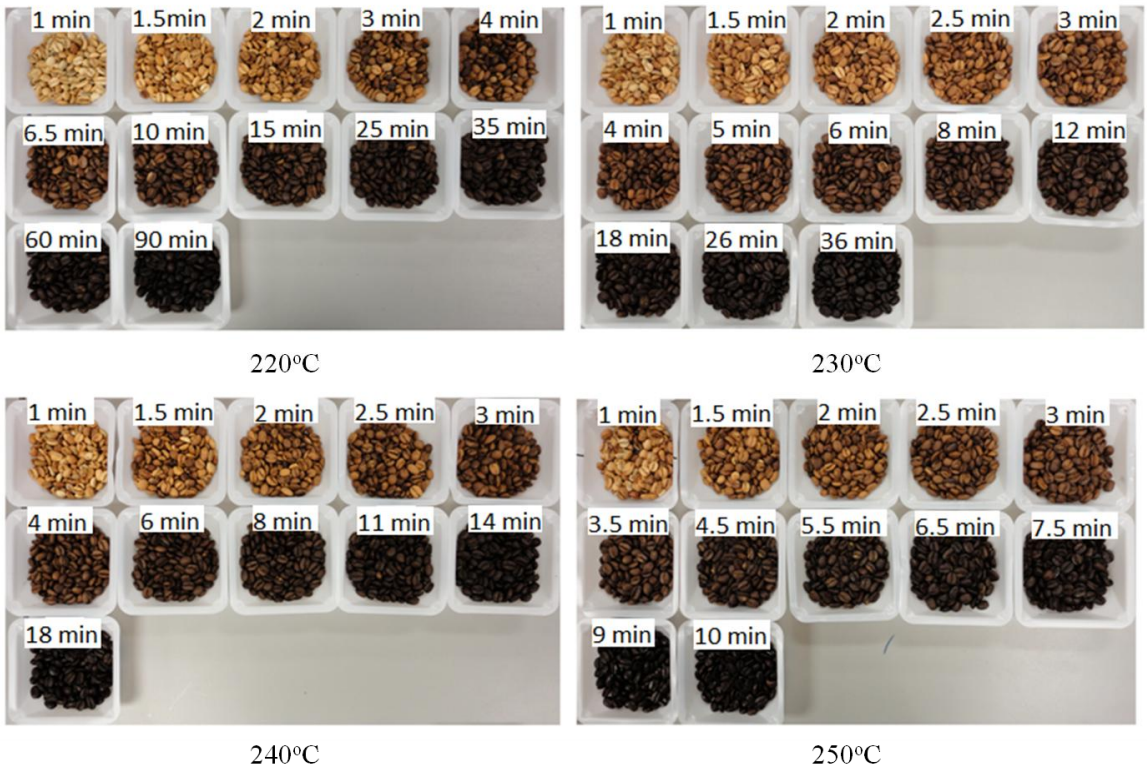

Figure 3.7- Color development of coffee beans roasted at 220, 230, 240 and 250°C for different roast times.

3.3.2 Kinetics of roast loss

Roast loss in coffee beans is mainly due to vaporization of water, formation of volatiles, and detachment of bean chaffs. This parameter is often used in conjunction with color to indicate the degree of roast in coffee (Schenker, 2000). In this study, rapid weight loss was observed during the initial stage of roast (Figure 3.8). As the beans were processed to ~15% roast loss level, a reduced rate of weight loss was observed. The 2-stage phenomenon suggested that there was a change in mechanism on the evolution of volatiles when the coffee beans reached ~15% roast loss level. The initial roast loss was predominantly caused by the rapid vaporization of water from the green beans. Since the initial moisture content of the green beans was 7.8% (wet basis), the weight loss must be also attributed to the evolution of CO_2 and other volatiles.

Similar to L^* kinetics data, although the first order kinetics model (Eq.3.7) fitted the RL data with high R^2 and low MSE value (Table 3.2), the model failed to describe the continual increasing trend when time is large (fitted plots not shown). Instead, the RL data were fitted with two separate zero-order kinetics model (Eq.3.5; Figure 3.7). As summarized in Table 3.2, the two-stage model resulted in R^2 ranging from 0.906 to 0.990 and MSE values from 0.079 to 0.508%, indicating its goodness of fit to the kinetic data. By comparison, the first-order equation (Eq.3.6) provided less accurate fit, resulting in R^2 and MSE values that were in the ranges of 0.881-0.972 and 0.090-1.245%, respectively (Fitted plots not shown). Therefore, the rate constants calculated from the zero-order model (Eq.3.5) were used for the activation energy determination. As temperature increased from 220 to 250°C, the rate constant increased from 1.778 to 3.946 %/min for the first stage, and from 0.070 to 0.991 %/min for the second stage. From the Arrhenius plot (Figure 3.9), the activation energies for the first and second stage were 53.49 and 184.15 kJ/mol, respectively, indicating that weight losses that occurred in the second stage were more temperature dependent than those in the first stage. Comparing Figures 3.4 and 3.8, it is evident that at any given temperature, the roast times at which the first-to-second stage transition occurred for both parameters were very similar. This observation suggested that L^* value and roast loss could be related.

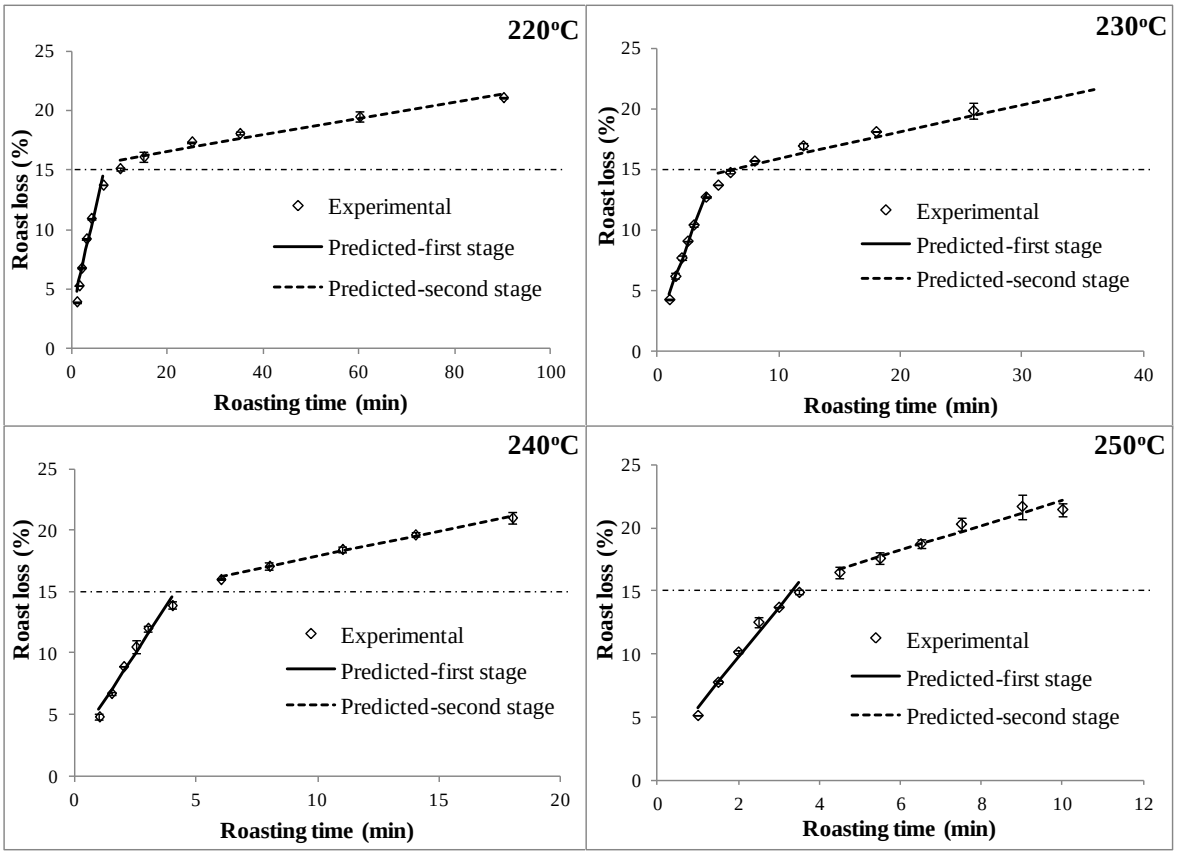

Figure 3.8- Kinetics of the roast loss for coffee beans roasted at 220, 230, 240 and 250°C. The horizontal lines indicate when the coffee beans attained the medium roast degree. Predicted plots are derived from zero-order kinetic model (Eq.3.5).

Table 3.2- Estimated equation parameters, coefficient of determination (R^2) and mean square errors (MSEs) obtained by fitting Eq. 3.5, 3.6 and 3.7 to RL values.

	Zero-order (Eq. 3.5)								First-order (Eq. 3.6)							
	1st stage				2nd stage				1st stage				2nd stage			
T, °C	*k*	RL_0	R^2	*MSE*	*k*	RL_0	R^2	*MSE*	*K*	RL_0	R^2	*MSE*	*k*	RL_0	R^2	*MSE*
220	1.778	2.955	0.955	0.508	0.070	15.150	0.945	0.223	0.173	4.714	0.881	1.345	0.004	15.391	0.929	0.284
230	2.785	1.913	0.990	0.079	0.221	13.632	0.932	0.409	0.299	4.012	0.944	0.424	0.012	14.053	0.908	0.554
240	3.066	2.332	0.968	0.303	0.415	13.700	0.980	0.064	0.287	4.673	0.906	0.886	0.022	14.271	0.972	0.090
250	3.946	1.825	0.972	0.327	0.991	12.286	0.906	0.370	0.348	4.703	0.917	0.974	0.050	13.448	0.891	0.426

First order (Eq. 3.7)				
Combined 1st and 2nd stages				
k	RL_0	RL_∞	R^2	*MSE*
0.165	1.967	18.900	0.968	0.968
0.221	1.183	19.485	0.980	0.523
0.272	0.514	20.128	0.988	0.327
0.316	-0.849	22.392	0.990	0.280

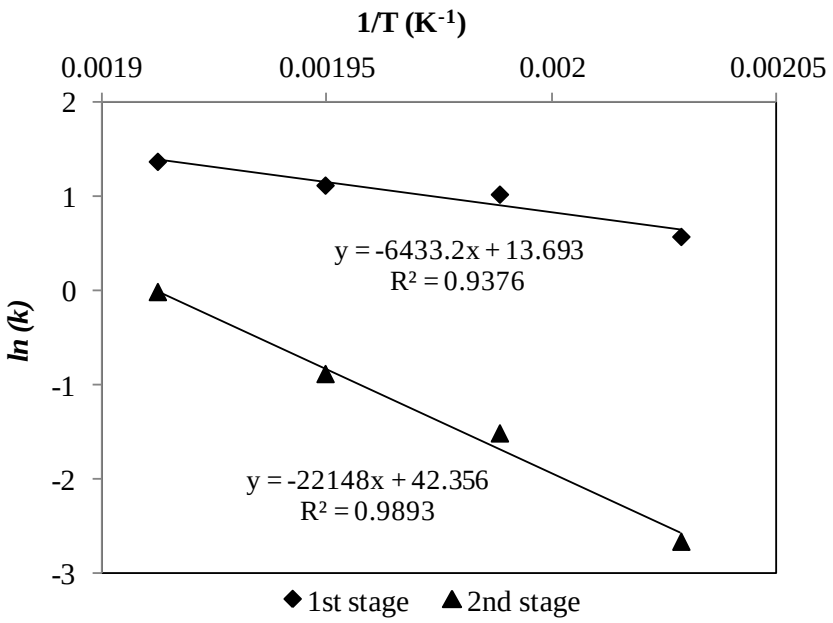

Figure 3.9- Arrhenius plots of rate constant of roast loss evolution, showing different activation energies for first and second stage roasting processes.

3.3.3 Changes in residual CO_2 content

Residual CO_2 contents in coffee beans roasted under different conditions are depicted in Figure 3.10a. As shown, the residual CO_2 contents increased with roast time to maximal values and then decreased to different levels at the end of the roast. The maxima observed for residual CO_2 (Figure 3.10a) was likely caused by the cracking of the coffee beans (commonly known to the industry as the "second crack"), as a result of pressure build up within the beans and the weakening of the cell wall structure due to pyrolysis of cellulose (Clarke and Vitztbum 2001; Redgwell et al. 2002; Illy and Viani 2005). The expanded bean microstructure after the second cracking might have allowed rapid degassing of CO_2, resulting in lower residual CO_2 contents. The maximum residual CO_2 content increased with increasing roast temperature, resulting in different CO_2 residual contents at the end of roast (~13.5 and 11.2 mg/g at 250 and 220°C, respectively). The lower residual CO_2 in beans roasted at lower temperature could be related to the larger amount of CO_2 evolved during roasting than those processed at higher temperature,

due to the longer roasting time involved in the former process. Since substantial microstructural changes occurred after the second crack, which will affect the residual CO_2, only the initial stage of roasting were fitted with zero-order kinetic model to get the CO_2 formation rate information. The rate constants followed the Arrhenius model well with activation energy of 96.6 kJ/mol (Figure 3.11).

The residual CO_2 was also plotted against L^* values to elucidate their correlation (Figure 3.10b). As shown, residual CO_2 content increased with roast degree, when the coffee beans were processed below the dark roast degree. At medium and dark roast degree, the residual CO_2 contents are ~11 and 15 mg/g, respectively. Furthermore, at any given L^* value, residual CO_2 content was not affected by roasting temperature, indicating L^* value could be used as an indicator of residual CO_2 content regardless of roasting conditions. This correlation is not unexpected because the color development and CO_2 formation are both due to browning reactions (e.g., Maillard, caramelization and pyrolysis reactions) taking place during coffee roasting. However, when processed beyond dark roast degree, a reversed correlation was observed, suggesting that lower amount of CO_2 would retain in the beans when processed beyond the second crack. This is probably due to more porous structure after second cracking which resulted in increased CO_2 loss during roasting.

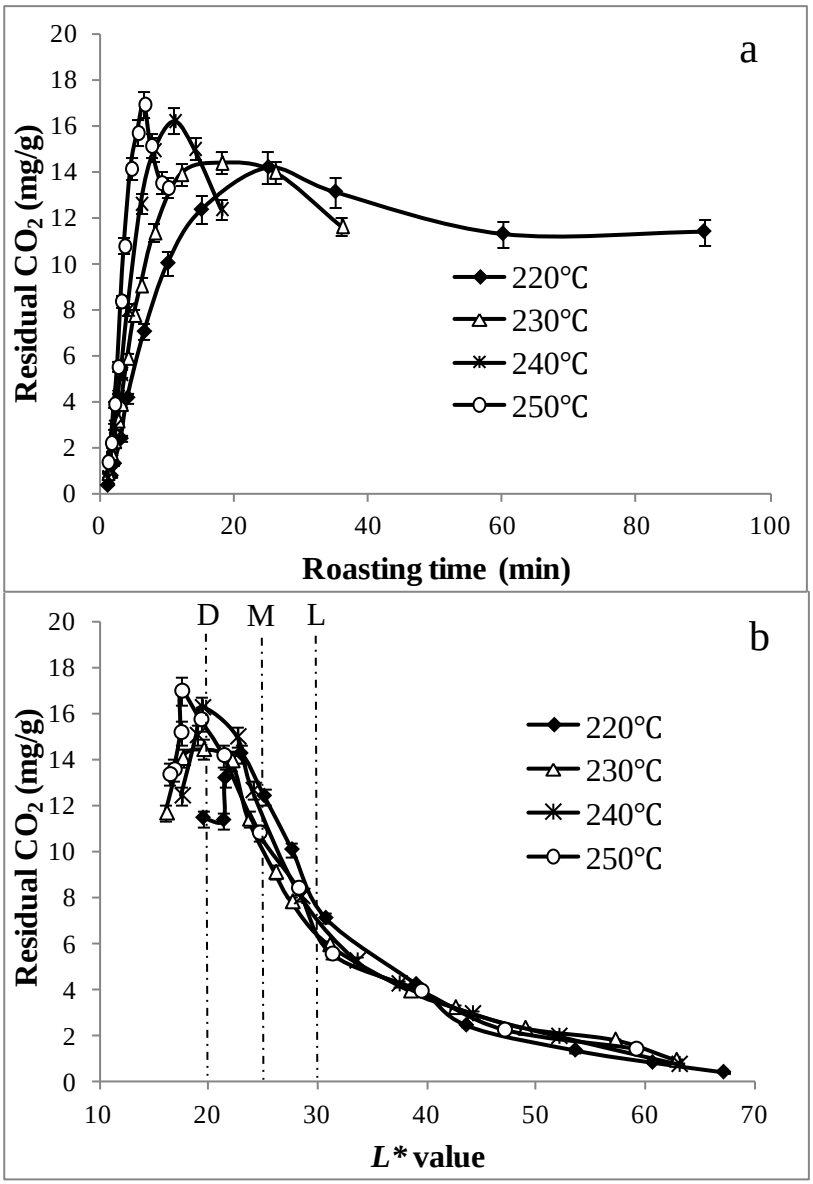

Figure 3.10- Residual CO_2 content at different roasting temperature-time conditions (a) and the plots between residual CO_2 with L^* value (b) (L: light roast; M: medium roast; D: dark roast).

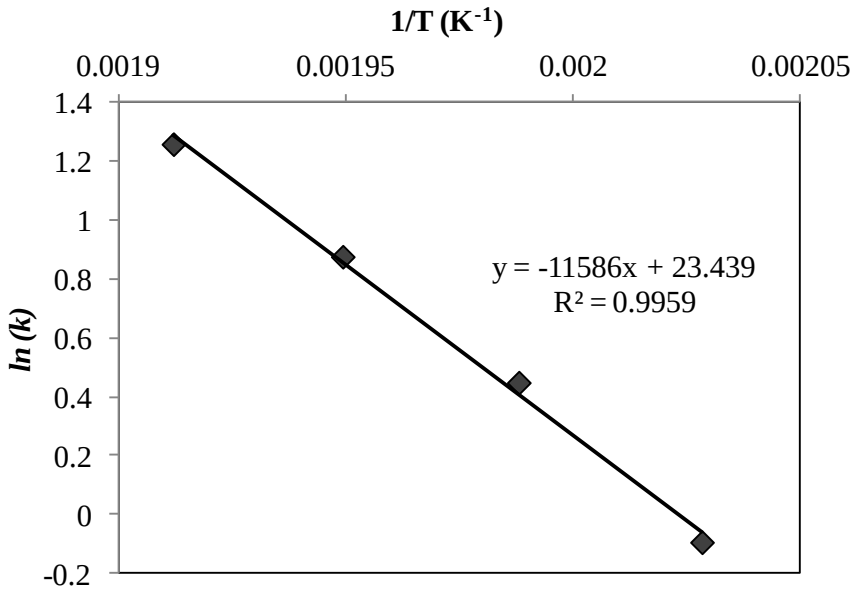

Figure 3.11- Arrhenius plots of rate constants, determined from zero-order kinetic models, for changes of residual carbon dioxide content during the initial phase of roasting.

3.3.4 Evolution of volatile compounds

One of the important events that occurred during the roasting of coffee beans is the formation of complex mixture of volatile compounds derived from Maillard and other pyrolysis reactions. Importantly, these volatiles contribute to the basic aroma characteristic of roasted coffee. Many previous studies on volatile compounds have been focused on the identification of aroma impact compounds (Semmelroch et al. 1995; Semmelroch and Grosch 1996; Mayer, Czerny, and Grosch 2000; Akiyama et al. 2008). In this study, the evolution of volatiles during roasting under different roasting temperatures was investigated. Figure 3.12 summarized the volatile profiles for coffee samples roasted at 220, 230, 240 or 250°C, reported as total peak area for 33 compounds detected (Table 3.3). As shown, bean roasted at higher roasting temperatures had higher rates and greater amounts of total volatiles formed than those processed at lower temperature.

Figure 3.13 shows the distribution of peak areas for the 33 volatile compounds. On the basis of *L** value, the peak area data were presented based on light, medium and dark roast degrees. As shown, the profiles of the volatile compounds were highly dependent on the roasting temperature. In general, at any given degree of roast, higher roasting temperature led to the formation of greater amounts of volatiles in the coffee beans, except peaks 6 (2-methylfuran), 11 (2,5-dimethyfuran), 12 (N/I), and 16 (pyridine), which showed an opposite trend. Moreover, peaks 6 (2-methylfuran) and 16 (pyridine) increased considerably as the coffee samples were processed to dark roast. These two compounds that may be related to the characteristic aroma of dark roast coffee were formed from Maillard browning reaction. To a lesser extent, peaks 18 (methylpyrazine), 30 (furfuryl acetate), 32 (dihydro-2(3H)-furanone) and 33 (2-furan ethanol) also exhibited a similar trend. By contrast, all other peaks tended to show smaller peak areas in dark roast as compared to the light roast counterpart, especially peaks 13 (2,3-butanedione), 14 (2,3-pentanedione), and 26 (furfural). These three compounds were generated at the beginning of roasting and their amount peaked at around L^*=30, followed by a rapid decrease when the beans were roasted to darker roast degrees. Moreover, higher amounts were generated at higher roasting temperatures (kinetics data not shown). This implies that high-temperature-short-time roasting could be desirable for increasing certain volatile compounds to increase the flavour complexity, especially when the coffee beans were to be processed to dark roasts.

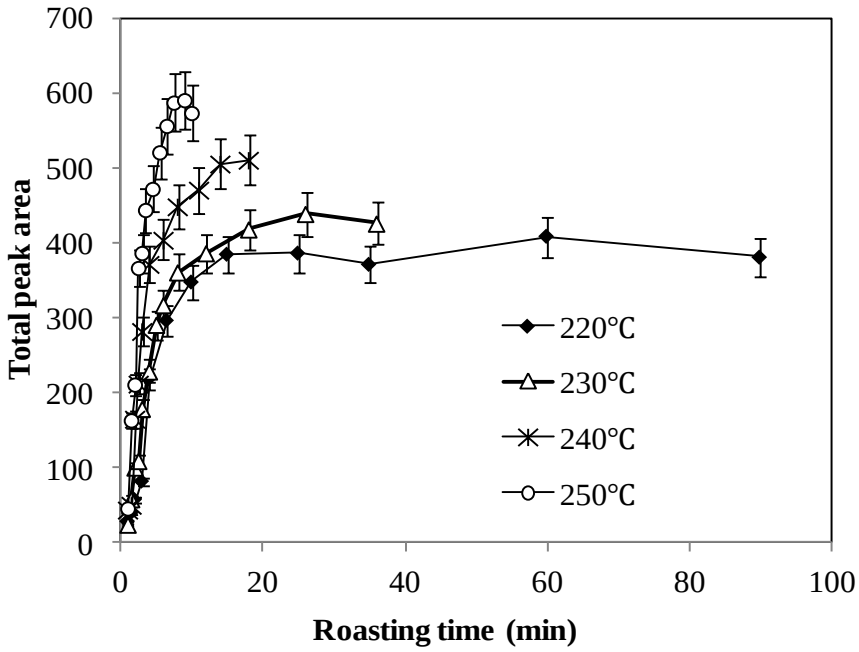

Figure 3.12- Changes of total peak area of coffee volatiles chromatogram with roasting time at roasting temperatures of 220, 230, 240 and 250°C.

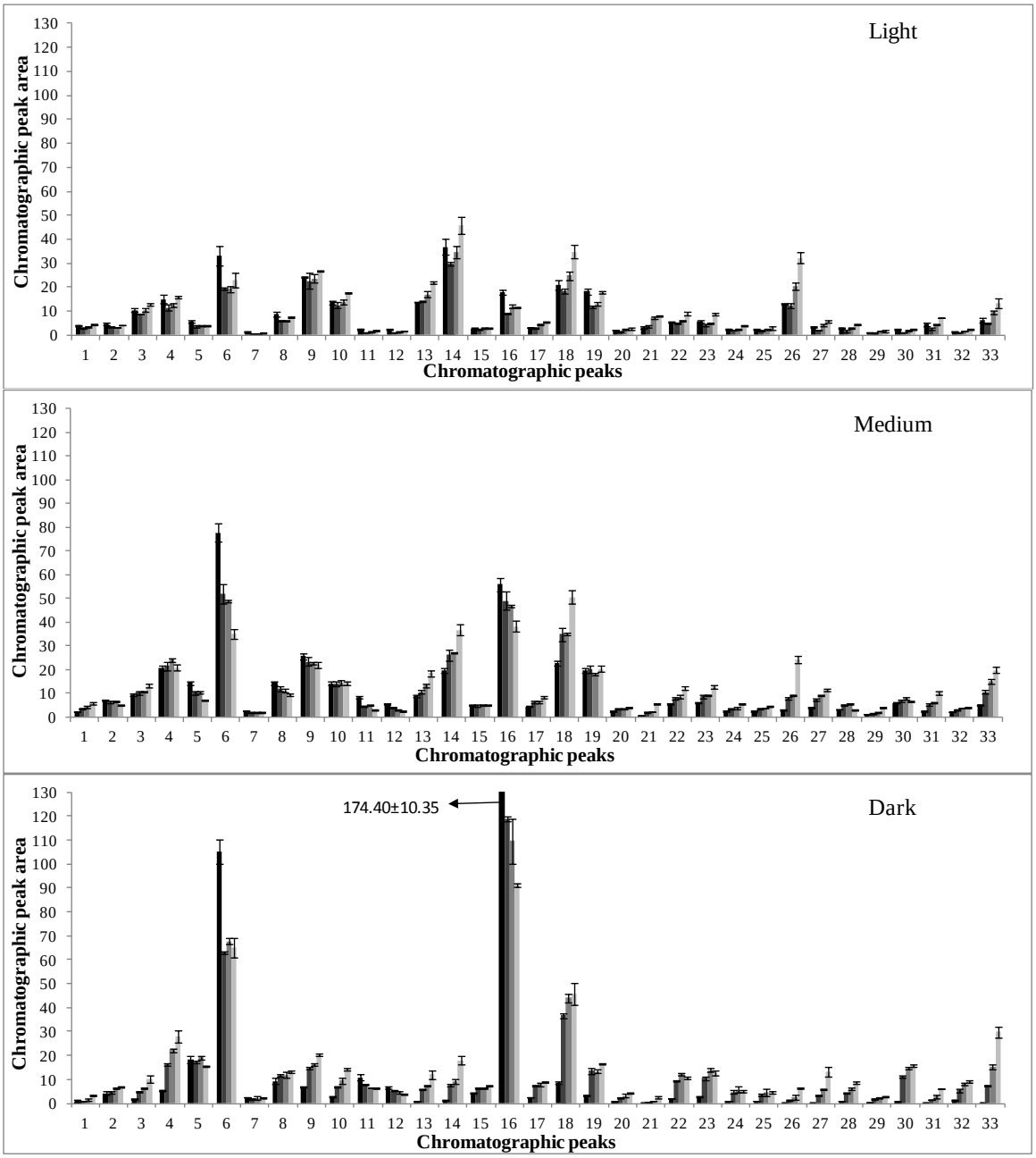

Figure 3.13- Volatile profiles, as indicated by chromatographic peak areas from SPME analysis, for light, medium and dark roasted coffee beans processed at different roasting temperatures (■: 220°C, ■: 230°C, ■: 240°C, ■: 250°C). Horizontal axis indicates 33 chromatographic peaks following the sequence of elution.

Table 3.3- Peak identification of 33 volatile compounds in Figure 3.13

Peaks	Compounds	Peaks	Compounds
1	1,3-pentadione	18	Methylpyrazine
2	N/I	19	N/I
3	Furan	20	2-butanone
4	N/I	21	2-propanone
5	N/I	22	2,5-dimethylpyrazine
6	2-methylfuran	23	2,6-dimethylpyrazine
7	3-methylfuran	24	Ethylpyrazine
8	Pentanedial	25	2,3-dimethylpyrazine
9	2-methylbutanal	26	Furfural (Furaldehyde)
10	3-methylbutanal	27	1-hydroxyl-2-propanone acetate
11	2,5-dimethyfuran	28	Furfurylformate
12	N/I	29	Pyrrole
13	2,3-butanedione	30	Furfury acetate
14	2,3-pentanedione	31	5-methyl-2-furaldehyde
15	1-methyl pyrrole	32	Dihydro-2(3H)-furanone
16	Pyridine	33	2-Furanethanol
17	Pyrazine		

N/I: not identified

3.4 Conclusions

Firstly, this study showed that the developed roasting apparatus could effectively control the roasting temperature. By studying the changes in color, roast loss, volatile compounds, and residual CO_2 at different roasting temperatures, this study provided an enhanced understanding of the physicochemical changes that occur in coffee beans during isothermal roasting. Kinetics studies of L^* value and roast loss, which are two of the most commonly used roast degree indicators, revealed that the coffee bean roasting process could be separated into two stages. The transition between these two stages was found to occur when the beans attained the medium roast degree. Residual CO_2 content increased with the roast degree until dark roast, after which lower values were determnied. In addition, it was found that residual CO_2 content was independent of the roasting temperature applied before attaining dark roast degree, which makes L^* a reliable indicator of residual CO_2 content. The effects of time-temperature on the formation of volatiles in coffee are highly complex and their formation was superimposed by an accelerated decay of some aroma compounds during the final roasting stage. The volatile profiles of the roasted coffee beans was not only dependent on the roast degree, but also on the temperature used during the roasting process, implying that coffee flavours will vary with the time-temperature profile used.

CHAPTER 4 : EFFECT OF ROASTING TEMPERATURE-TIME CONDITIONS ON CO_2 DEGASSING BEHAVIOUR IN ROASTED COFFEE

4.1 Introduction

Green coffee beans are normally roasted above 200°C to develop the characteristic flavour, color, aroma, and structure of roasted coffee beans (Schenker et al. 2002; Yeretzian et al. 2002; Baggenstoss et al. 2008; Moon and Shibamoto 2009). As a result of the roasting process, CO_2 is produced that accounts for more than 80% of the gases formed (Clarke and Macrae 1987; Geiger et al. 2005). By and large, the formation of CO_2 in roasted coffees is attributed to Maillard, Strecker, and pyrolysis reactions (Shimoni and Labuza 2000; Anderson et al. 2003; Geiger et al. 2005).

During the roasting process, the formations of CO_2 and other volatile compounds result in an increased internal pressure, causing the beans to expand and eventually crack (Schenker et al. 2000; Clarke and Vitztbum 2001). A typical roasting process can cause the beans to swell 40~60% at about 20% roast loss (Illy and Viani 1995). The porous structure developed, which is dependent on the roasting temperature-time conditions applied, determines the residual CO_2 content after roasting, as well as the subsequent mass transport phenomena that occurs during storage (Illy and Viani 1995; Schenker 2000; Clarke and Vitztbum 2001; Geiger et al. 2005). The expanded porous matrices of roasted coffee beans are made up of evacuated cells with a framework of cell walls. The evacuated cells, with a diameter of 20-40 μm, can be regarded as macropores based on the pore size classification of International Union of Pure and Applied Chemistry (Schenker et al. 2000; Anderson et al. 2003). These macropores are the main contributors to the porosity of roasted coffee beans. Porosity values

of roasted coffee beans varies from 0.474-0.738 depending on the measurement technique used and roasting conditions (Schenker et al. 2000; Shimoni and Labuza 2000). Part of the residual CO_2 is believed to be trapped within these evacuated cells as occluded gas, which is in equilibrium with absorbed/adsorbed CO_2 in oil, moisture, and polysaccharides (Illy and Viani 1995; Schenker 2000; Clarke and Vitztbum 2001). Besides, the aforementioned cell walls are porous as well with typical pores diameter ranging from 20 to 50 nm, which can be regarded as mesopores (Schenker et al. 2000; Anderson et al. 2003). High-temperature roasted coffees were found to have larger mesopores in the cell wall as compared to low-temperature roasted beans (Schenker et al. 2000). Due to the complicated porous structure, the mass transfer of CO_2 in roasted coffee matrices is complex, involving Knudsen diffusion, transition-region diffusion, pressure driven viscous flow, surface diffusion, and desorption from various constituents (Anderson et al. 2003).

Although much of the CO_2 produced is lost during roasting, a significant amount remains trapped in the roasted beans. Thus, roasted coffee is tempered to remove the CO_2 before packaging to prevent package swelling or failure. Alternatively, coffees are partially tempered to minimize aroma loss and packaged in active packaging systems that are equipped with a one-way vent valve to allow the releasing of CO_2 during storage. In order to strike a balance between adequate CO_2 degassing and minimized aroma loss during the tempering process, a systematic understanding of CO_2 degassing kinetics as affected by roasting conditions is important. This information will also be useful during the design optimization of pressure relief valve for active packages of coffee. The first objective of this study was to investigate the CO_2 degassing behaviour of an Arabica coffee, processed using a fluidized bed hot air roaster under high-temperature-short time (HTHT) and low-temperature-long-time (LTLT) processing conditions. The second objective was to

understand the different degassing phenomena observed by investigating various physicochemical properties of the roasted coffee beans. In addition, the effects of temperature and relative humidity (RH) on CO_2 degassing behaviour were investigated.

4.2 Materials and Methods

Brazilian Arabica green coffee beans (Strictly Soft grade) were supplied by Mother Parkers Tea & Coffee (Mother Parkers Tea & Coffee Inc., Mississauga, ON, Canada). Sodium carbonate, hexane, sodium hydroxide, tri-sodium citrate, 1N sulphuric acid, concentrated sulfuric acid, Drierite desiccant, and Ascarite II column (sodium hydroxide coated silica gel) were all purchased form Fisher Scientific International Inc. (Ottawa, ON, Canada).

4.2.1 Roasting procedure and sample preparation

Green coffee beans were roasted using a modified fluidized bed roaster (Fresh Roast SR 500 roaster; Fresh Beans Inc., UT, USA). A microprocessor temperature process controller was connected to the roaster to allow accurate hot air temperature control (Model CN 7200, Omega Engineering, Inc., Stamford, CT, USA) (Wang and Lim 2014). More detailed information about the apparatus was presented in section 3.2.1. Green coffee beans were roasted using either LTLT process at 230°C or HTST process at 250°C to achieve light (L), medium (M), dark (D) and very dark (VD) roast degrees. The roast degree was determined by comparing the color of the roasted coffee fine grinds with SCAA (Specialty Coffee Association of America) standard disks, and expressed as CIE L^* value determined

using a spectrophotometer reflectance system (Model CM-3500d, Konica Minolta Sensing, Inc., Osaka, Japan).

Medium and dark roasted coffee beans (LTLT-M, LTLT-D, HTST-M and HTST-D) were ground to coarse, medium, and fine grinds, using a commercial blur grinder (BODUM® Inc., NY, USA). Approximately 20 g of the roasted coffee samples were loaded into the grinder, which took about 10 s to grind. The particle size distribution of these three grinds was measured by a series of sieves and presented in Figure 4.1. Table 4.1 summarizes the roasting conditions used to obtain various coffee samples.

Table 4.1- Roasting temperature-time conditions used to obtain roasted coffee samples

Sample abbreviations	Roasting temperature (°C)	Time (min)
LTLT-L	230	4
LTLT-M		8
LTLT-D		18
LTLT-VD		26
HTST-L	250	2.5
HTST-M		3.5
HTST-D		5.5
HTST-VD		7.5

HTST: high-temperature-short-time; LTLT: low-temperature-long-time; L: light roast degree; M: medium roast degree D: dark roast degree; VD: very dark roast degree.

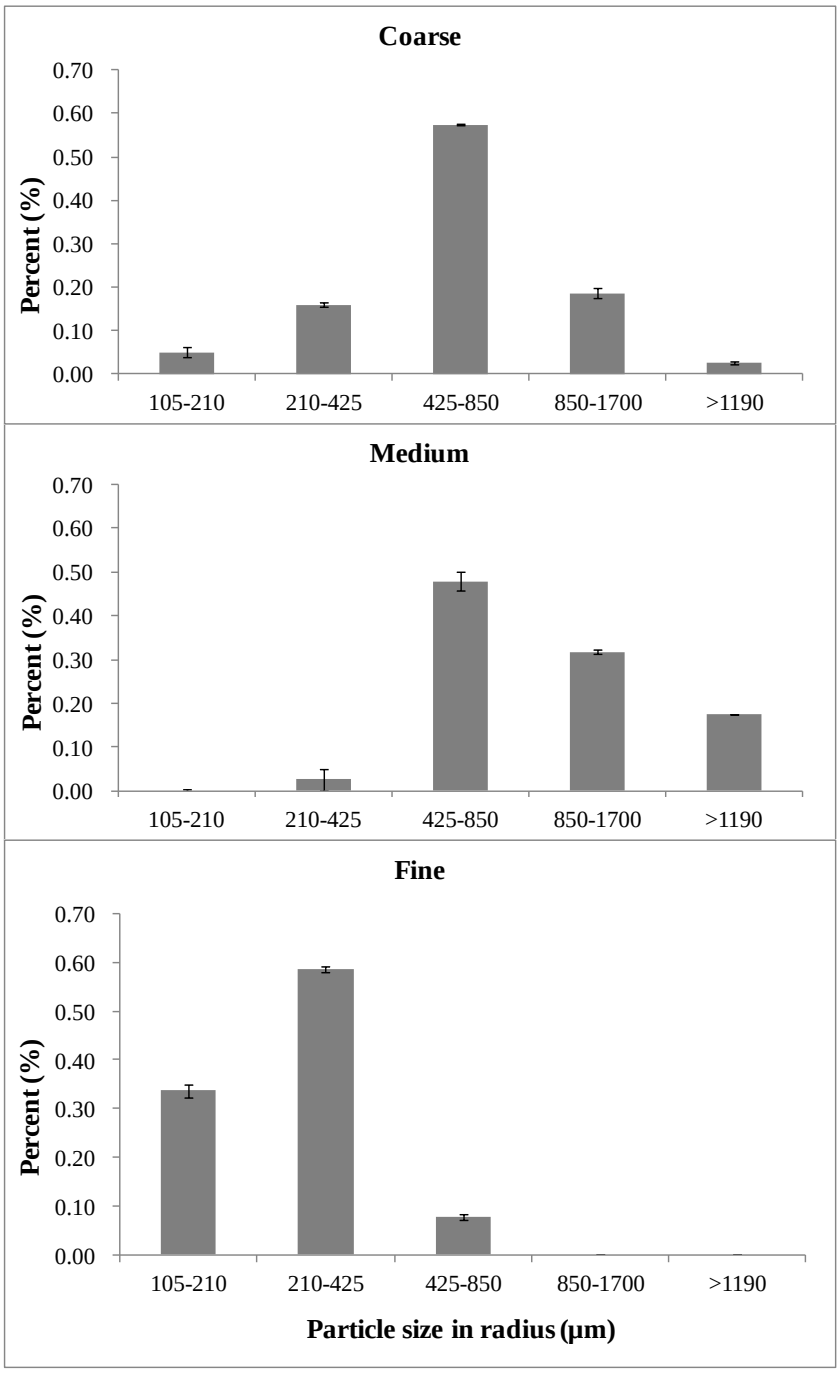

Figure 4.1- Averaged particle size (in radius) distribution of coarse, medium and fine ground coffee.

4.2.2 Determination of residual CO_2 content

Residual CO_2 content was determined by a gravimetric method as described in section 3.2.4 (Shimoni and Labuza 2000; Anderson et al. 2003; Wang and Lim 2014).

4.2.3 CO_2 degassing behaviour test

The degassing of CO_2 from roasted coffee at 25°C was monitored by a Fourier transform infrared (FTIR) spectrometer (IR Prestige-21; Shimadzu Corp., Tokyo, Japan). Two and a half grams of coffee was placed into a modified 250 mL clear French squares glass bottle (Fisher Scientific International Inc., Ottawa, ON, Canada) equipped with a PTFE lined closure. Two 15 mm diameter holes were drilled on the opposite side walls of the bottle, which were sealed with CaF_2 windows (Pike Technologies, Madison, WI, USA) using epoxy adhesive. The CaF_2 windows allowed the infrared beam of the spectrometer to transmit across the headspace of the bottle, allowing the detection of CO_2 without disrupting the headspace air (Figure 4.2a). At predetermined time intervals, the headspace air was analyzed. A typical FTIR spectrum of the headspace air is shown in Figure 4.2b, showing a strong absorbance at 2341 cm^{-1} wavenumber that can be attributed to CO_2 gas. To determine the CO_2 concentration, a calibration curve was established by mixing various known amounts of sodium carbonate with excess amount of 1N sulfuric acid solution to generate headspace air with different levels of CO_2. High linear correlation was observed between the absorbance value and CO_2 concentration, with a coefficient of determination (R^2) of 0.998.

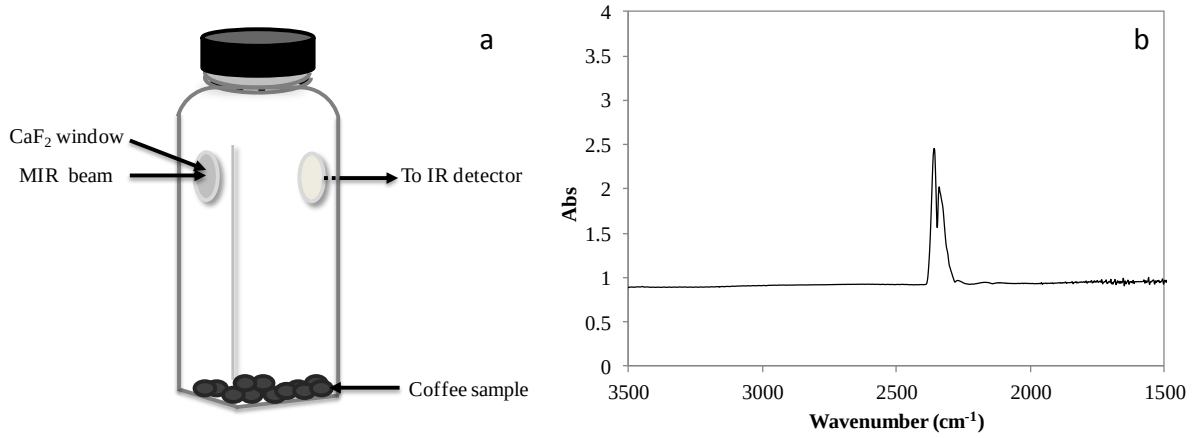

Figure 4.2- Schematic diagram of CO_2 degassing test apparatus (a) and typical FTIR spectrum of headspace air, showing the strong absorbance at 2341 cm^{-1} due to CO_2 (b)

The effect of temperature on CO_2 degassing was investigated by storing the testing apparatus in environmental chambers (Sanyo Versatile Environmental Test Chamber, Sanyo Electric Co. Ltd., Gunma, Japan) at temperature of 4, 15, 25 or 40 °C.

To investigate the effect of environmental humidity on CO_2 degassing, the headspace relative humidity (RH) (0, 33, 58, and 81%) of the degassing bottle was adjusted by desiccant (0%) and saturated salt solutions of $MgCl_2$ (33%), NaBr (58%) and $(NH_4)_2SO_4$ (81%). A small container with 1.5 mL saturated salt solution was placed within the degassing bottle and fixed on the wall with adhesive tape. For 0% RH condition, three grams of Drierite desiccant was added to the bottle instead of saturated salt solution. Before adding the coffee sample, the degassing bottles with saturated solution or desiccant were stored at 25 °C overnight to enable the equilibration with the headspace.

HTST-D sample was used to investigate the effect of temperature and RH on CO_2 degassing.

4.2.4 CO_2 degassing modeling

The CO_2 degassing plots of the coffee beans and ground coffee were fitted with Weibull distribution model, which is an empirical model applied to describe various kinetics in food, such as drying and hydration processes (Menges and Ertekin 2006; Cunningham et al. 2007; Bakalis et al. 2009; Meisami-sal et al. 2010):

$$C = C_{\infty} * [1-\exp [-(t/\alpha)^{\beta}]] \quad \text{(Eq. 4.1)}$$

where t is degassing time (h); C (mg/L) is CO_2 concentration in the headspace at time t; C_{∞} (mg/L) is headspace CO_2 concentration at infinity time; α is scale parameter (h) and β is shape parameter (dimensionless). The α parameter determines the rate and is related to the reciprocal of the process's rate constant, representing the time needed to accomplish approximately 63% of the process. The calculated diffusion coefficient (D_{calc}) can be obtained from α parameter by taking the sample geometries into account (Marabi et al. 2003; Marabi and Saguy 2004; Corzo et al. 2008):

$$D_{calc} = \frac{L^2}{\alpha} \quad \text{(Eq. 4.2)}$$

where L is the sample radius for spherical samples. The L of roasted coffee beans is calculated by the equation (Dutra et al. 2001):

$$L = \frac{1}{2} a + \frac{1}{2} b + \frac{1}{2} c \quad \text{(Eq. 4.3)}$$

where a, b, c represent the measurements of major, minor, and intermediate diameters of individual bean. For the ground coffee, the average radius for each grinding level was calculated based on particle size distribution in Figure 4.1. Coarse grinding resulted in an average particle size of 654 μm in radius. For medium and fine grounds, the values were 467 and 299 μm, respectively. The shape parameter β is related to velocity of the mass transfer at the beginning; the lower the value, the faster the degassing rate at the beginning. When β=1,

the Weibull distribution model reduces to 1st order kinetic equation, while a larger β value (>1) indicates the presence of a lag phase in the mass transport process (Marabi et al. 2003; Marabi and Saguy 2004; Saguy, Marabi, and Wallach 2005; Corzo et al. 2008).

4.2.5 Attenuated Total Reflectance (ATR)-FTIR analysis of roasted coffee powder

Roasted coffees were ground using a laboratory ball mill (PM 200; Retsch Inc., Newtown, PA, USA) at 450 rpm for 30 min to obtain a fine power. The power samples were then analyzed with Shimadzu FTIR spectrometer (IR Prestige-21; Shimadzu Corp., Tokyo, Japan) equipped with an ATR accessory (Pike Technologies, Madison, WI, USA). During the analysis, the coffee powder was spread onto the crystal and then compressed using a clamp. Five samples from each treatment were scanned from 600 to 4000 cm^{-1} wavenumber in absorbance mode at a resolution of 4 cm^{-1}. Each spectrum represented an average of 40 scans. For chemometric analysis, the FTIR spectra obtained were exported as ASCII format, organized in Excel spreadsheets and then analyzed using Pirouette v.4.0. chemometric software package (Infometrix, Inc., Bothell, WA, USA). Before the principal component analysis (PCA), second derivative and mean-center treatments were applied to reduce the noise from baseline variation and to enhance spectral features.

4.2.6 Moisture, oil content and density

Samples of roasted beans were finely ground and then analyzed using a moisture analyzer (IR-50; Denver Instruments, Bohemia, NY, USA). Approximately 1 g of ground coffee was weighted accurately onto the loading tray and the temperature was increased from 60°C to 105°C in 2 min and then kept at 105°C for 10 min. The Soxhlet method was used to measure the oil content of roasted coffee by using hexane as the extraction solvent. About 5

grams of coffee were used for the test and the extraction cycle was allowed to repeat for 6 hours. Bean density was determined using a displacement method as reported by Schenker (2000). Briefly, a known quantity of roasted beans was added to a 100 mL graduated cylinder filled with 70 mL of water. A customer-made plunger was used to submerge the floating beans into the water, followed by sliding the plunger up and down to remove the entrapped air. The final volume was then noted. Similarly, the plunger was submerged into the graduate cylinder without the beans. From the volume difference, the bean volume and thus the bean density were calculated. Three measurements were taken for each sample during moisture content, oil content, and density analyses.

4.2.7 Cell wall porosity test by mercury intrusion porosimetry

A mercury-porosimeter (PoreMaster 60; Quantachrome Instruments, FL, USA) was used to determine the cell wall porosity of coffee samples (Schenker 2000). To exclude the effect of the evacuated cells, the roasted coffee beans were ground with a laboratory ball mill (PM 200; Retsch Inc., Newtown, PA, USA) to disrupt the cells. In order to confirm the efficiency of the grinding, the particle size after grinding was determined by light microscopy after dispersing the coffee particles in vegetable oil. About 0.4 g ground sample was used and the measurement was conducted at 20°C. Applied intrusion pressure ranged from 0 to 60000 psia, which corresponded to pore diameters of 1068.83 to 0.0036 μm. The measured intrusion pressure was converted to equivalent pore diameter by using the Washburn equation:

$$\Delta p = \frac{4\gamma \cos\theta}{d_{pore}} \qquad \text{(Eq. 4.4)}$$

where Δp is the intrusion pressure (psia); γ is surface tension of the mercury (480 mN/m); θ is contact angle between solids and mercury (140°); d_{pore} is the diameter of the pores.

4.2.8 Moisture isotherm of roasted coffee bean

Different relative humidity conditions were established inside wide mouth one-litre jars using saturated salt solutions. The salts used and the corresponding RH were shown in Table 4.2 (Gennadios and Weller 1994). For 0% RH humidity, Drierite desiccant was added to the jar instead.

Table 4.2- Saturated salt solution used in the moisture isotherm determination of the roasted coffee bean HTST-D at 25 °C

Relative humidity (%)	Salt	Relative humidity (%)	Salt
11.2	LiCl	57.7	NaBr
22.6	CH_3COOK	68.9	KI
32.7	$MgCl_2$	75.3	NaCl
43.8	K_2CO_3	84.3	KCl
52.9	$Mg(NO_3)_2$	93.6	KNO_3

HTST-D beans were freeze-dried for 24 h before the sorption experiments. Approximately 5 g of roasted coffee beans were accurately weighted and placed onto aluminum pans, and suspended over the salt solution in the sealed jars. The jars were kept inside an environmental chamber (Sanyo Versatile Environmental Test Chamber, Sanyo Electric Co. Ltd., Gunma, Japan) maintained at 25 °C. The weight of samples was recorded to the nearest 0.0001 g every two days until equilibrium. Equilibrium was assumed to have

been reached when the change in moisture content of samples was less than 0.001g water/g dry matter.

The GAB (Guggenheim- Andersen-de Boer) equation was used to fit the water sorption isotherm of roasted coffee beans (Timmermann 2003).

$$m = \frac{C_G k_G a_w m_0}{(1-k_G a_w)(1-k_G a_w + C_G k_G a_w)} \quad \text{(Eq. 4.5)}$$

where m is the amount of moisture sorbed by 1 g of coffee at water activity a_w; m_0 is the monolayer moisture content, and C_G and k_G are the GAB energy constants.

4.2.9 Statistical analysis

The non-linear regression method (IBM SPSS Statistics 21, New York, United States) was utilized to estimate the parameters of Weibull distribution model and GAB model. The goodness of fit was evaluated on the basis of coefficient of determination (R^2) and root-mean-square error (RMSE). Statistical comparison of values in this study was conducted based on Tukey's multiple comparisons using Minitab 15 software (Minitab Inc, State College, United States).

4.3 Results and Discussion

4.3.1 Effect of roasting conditions on the residual CO_2 content in roasted coffee

4.3.1.1 Roasted coffee beans

The residual CO_2 contents in the roasted coffee beans increased from 6.29 ± 0.47-6.70 ± 1.01 mg/g to 11.04 ± 0.99-11.51 ± 0.50 mg/g as the coffee beans were roasted from light to medium roast (Table 4.3). These values are comparable with the value reported by Geiger et al., who observed 9.9 mg/g of residual CO_2 in medium roast coffee (Geiger et al. 2005).

Roasting the coffee to dark degree resulted in more than double the residual CO_2 (15.62 ± 0.72-15.36 ± 0.52 mg/g) as compared to the light roast counterparts. However, processing the beans to very dark roast degree did not cause further increase in residual CO_2 (15.11 ± 0.92-15.97 ± 2.46 mg/g). This observation may be due to the depletion of the CO_2 precursors (e.g., sucrose, amino acids, chlorogenic acid) and the rapid release of trapped CO_2 when the beans underwent the "second crack" that occurred as roasted to dark roast. On the other hand, the residual CO_2 contents of HTST and LTLT coffee beans, at any given degree of roast, were not significantly different ($P>0.05$; Table 4.3), suggesting that roast degree is an important determinant for the amount of CO_2 trapped in roasted coffee, but not the roast temperature tested (230 and 250°C). On the basis that the roast time needed to achieve the same roast degree was considerably longer at 230°C than at 250°C (Table 4.1), one can infer that the rate of CO_2 formation was highly temperature dependent.

Table 4.3- Residual CO_2 content of roasted coffee beans at various temperature-time roasting conditions

Samples	Roast degree	*L** value [n]	Residual CO_2 content (mg/g) [n]
LTLT-L	Light	32.64 ± 0.38[a]	6.29 ± 0.47[a]
HTST-L		33.15 ± 0.33[a]	6.70 ± 1.01[a]
LTLT-M	Medium	24.07 ± 0.34[b]	11.51 ± 0.50[b]
HTST-M		24.44 ± 0.90[b]	11.04 ± 0.99[b]
LTLT-D	Dark	20.75 ± 0.34[c]	15.62 ± 0.72[c]
HTST-D		20.27 ± 0.81[c]	15.36 ± 0.52[c]
LTLT-VD	Very dark	18.53 ± 0.22[d]	15.11 ± 0.92[c]
HTST-VD		18.14 ± 0.29[d]	15.97 ± 2.46[c]

[n] In the same column, the values with same letter means there is no significant difference ($p>0.05$) by Tukey's multiple comparison test. HTST: high-temperature-short-time; LTLT: low-temperature-long-time; D: dark roast degree; M: medium roast degree.

4.3.1.2 Ground coffee

The residual CO_2 can be trapped as gaseous phase within the evacuated cells, or be solubilized in moisture, lipid and solid matrices. To gain better understanding of the CO_2 that were trapped in the cellular voids, roasted coffee beans were ground into coarse, medium and fine grinds. The particle size distributions of these three grinds, determined by passing the ground samples through a series of sieves, are shown in Figure 4.1, and the corresponding CO_2 contents are summarized in Table 4.4. As shown, substantial amount of CO_2 was lost during grinding; the finer the grind, the greater the amount of CO_2 loss. Compared with the whole beans, approximately 26-30, 33-38 and 45-59% of residual CO_2 were lost when the samples were ground to coarse, medium, and fine grinds, respectively. These observations

indicated that a substantial amount of CO_2 was trapped in the evacuated cells of coffee beans, the breakage of which allowed the gas to escape during grinding. Conceivably, the frictional heat generated during grinding, which was greater in finely ground samples, would have also contributed to the increased CO_2 desorption from the lipid and solid matrices.

Table 4.4- Effect of grinding on residual CO_2 content in ground coffee samples

Ground coffee Samples	Residual CO_2 content (mg/g)	Percentage of loss due to grinding (%) [a]
LTLT-M-coarse	8.54 ± 0.08	26
LTLT-M-medium	7.66 ± 0.18	33
LTLT-M-fine	5.49 ± 0.23	52
HTST-M-coarse	7.75 ± 0.10	30
HTST-M-medium	6.80 ± 0.21	38
HTST-M-fine	4.46 ± 0.15	59
LTLT-D-coarse	11.63 ± 0.07	26
LTLT-D-medium	10.26 ± 0.09	34
LTLT-D-fine	8.54 ± 0.09	45
HTST-D-coarse	11.82 ± 0.34	29
HTST-D-medium	9.56 ± 0.16	38
HTST-D-fine	6.62 ± 0.20	57

[a] the value was calculated by the following equation: (1- residual CO_2 content in ground coffee/ residual CO_2 content in roasted coffee beans) ×100%. HTST: high-temperature-short-time; LTLT: low-temperature-long-time; L: light roast degree; M: medium roast degree; D: dark roast degree.

4.3.2 Effect of roasting conditions on CO_2 degassing behaviour

CO_2 degassing in whole beans is a slow process. As shown in Figure 4.3, beans subjected to HTST-D treatment took more than 800 h (~33 days) to degas ~14 mg/g of CO_2, which accounted for about 90% of the residual CO_2 (15.36 mg/g; Table 4.3). In comparison, the degassing process was relatively slower for LTLT-D sample; about 42% of CO_2 was still trapped with the same degassing duration. Similar trends were observed with the medium roasted beans that were processed using HTST and LTLT processes, except that the amount of CO_2 evolved were lower than for the dark roast beans. These results indicated that CO_2 degassing rates for coffee beans roasted at higher temperature were faster than those roasted at lower temperature. This phenomenon can be attributed to the greater porosity of coffee samples produced by the HTST process than those with the LTLT process (Schenker et al. 2000).

For ground coffee, the degassing rates were greater than for the whole beans (Figure 4.4). The degassing plots for the fine grind reached the plateau within 50 h, even though the coarse and medium grinds continued to degas slowly at the end of the test period. The greater degassing rate for the ground coffee can be attributed to the partial disruption of pore structures and increased surface-to-volume ratio of the coffee particles due to size reduction.

To further evaluate the CO_2 degassing kinetics, the Weibull distribution model was fitted to the degassing data. The coefficient of determinations (R^2) for all best fit lines are greater than 0.99 with root mean square deviation (RMSD) less than 2 mg/L, indicating the predicted values agreed with the experimental data (Table 4.5). The α parameter ranges from 190 to 335 h for coffee beans, and from 2 to 25 h for ground coffee, confirming that the CO_2 degassing were faster in the latter. Furthermore, the smaller the grind size, the smaller the α value. On the other hand, the roast degree had lesser effect on the magnitude of the α

parameter than the roasting temperature. For instance, α values for LTLT-M-coarse and LTLT-D-coarse samples are 21 h and 25 h respectively, while the values for HTST-M-coarse and HTST-D-coarse are 12 h and 13 h, respectively. These results imply that smaller grinding size and higher roasting temperature will favour the rapid degassing of CO_2, while roast degree had a relatively less effect.

The D_{calc} values were calculated from the α parameter to normalize the effect of particle size on CO_2 degassing rate (Eq. 4.2). As shown in Table 4.5, the D_{calc} values for beans (13.2×10^{-12} to 22.9×10^{-12} m^2/s) were greater than those for the ground samples (4.9×10^{-12} to 15.4×10^{-12} m^2/s), despite the lower CO_2 degassing rates in the whole beans. The larger D_{calc} values for the whole beans than the ground coffees can be attributed to the greater plasticization of wall matrices in the former due to higher amount of dissolved CO_2. The presence of large pores in whole beans could also serve as channels to increase the overall diffusivity of CO_2. Fitting the Fick's law diffusion model for spherical geometry to their coffee CO_2 degassing data, Anderson et al. (2003) determined that the effective diffusion coefficients for short and long times were in the ranges of 3.7×10^{-12} to 9.7×10^{-12} m^2/s and 0.5×10^{-13} to 9.7×10^{-13} m^2/s, respectively. These values are comparable with the D_{calc} values observed in the present study.

The β values are in the range of 0.70-0.73 for the beans and 0.46-0.53 for the ground coffee (Table 4.5). The lower values for the ground coffee samples are indicative of higher degassing rates in the initial stage of the degassing process. On the other hand, no specific trend was observed between the β value and grind size. The shape parameter β in the Weibull distribution model has been utilized by researchers for elucidating diffusion mechanisms in a number of food systems (Marabi et al. 2003; Marabi and Saguy 2004; Corzo et al. 2008). For

instance, during the rehydration of food particulates, β parameter in the range of 0.67-0.81 indicates that mass transfer diffusion predominates, while higher β value in the range of 0.97-1 is indicative of the presence of external resistance (Marabi et al. 2003). Due to coffee's complex microstructures and multiple components that interact with the CO_2, the actual diffusion mechanism for CO_2 degassing in coffee cannot be explicitly explained with β parameter alone. However, the different β values observed between whole beans and ground coffee samples may suggest that the mechanisms involved were different. A previous study speculated that the CO_2 transfer through the outer cell barrier (epidermis) might be a limiting factor for CO_2 degassing in roasted coffee beans (Baggenstoss et al. 2007). Therefore, destruction of the outer cell barrier caused by grinding might explain the faster CO_2 degassing rate at the beginning (lower β value) in ground coffee than in whole beans.

The C_∞ predicts the headspace CO_2 concentration at time infinity. By comparing the predicted C_∞ values of the roasted coffee beans (Table 4.5) with their residual CO_2 content (Table 4.3), it could be concluded that at the same degree of roast more CO_2 could be degassed from HTST roasted coffee beans than LLTT roasted ones, although their residual CO_2 contents were comparable. This might be due to the more compact structure of low temperature roasted coffee.

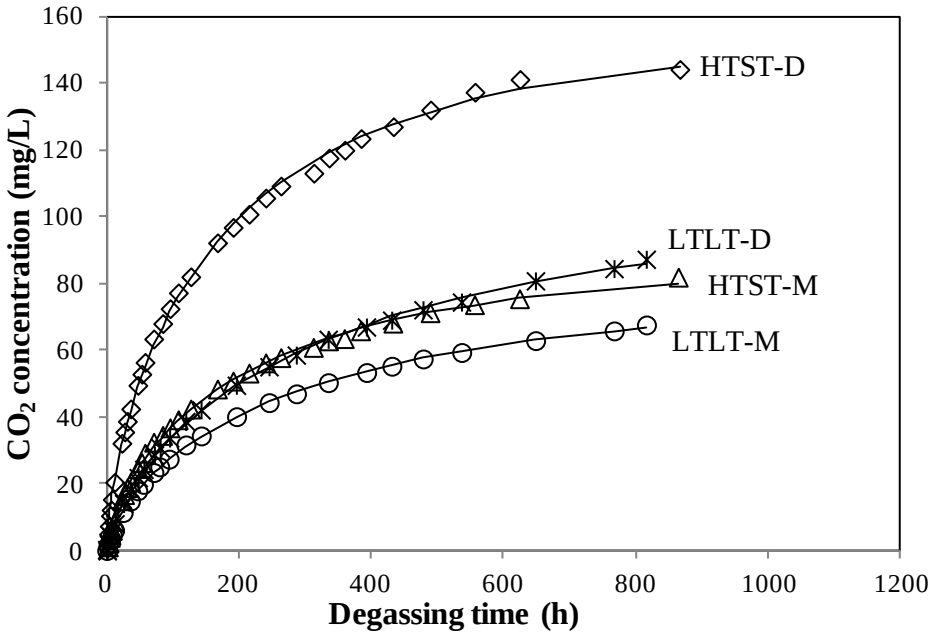

Figure 4.3- Representative CO_2 degassing data (symbols) at 25 °C for coffee beans roasted using different temperature-time conditions. Solid line represents the best fit curves of Weibull distribution model, showing its goodness of fit to the experimental data. HTST: high-temperature-short-time; LTLT: low-temperature-long-time; D: dark roast degree; M: medium roast degree.

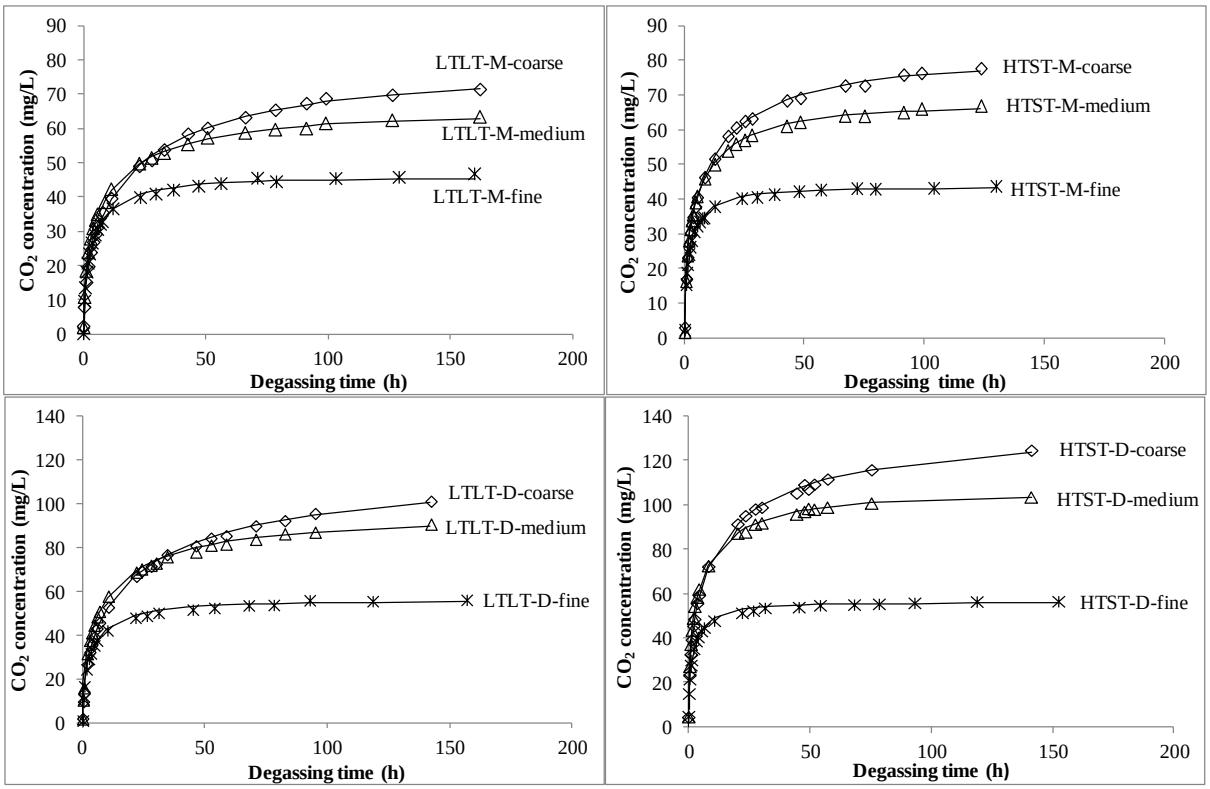

Figure 4.4- Representative CO_2 degassing data (symbols) at 25 °C for coffee samples ground to different sizes (coarse, medium and fine). Solid lines represent the best fit curves of Weibull distribution model to the experimental data. HTST: high-temperature-short-time; LTLT: low-temperature-long-time; D: dark roast degree; M: medium roast degree.

Table 4.5- Derived Weibull distribution model parameters (α, β, C_∞), D_{cacl} (calculated diffusion coefficients), coefficient of determination (R^2), and RMSE (root mean square error).

Coffee sample	α (h)	β	C_∞ (mg/L)	D_{cacl} (m^2/s, $\times 10^{-12}$)	R^2	RMSE (mg/L)
Coffee beans						
LTLT-M	335.2 ± 54.6	0.72 ± 0.00	72.5 ± 5.4	13.2 ± 2.2	0.999	0.52
HTST-M	222.9 ± 1.3	0.73 ± 0.01	82.4 ± 5.3	19.6 ± 0.1	0.998	1.02
LTLT-D	305.3 ± 69.5	0.73 ± 0.03	101.0 ± 2.3	14.7 ± 3.4	0.999	0.73
HTST-D	190.9 ± 4.2	0.70 ± 0.01	149.1 ± 5.9	22.9 ± 0.5	0.999	1.58
Ground coffee						
LTLT-M-coarse	20.7 ± 1.7	0.52 ± 0.01	73.4 ± 4.1	5.8 ± 0.3	0.998	0.86
LTLT-M-medium	9.5 ± 0.8	0.48 ± 0.00	68.9 ± 6.4	9.5 ± 0.8	0.999	0.81
LTLT-M-fine	4.8 ± 0.1	0.53 ± 0.00	45.5 ± 0.3	5.2 ± 0.1	0.998	0.63
HTST-M-coarse	11.5 ± 0.5	0.49 ± 0.00	80.4 ± 0.6	10.4 ± 0.5	0.999	0.76
HTST-M-medium	6.6 ± 0.6	0.47 ± 0.00	69.1 ± 2.7	13.6 ± 1.2	0.998	0.70
HTST-M-fine	2.8 ± 0.0	0.48 ± 0.00	42.9 ± 0.5	9.0 ± 0.1	0.997	0.63
LTLT-D-coarse	24.9 ± 1.2	0.51 ± 0.01	110.3 ± 1.4	4.9 ± 0.2	0.999	0.85
LTLT-D-medium	11.7 ± 0.6	0.48 ± 0.01	92.2 ± 0.3	7.6 ± 0.4	0.998	1.10
LTLT-D-fine	4.7 ± 0.1	0.52 ± 0.01	55.7 ± 0.8	5.3 ± 0.1	0.995	1.14
HTST-D-coarse	12.8 ± 0.8	0.47 ± 0.01	128.6 ± 2.0	9.3 ± 0.6	0.998	1.50
HTST-D-medium	5.8 ± 0.4	0.46 ± 0.01	104.1 ± 0.5	15.4 ± 1.0	0.997	1.44
HTST-D-Fine	2.2 ± 0.1	0.49 ± 0.01	55.2 ± 0.5	11.1 ± 0.3	0.996	0.94

4.3.3 Effect of roasting conditions on chemical compositions of roasted coffee

Results presented in sections 4.3.1 and 4.3.2 show that at the same degree of roast, CO_2 degassing rates for both HTST beans and grounds were greater than the LTLT counterparts, although the residual CO_2 contents were comparable. To better understand this phenomenon, the chemical compositional differences between HTST and LTLT processed coffees were investigated. As shown in Table 4.6, at any given degree of roast, HTST processed coffees had significantly higher ($p<0.05$) water and oil contents than those roasted using LTLT process. The majority of moisture detected in the roasted beans was derived from the reactions (e.g., Maillard browning) that occurred during roasting, rather than from the initial moisture present in the green beans (Wang and Lim 2012). Due to the longer roasting time with the LTLT process, the lower moisture contents observed in LTLT beans could be attributed to the depletion of reaction substrates (Geiger et al. 2005). This explanation agrees with the greater roast loss for LTLT beans than the LTLT beans (Table 4.6). The higher moisture content of HTST beans might partly explain their higher CO_2 degassing rates – a phenomenon that has been reported by other researchers (Baggenstoss et al. 2008). On the other hand, the lower oil contents measured for the LTLT beans, as compared with the HTST counterparts, were likely due to the greater amount of oil loss during in the LTLT process due to the extended roast time (Table 4.6).

Table 4.6- Some physiochemical properties of roasted coffee

Coffee samples	Total roast loss (%)	Oil content (dry basis, %)	Moisture content (%)	Density (g/ml)
LTLT-M	15.7 ± 0.2^{a}	13.7 ± 0.1^{a}	1.3 ± 0.0^{a}	0.626 ± 0.000^{a}
HTST-M	14.9 ± 0.2^{a}	14.5 ± 0.3^{b}	1.5 ± 0.1^{b}	0.585 ± 0.006^{b}
LTLT-D	18.1 ± 0.3^{b}	14.1 ± 0.0^{b}	0.9 ± 0.1^{c}	0.561 ± 0.002^{c}
HTST-D	17.6 ± 0.4^{b}	15.0 ± 0.3^{c}	1.3 ± 0.1^{a}	0.522 ± 0.010^{d}

In the same column, the values with same letter means there is no significant difference ($p>0.05$) by Tukey's multiple comparison test. HTST: high-temperature-short-time; LTLT: low-temperature-long-time; D: dark roast degree; M: medium roast degree.

To further evaluate the differences in chemical composition, ATR-FTIR spectroscopy and PCA methodologies were applied. The FTIR technique allows rapid and non-destructive determination of infrared fingerprints of test samples, which has been successfully applied in coffee authentication studies and in studies investigating chemical compositional changes in coffee during roasting (Lyman et al. 2003; Nalawade et al. 2006; Wang et al. 2009; Wang, Fu, and Lim 2011; Wang and Lim 2012).

FTIR spectra of medium and dark roast coffees, produced using LTLT and HTST processes, are shown in Figure 4.5a. As shown, medium roast coffees (HTST-M, LTLT-M) have stronger absorbance at 2918, 2850 and 1743 cm^{-1}, which correspond to the stretching of C-H and C=O. In addition, some differences were observed in 1000-1600 cm^{-1} wavenumber region, which includes C-H, C-O, C-N, and P-O vibrations (Wang et al. 2009). This region is unique for every organic molecule and is believed to represent the overall "fingerprints" of many different compounds in coffee (Lyman et al. 2003; Nalawade et al. 2006; Wang et al.

2009; Wang, Fu, and Lim 2011; Wang and Lim 2012). To evaluate if the infrared spectra can be used to discriminate the different roasted coffee samples, the PCA was employed. The resulting score plot is presented in Figure 4.5b, showing that the four samples (LTLT-M, HTST-M, LTLT-D, HTST-D) are well separated. The clusters for the medium and dark roasted coffees from the LTLT process (LTLT-M and LTLT-D) were farther apart than those from the HTST process (HTST-M and HTST-D). This observation suggests that the LTLT process resulted in greater overall chemical compositional differences between medium and dark roast coffees, as compared to those processed using the HTST process. Further inspection of the loading plot (Figure 4.5c) revealed that the main spectral regions that contributed to the differences observed were 2850-2920, 1714-1739, and 600-1500 cm^{-1} wavenumbers, which corresponds to C-H stretching, C=O stretching, and IR fingerprint, respectively. The C=O absorbance can be attributed to a number of characteristic components present in coffee, including aromatic acids, aliphatic acids, ketones, aldehydes, aliphatic/vinyl esters, and lactones (Lyman et al. 2003; Wang et al. 2009; Wang, Fu, and Lim 2011). CO_2 has been reported to interact with carbonyl groups in polymers (Nalawade et al. 2006; Perko and Marko 2011), affecting the solubility of the gas. Therefore, the different degassing behaviours observed in coffee samples could be partially explained by their different C=O contents in the coffee matrices.

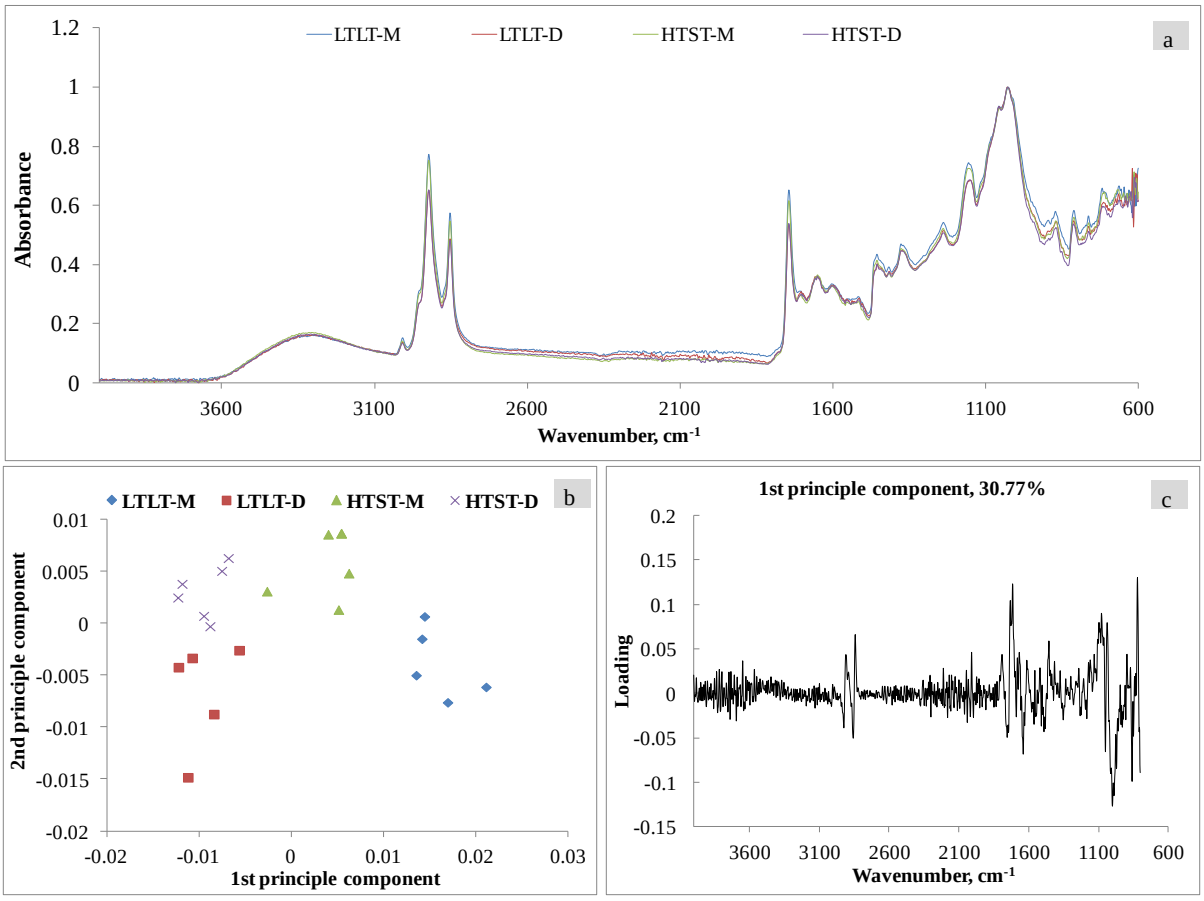

Figure 4.5- (a) Representative FTIR spectra of ground LTLT-M, LTLT-D, HTST-M, and HTST-D samples; (b) two factor score plots of PCA analysis of FTIR data; (c) loading plot of first principle component. HTST: high-temperature-short-time; LTLT: low-temperature-long-time; D: dark roast degree; M: medium roast degree.

4.3.4 Effect of roasting conditions on the cell wall porosity of roasted coffee

The CO_2 trapped in the cell luminas is in equilibrium with the CO_2 absorbed or adsorbed in the coffee matrix and makes the pressure in the cell lumina higher than atmosphere pressure. The internal pressure has been calculated as 4-6.4 atm by previous researchers based on ideal gas law (Clarke and Macrae 1987; Anderson et al. 2003). Due to the pressure difference between the surrounding atmosphere and cell luminas along the outer sphere, the absorbed and adsorbed CO_2 desorbed and the CO_2 trapped in the luminas diffused

across the cell walls to the environment mainly by viscous flow through the cell wall pores and by ordinary diffusion through the coffee matrix (mainly cellulose) (Kast and Hohenthanner 2000; Malek and Coppens 2003). Thus, roasting conditions that would affect the cell wall porosity will affect the CO_2 degassing behaviour. Figure 4.6 shows the development of cumulated pore volume as function of intrusion pressure and pore diameter during mercury porosimetry analysis for HTST-M, HTST-D, LTLT-M, and LTLT-D. The averaged particle size distribution of the finely ground coffee samples was in the range of 3-26 µm (inset of Figure 4.6). Since the size of macropores in roasted coffee beans are typically in 20-40 µm (Schenker et al. 2000), one can conclude that the grinding process had destroyed the majority of the evacuated cells. Accordingly, the cumulated increases in pore volume as the intrusion pressure increased up to pore diameters of ~2.5-3.5 µm can be attributed to the filling of inter-particle spaces of the powder samples. Further increase in the intrusion pressure did not result in the increasing of cumulated pore volume. However, at intrusion pressure of around 4,000-10,000 psi (corresponded to ~15-35 nm pore size), an increase in the intruded volume was observed, indicating that filling of the mesopores in the cell walls had occurred. This observation is in agreement with the results by Schenker (2000), who reported 20-50 nm pores in the cell walls of roasted coffee. The increasing trend of the intruded volume above 30,000 psi pressure (corresponded to ~3.6 nm pre size) indicated the presence of smaller pores (micropores), which were too small to be determined due to the limitation of the mercury porosimeter. Overall, the mercury porosimetry data did not reveal any detectable differences in cell wall porosity between the four coffee samples tested. However, the increasing trend of the intruded volume above the maximum pressure of this technique indicated the presence of smaller pores (< 3.6 nm) including micropores (<2 nm). The formation of microspores during coffee roasting could be attributed to the cell wall

polysaccharides degradation (Redgwell et al. 2002; Redgwell and Fischer 2006). It was reported that the degree of polymerization and branching of the galactomannans, the size of the arabinosyl side chains of the arabinogalactans decreased with the increasing of roast degree (Nunes and Coimbra 2002). Although there is no reported study about roasting temperature on the degradation of polysaccharide in coffee yet, we can speculate that the LTLT roasted coffee beans might contains more microspores which increased the tortuosity and thus decreased the degassing rate.

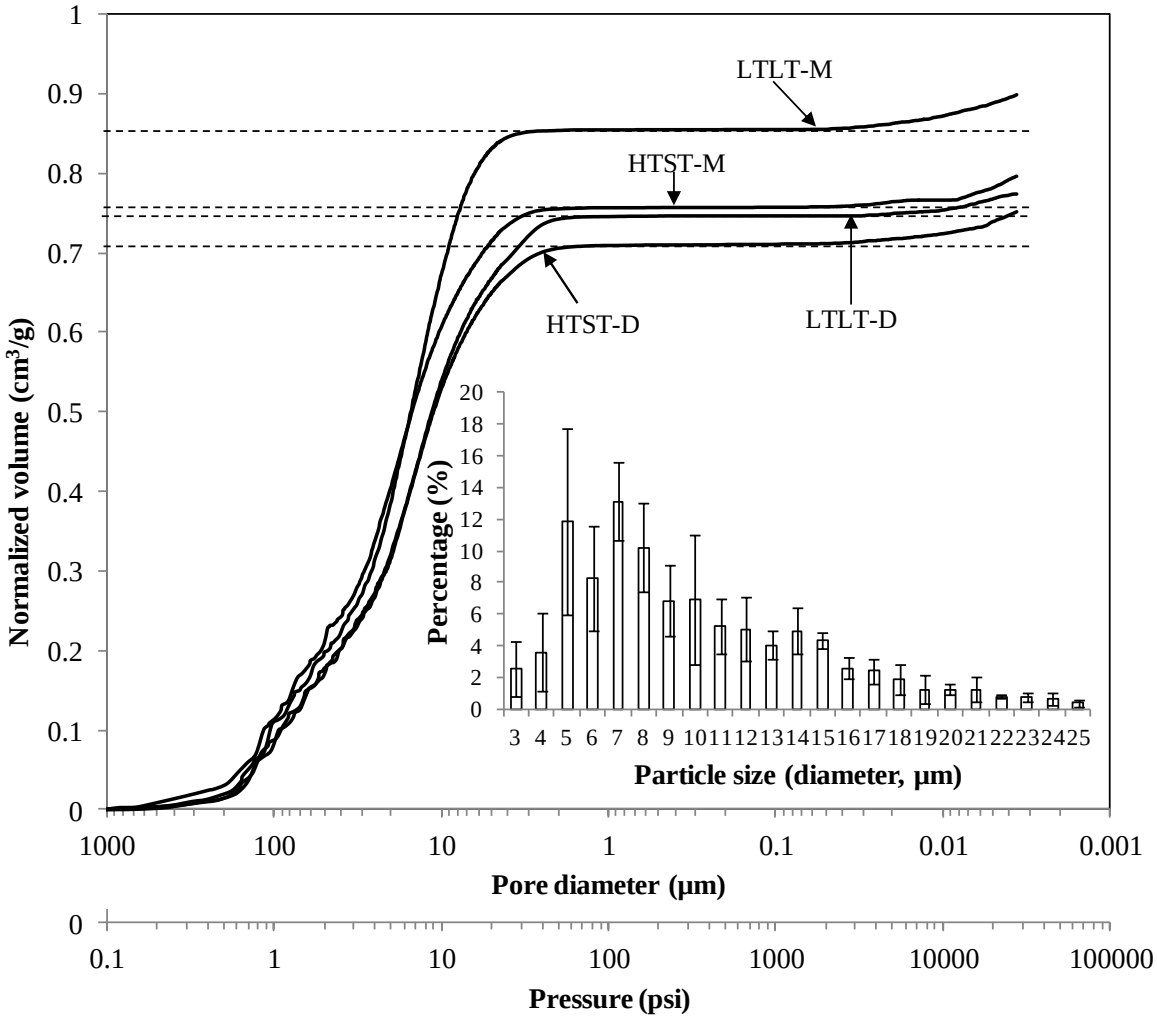

Figure 4.6- Representative porosimetric curves of finely ground coffee LTLT-M, LTLT-D, HTST-M, and HTHT-D samples, showing mesopores (2-50 nm) present in the cell walls. The inset summarizes the averaged particle size (in diameter) distribution of coffee samples subjected to the mercury porosimetry analysis, indicating that the particles were less than 30 µm. HTST: high-temperature-short-time; LTLT: low-temperature-long-time; D: dark roast degree; M: medium roast degree.

4.3.5 Effect of temperature on CO_2 degassing in roasted coffee beans

After roasting, coffee may be exposed to various temperature and RH environmental conditions, which may affect the CO_2 degassing rate. To better understand the CO_2 degassing mechanisms, the effect of temperature and humidity were investigated. The CO_2 degassing

plots at 4, 15, 25 and 40 °C are shown in Figure 4.7. As expected, increasing of temperature increased the CO_2 degassing rate. The degassing approached completion at around 800 h for both 25 and 40 °C, while it took much longer for 4 and 15 °C degassing. The faster degassing rate at higher temperature could be explained by the faster CO_2 molecular movement when temperature was increased (Welty et al. 2008). Moreover, the solubility of CO_2 in the coffee would decrease as temperature increased.

The α value from Weibull distribution model decreased from 562 to 101 h as temperature increased from 4 to 40 °C, while for the β parameter, no significant change was found (Table 4.7). The negligible effect of temperature on β value may be related to the predominant degassing mechanism during the initial phase of the degassing process. Since the pressure of CO_2 within the beans is greater than one atmosphere, it is believed that degassing at the beginning was controlled by the pressure-driven viscous flow, instead of activated diffusion that is temperature-dependent (Anderson et al. 2003). To evaluate the temperature effect on the reaction rate, Arrhenius plot of D_{cal} was presented in Figure 4.8. As shown, a straight line was obtained, and the activation energy was calculated as 29.73 kJ/mol.

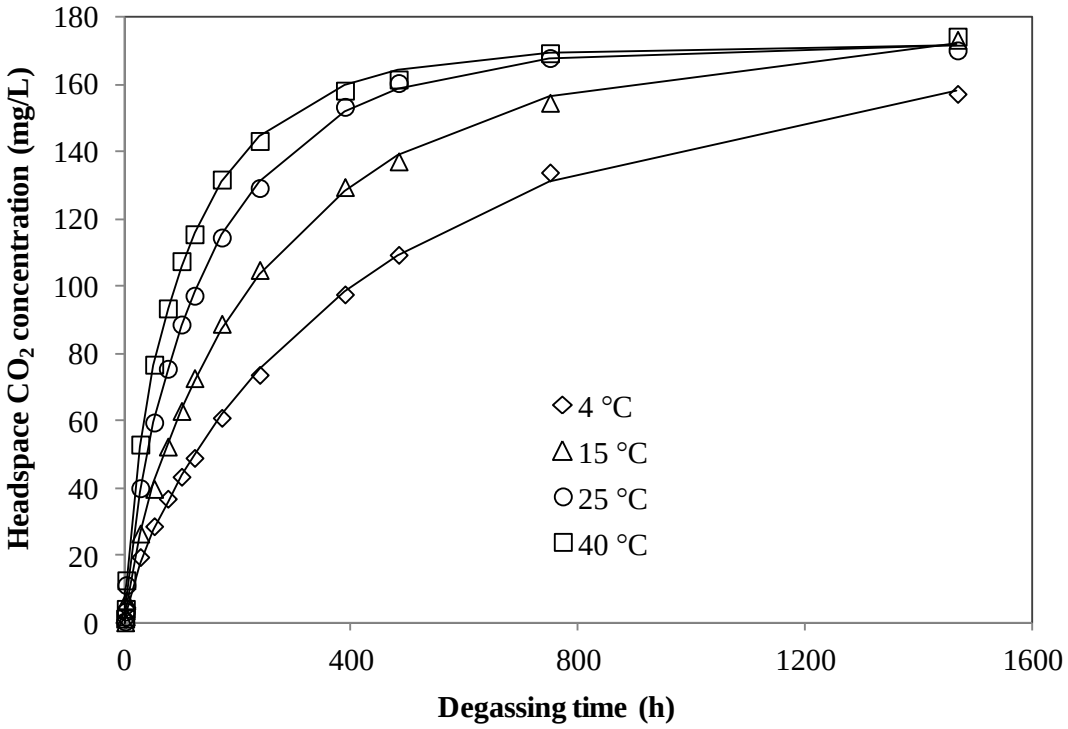

Figure 4.7- Representative CO_2 degassing data (symbols) at different degassing temperatures. Solid line represents the best fit curves of Weibull distribution model, showing its goodness of fit to the experimental data.

Table 4.7- Derived Weibull distribution model parameters (α, β, C_∞), D_{cacl} (calculated diffusion coefficients), coefficient of determination (R^2), and RMSE (root mean square error) from CO_2 degassing experiments at temperature of 4, 15, 25 and 40°C.

Temperature (°C)	α (h)	β	C_∞ (mg/L)	D_{cacl} (m^2/s, $\times10^{-12}$)	R^2	RMSE (mg/L)
4	562.9±89.2	0.79±0.02	174.2±1.6	7.87±1.2	0.998	0.93
15	280.5 ± 5.3	0.80±0.01	170.5±7.8	15.61±0.3	0.997	1.35
25	166.9±21.7	0.80±0.00	165.8±8.9	26.46±3.4	0.999	2.07
40	101.2±6.3	0.72±0.05	162.1±13.1	43.34±2.7	0.999	4.27

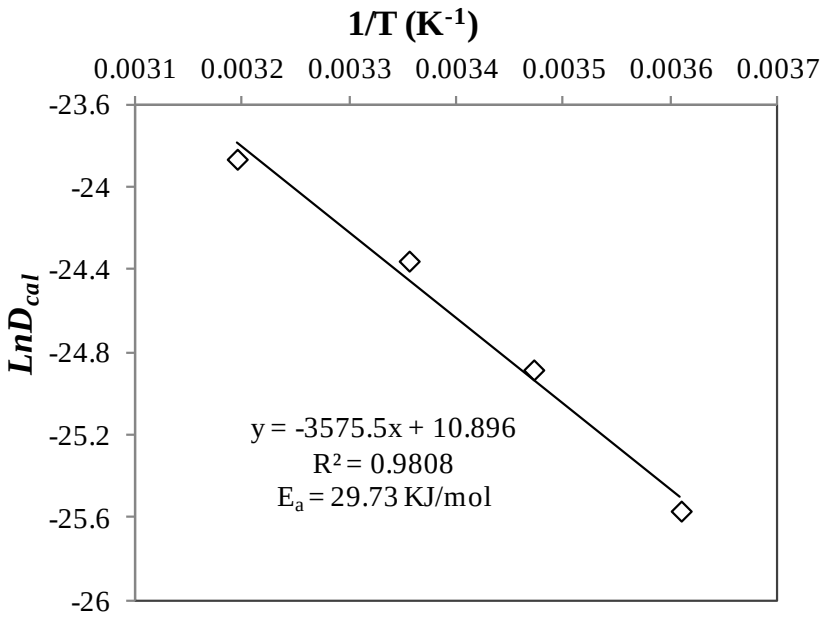

Figure 4.8- Arrhenius plot of D_{cal} of CO_2 degassing, showing activation energy of 29.73 KJ/mol.

4.3.6 Effect of RH on CO_2 degassing in roasted coffee beans

The CO_2 degassing plots under different RH conditions are shown in Figure 4.9. As shown, the CO_2 degassing rate increased with increasing of humidity. The degassing attained equilibrium in 90 h at 81% RH, while only ~60 % of CO_2 in roasted beans was degassed at 0% RH, even after an extended degassing period (1100 h). The predicted α values from Weibull model decreased from 294 to 45 h with the increasing of RH, indicating the faster degassing rate at higher RH. The increased degassing rate of the beans at elevated RH could be explained by the plasticizing effect of moisture on the cellulose matrix that increased the diffusivity of CO_2, whereas, under the dry conditions, cellulose mainly existed in a glass state. For shape parameter β, the value increased with increasing of RH, implying that initial CO_2 degassing rate tended to be higher when RH was lower. At 81% RH, the predicted β value was 1.62 (>1), indicating that there was a brief lag phase during the initial phase of degassing

(shown in the insert of Figure 4.9). The lag phase could be explained by the simultaneous moisture (from environment to beans) and CO_2 (from beans to environment) mass transfers during the degassing experiments. Table 4.9 also shows that the predicted C_∞ increased from 108 to 167 mg/L with the increasing of RH. The predicted low C_∞ for low RH experiments is likely due to the lack of data point for regression analysis when time is large, i.e., the degassing has not truly attained equilibrium for low RH experiments due to slow CO_2 diffusion in glassy coffee matrices.

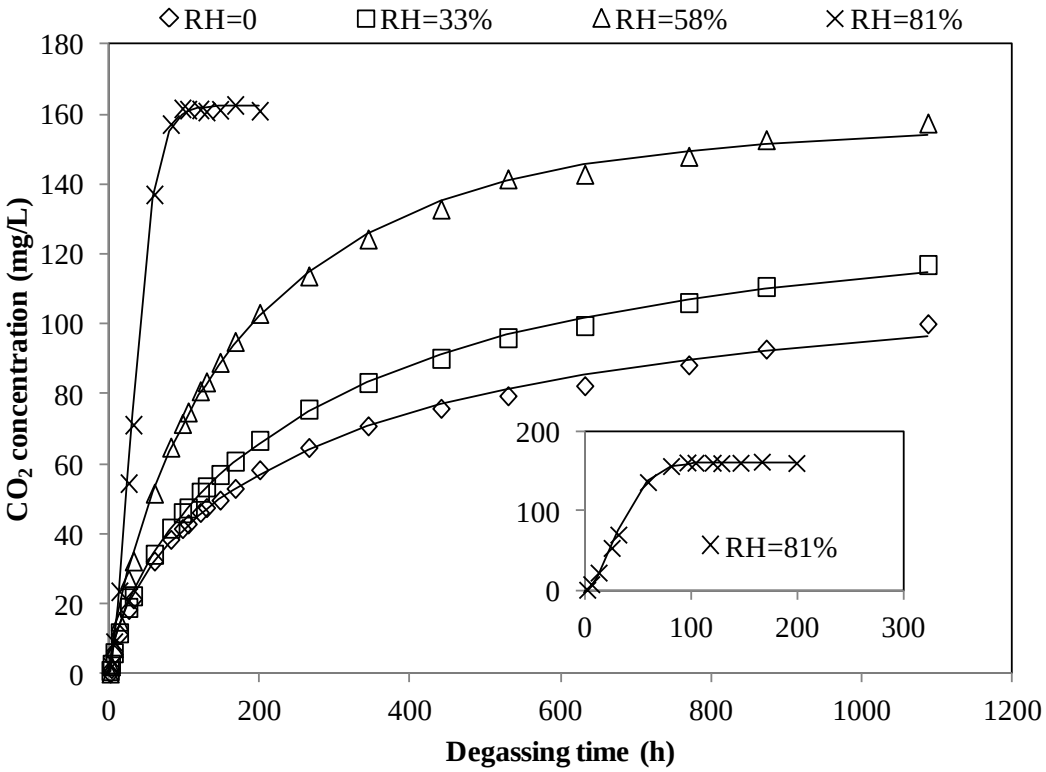

Figure 4.9- Representative CO_2 degassing data (symbols) at 25°C with different relative humidity control. Solid line represents the best fit curves of Weibull distribution model, showing its goodness of fit to the experimental data. Insert shows the CO_2 degassing kinetic at RH 81%.

Table 4.8- Derived Weibull distribution model parameters (α, β, C_∞), D_{cacl} (calculated diffusion coefficients), coefficient of determination (R^2), and RMSE (root mean square error) from CO_2 degassing at RH of 0, 33, 58 and 81%.

RH (%)	α (h)	β	C_∞ (mg/L)	D_{cacl} (m^2/s, $\times 10^{-12}$)	R^2	RMSE (mg/L)
0	294.0±19.7	0.63±0.01	108.8±3.4	14.92±1.0	0.998	2.09
32.73	309.7±14.2	0.70±0.00	125.0±4.6	14.14±0.6	0.997	1.36
57.70	168.4±23.7	0.80±0.01	163.2±9.4	26.00±3.7	0.998	2.22
80.99	44.8±3.1	1.62±0.10	167.1±5.1	97.66±6.7	0.998	2.68

In order to understand the different degassing behaviours observed in Figure 4.9, moisture sorption isotherm at 25 °C was determined (Figure 4.10). By fitting the data with the GAB equation, the monolayer moisture (M_0) was calculated as 2.7%, which is equivalent to ~0.33 $a_{w.}$ The calculated M_0 is consistent with the value reported by previous researchers (Hayakawa, Matas, and Hwang 1978; Pittia, Nicoli, and Sacchetti 2007; Andrade, Lemus, and Perez 2011). Based on the moisture isotherm, the moisture contents of coffee after attaining equilibrium at 33, 58, and 81% RH are predicted as 2.6, 6.3, and 16.9% on a dry weight basis, respectively. Thus, the tremendous increasing of degassing rate at RH 81% as compared to RH 58% could be attributed to the substantial increase of moisture content (6.3 to 16.9%).

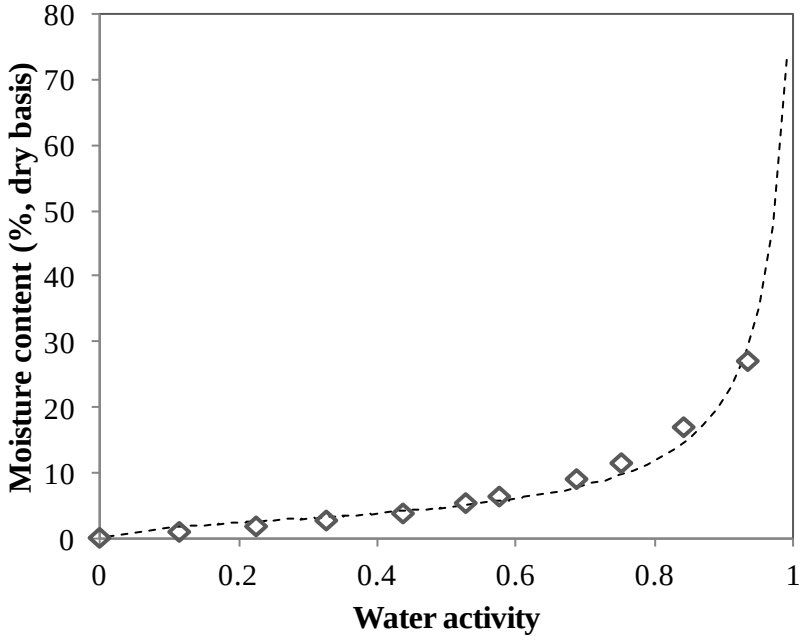

Figure 4.10- Representative moisture sorption isotherm of roasted coffee beans at 25° C. The dotted line represents the best fit curves of GAB equation, showing its goodness of fit to the experimental data (symbols).

4.4 Conclusion

This study showed that the amounts of CO_2 retained in roasted coffee beans, at any given roast degree, were independent from the roast temperature (230 and 250°C). However, the CO_2 degassing rates for coffee beans roasted at higher temperature were significantly faster than those roasted at lower temperature. As the roasted beans were ground from coarse to fine grinds, 26 to 59% of CO_2 were lost. As expected, the degassing rates of ground coffee were greater than the whole beans due to increased particle surface area and decreased diffusion distance. The reasons for the different CO_2 degassing behaviours observed could be partially attributed to the different water and oil contents of beans roasted at different temperature and roast degree, as well as the different chemical compositions as determined by the FTIR data. As expected, increasing the temperature will speed up the CO_2 degassing. In addition, environmental RH has a great effect on CO_2 degassing rate as well as the

maximum CO_2 that could be degassed. Therefore, the conditioning process control and the degassing valve design should take the coffee roasting profile as well the environmental factors into consideration in order to best maintain the coffee quality.

Mercury porosimetry test did not reveal any detectable difference in cell wall porosity, but indicated the presence of pores with the sizes less than 3.6 nm, which should be further studied in order to better understand the CO_2 degassing mechanism.

CHAPTER 5 : INVESTIGATION OF CHLOROGENIC ACIDS AS THE PRINCIPAL CO_2 PRECURSOR IN COFFEE

5.1 Introduction

CO_2 is the major gas produced during coffee roasting, accounting for ~87% of the gases released from roasted coffee (Clarke and Macrae 1987; Anderson et al. 2003; Baggenstoss et al. 2007). Part of the CO_2 produced evolves directly during roasting, while a considerable fraction remains retained within the coffee matrix that releases slowly during storage. The residual CO_2 within the roasted coffee must be adequately degassed before packaging to prevent package swelling or even bursting. Alternately, the roasted coffee must be packaged in package equipped with a vent valve to release the internal pressure. Thus, understanding the formation and degassing of CO_2 in roasted coffee is important to overcome the degassing and packaging challenges faced by the coffee industry.

In general, the generation of CO_2 in roasted coffee has been hypothesized to be originated from Maillard reactions (Shimoni and Labuza 2000; Anderson et al. 2003; Geiger et al. 2005). However, some researchers believe that chlorogenic acid (CGA) is also an important CO_2 precursor (Small and Horrel 1993; Clarke and Vitztbum 2001). It is well known that Robusta green coffee has significantly higher CGA and lower sucrose content than Arabica green coffee beans (Clarke and Vitztbum 2001; Illy and Viani 2005; Belitz, Grosch, and Schieberle 2009). The lower sucrose content in Robusta green coffee might be the reason for its lesser extent of Maillard reaction than in Arabica coffee. However, the fact that Robusta coffee tends to exhibit higher CO_2 content after roasting (Anderson et al. 2003) also implies that sugar is likely not the main contributor of CO_2. Alternatively, we hypothesize that CGA could play an important role in the generation of CO_2, considering that

Robusta beans have a greater CGA content than Arabica counterparts. The idea of CGA involvement in CO_2 generation during coffee roasting is further reinforced based on the study conducted by Sharma et al. (2002), who demonstrated that CO_2 is the major volatile compound formed during the pyrolysis of CGA.

CGA is a trivial name used to describe a family of esters formed between quinic acid and trans-cinnamic acids (mainly caffeic, ferulic and *p*-coumaric acid in coffee). The most abundant group of CGA in green coffee beans is the caffeoylquinic acid (CQA), representing more than 80% of the total CGA, of which 5-CQA is the major one (Trugo and Macrae 1984; Ky et al. 2001; Farah et al. 2005). The content of CGA in green coffee is around 3-12% (dry weight basis) and Robusta coffee generally contains more CGA than coffee Arabica (Trugo and Macrae 1984; Campa et al. 2005; Farah et al. 2005). CGA has a melting temperature of about 207°C. It is susceptible to thermal degradation under coffee roasting temperature, which is typically in the range of 220-240°C. Not surprisingly, the extent of degradation is dependent on the degree of roast. About 60% CGA loss was observed for medium roast coffee, while in dark roast coffee, most of the CGA is degraded (Trugo and Macrae 1984; Farah et al. 2005; Belitz, Grosch, and Schieberle 2009).

Based on the information collected, we hypothesize that CGA is the principal CO_2 precursor in coffee. To test this hypothesis, a series of experiments were conducted: (1) to study the CGA degradation and CO_2 formation kinetics during coffee roasting simultaneously and to explore their relationship; (2) to elucidate the thermal degradation behaviour of 5-CQA, the most abundant CGA in green coffee, under typical coffee roasting temperature conditions; and (3) to employ a green bean model system, which was spiked with CGA to investigate the CO_2 formation behaviour during roasting.

5.2 Materials and Method

Columbian (Excelso European Preparation) and Ethiopian (Limu) green coffee beans were supplied by Mother Parkers Tea & Coffee (Mother Parkers Tea & Coffee Inc., Mississauga, ON, Canada). Sodium carbonate, methanol (HPLC grade), sodium hydroxide, tri-sodium citrate, concentrated sulfuric acid, Folin-Ciocalteu reagent, Drierite^{TM} desiccant, Ascarite® II column (sodium hydroxide coated silica gel), D(-)-Quinic acid (purity > 98%, Acros Organics, Ottawa, Canada), and standard CGA 5-caffeoylquinic acid (*trans* isomer, purity > 99%, Acros Organics, Ottawa, Canada) were all purchased form Fisher Scientific International Inc. (Ottawa, ON, Canada). Caffeic acid was purchased from Sigma-Aldrich Canada Co. (Oakville, Ontario, Canada).

Green coffee CGA extract (ECGA, 5-caffeoylquinic acid, purity > 98%) for pure CGA thermal degradation test and spiking experiments was purchased from Changsha Ya Ying Bio-Technology Co., Ltd. (Changsha, Hunan, China). The ECGA was subjected to Differential Scanning Calorimetry and Attenuated Total Reflectance-Fourier Transform Infrared (ATR-FTIR) analysis to get the melting temperature and FTIR spectrum. By comparing with CGA standard, the product was proved to be chlorogenic acid. The purity of ECGA was validated by HPLC analysis.

5.2.1 Coffee roasting

Green coffee beans were roasted in a commercial fluidized bed roaster (Fresh Roast SR 500 roaster; Fresh Beans Inc., UT, USA), which was modified to allow accurate hot air temperature control by means of a microprocessor temperature controller (Model CN 7200, Omega Engineering, Inc., Stamford, CT, USA) (Wang and Lim 2014). Coffee beans were

roasted at 230°C or 250°C for different times, to produce batches of sample with different roast degree. Roast loss (RL) was determined by measuring the weight of green beans and roasted beans immediately after cooling:

$$RL = \frac{m_{green} - m_{roast}}{m_{green}} \times 100\ (\%)$$

where m_{green} (g) and m_{roast} (g) are weights of green and roasted coffee beans, respectively.

5.2.2 Determination of residual CO_2 content

Residual CO_2 content was determined by a gravimetric method as described in section 3.2.4 (Shimoni and Labuza 2000; Anderson et al. 2003; Wang and Lim 2014).

5.2.3 Volume of roasted coffee beans

Bean volume was determined using a displacement method based on Schenker (2000). Briefly, a known quantity of roasted bean samples was added to a 100 mL graduated cylinder filled with 70 mL of water. A customer-made plunger was used to submerge the floating beans into the water, followed by sliding the plunger up and down to remove the entrapped air. The final volume was then recorded. To determine the volume of the plunger, it was submerged into the graduated cylinder without the beans. From the volume difference, the bean volume was calculated. To normalize the effect of roast loss, the volume was expressed as mL/100 g green coffee.

5.2.4 Analysis of CGA and total polyphenol

Extraction

Roasted coffee samples were ground to fine grind using a commercial blur grinder (Bodum® Inc., NY, USA) and passed through a 0.046 mm sieve. To facilitate the grinding of green coffee beans, samples were frozen in liquid nitrogen before introducing into the grinder. Half gram of ground coffee was added in 60 mL 70% aqueous methanol and the mixture was stirred at room temperature for 60 min at 300 rpm. The mixture was allowed to stand for 10 min and 20 mL supernatant was transferred to a 40 mL vial. An aliquot of 0.2 mL of each of the Carrez's solutions, $K_2Fe(CN)_6$ (0.3 M) and $Zn(OAc)_2$ (1.0 M), were added to the vial to precipitate the proteins and other high molecular weight compounds (Ky, Noirot, and Hamon 1997; Farah et al. 2005). The mixture was shaken for 5 s and let stand for 10 min. The supernatant was filtered through 0.22 µm filter and was used for high pressure liquid chromatography (HPLC) and total polyphenol analyses. Three extractions were conducted for each sample.

HPLC Analysis of CGA

CGA was analyzed by a HPLC gradient system (Waters 2690 separation module, Milford, MA., USA), equipped with a photodiode array detector (Waters 996, Milford, MA., USA) and an Ultrasphere ODS-C_{18} column (250 mm × 4.5 mm × 5 µm, Beckman Coulter, USA). Chromatographic data were recorded and integrated in the Millennium 32 software. The chromatographic conditions and the gradient program were according to the study of Farah et al. (2005). The chromatographic conditions for the gradient were: eluent A: 80% 10 mM citric acid solution, acidity adjusted to pH 2.5 with phosphoric acid and 20% methanol.

Eluent B: methanol. The flow rate was 1 mL/min and run time was 60 min. The gradient program was as follows:

Time (min)	Eluent A (%, v/v)	Eluent B (%, v/v)
0.01	100	0
19	100	0
25	80	20
35	80	20
50	80	40
60	60	40
61	100	0

The identification of 5-CQA was performed by comparing the retention time with the CGA standard. The identification of other chlorogenic acids was achieved by comparing the chromatogram with that reported by Farah et al. (2005), who adopted the same chromatographic conditions and column during their HPLC analysis. Since the CGA has the maximum absorption at wavelength ~325 nm, the above identification process was validated by examining the maximum absorption point of the UV spectrum of each peak. The total CGA content was calculated based on the total peak area of all the identified chlorogenic acids at 325 nm and was expressed as 5-CQA equivalent.

Total polyphenol

The total polyphenol was determined using the Folin-Ciocalteau method (Vignoli, Bassoli, and Benassi 2011). An aliquot of 400 μL coffee extract or blank (deionized water) was pipetted into separate vials, to which 5 mL ten times diluted Folin-Ciocalteau reagent was added. The mixture was hand shaken for 5 s, and 4 mL 7.5% $NaCO_3$ solution was added. At the same time, 600 μL deionized water was added to make the total volume to 10 mL.

After shaking, the solution was left at room temperature to react (22 °C) for 2 h. The absorbance of each solution at 765 nm was determined by using a spectrophotometer. Results were expressed as % gallic acid equivalent.

5.2.5 Heating of pure CGA

About 0.05 grams of ECGA was weighted accurately into uncapped 15 mL silanised vials (Fisher scientific, Ottawa, ON, Canada) and heated at 210, 230, 250, and 270°C for up to 15 min (Casal, Oliveira, and Ferreira 2000) using a gas chromatograph oven (Agilent 5890, Agilent Technologies, Santa Clara, USA). The oven was allowed to equilibrate at the target temperature for 5 min before vial was inserted for heating. Immediately after the predetermined heating time was up, the vial was removed from the oven and allowed to cool down to room temperature in a desiccator before weight loss measurement. The weight loss was expressed as the ratio of weight after heating (W_t) to initial weight (W_i). The residual char was subjected to ATR-FTIR analysis to investigate the changes in IR active group. In addition, the total residual char was dissolved in 3 mL methanol and then diluted by 250 folds with 20% methanol for residual CGA analysis by HPLC using the method as described in Section 5.2.4. The extent of CGA degradation was expressed as:

$$\mathrm{D}egradation\ ratio = \frac{CGA_{original} - CGA_{residual}}{CGA_{original}}$$

5.2.6 ATR - FTIR analysis of CGA and CGA char

The CGA and its char samples were ground with pestle and mortar and then analyzed with Shimadzu FTIR spectrometer (IR Prestige-21; Shimadzu Corp., Tokyo, Japan) equipped with an ATR accessory (Pike Technologies, Madison, WI, USA). During the analysis, the

powder was spread onto the ATR crystal and then compressed using a clamp. Three samples from each treatment were scanned from 600 to 4000 cm^{-1} wavenumber in absorbance mode at a resolution of 4 cm^{-1}. Each spectrum represented an average of 60 scans.

5.2.7 CGA spiking of green coffee beans

Six grams of ECGA was dissolved in 74 g of distilled water at 80°C. After cooling, 100 g Columbian green coffee beans were added for soaking at room temperature. A control sample was prepared by adding 100 g Columbian green coffee beans to 80 grams distilled water and soaking at room temperature until all the liquid was absorbed by the bean. The control and CGA spiked green coffee beans were dried at 40°C for 12 h to remove the moisture and then stored in a 55% RH environmental chamber for one week to further equilibrate the moisture content.

5.2.8 Determination of evolved CO_2 during roasting of coffee and pure CGA

To account for the total CO_2 produced due to the roasting process, both the CO_2 trapped after roasting (Section 5.2.2) and CO_2 evolved during the roasting process will need to be determined. To this end, an experimental setup was developed to determine the amount of CO_2 evolved during roasting of coffee (Figure 5.1). A 500 mL Pyrex® volumetric flask was used as a reactor in which coffee beans or pure CGA was heated. The volumetric flask was connected to Drierite and Ascarite II column from one exit and to N_2 gas cylinder from another exit port. During the heating process, the valve to the N_2 cylinder was closed, forcing the evolved gases (CO_2, water vapour, organic volatiles) to vent through the Drierite column where moisture was removed, followed by CO_2 entrapped in the Ascarite II column, while all other vapours and gases were vented to the air. At the end of roasting, the remaining CO_2 in

the flask was captured by opening the valve, flushing the headspace for 10 min with N_2 gas through the same Drierite and Ascarite II columns. By measuring the weight increase of the Ascarite II column, the CO_2 evolved could be calculated. The CO_2 trapping efficacy of the system was validated by heating sodium bicarbonate at 230 °C. The average yield of CO_2 (measured value/theoretical value) of five sodium bicarbonate tests was about 98%, indicating the feasibility of using this setup for measuring evolved CO_2.

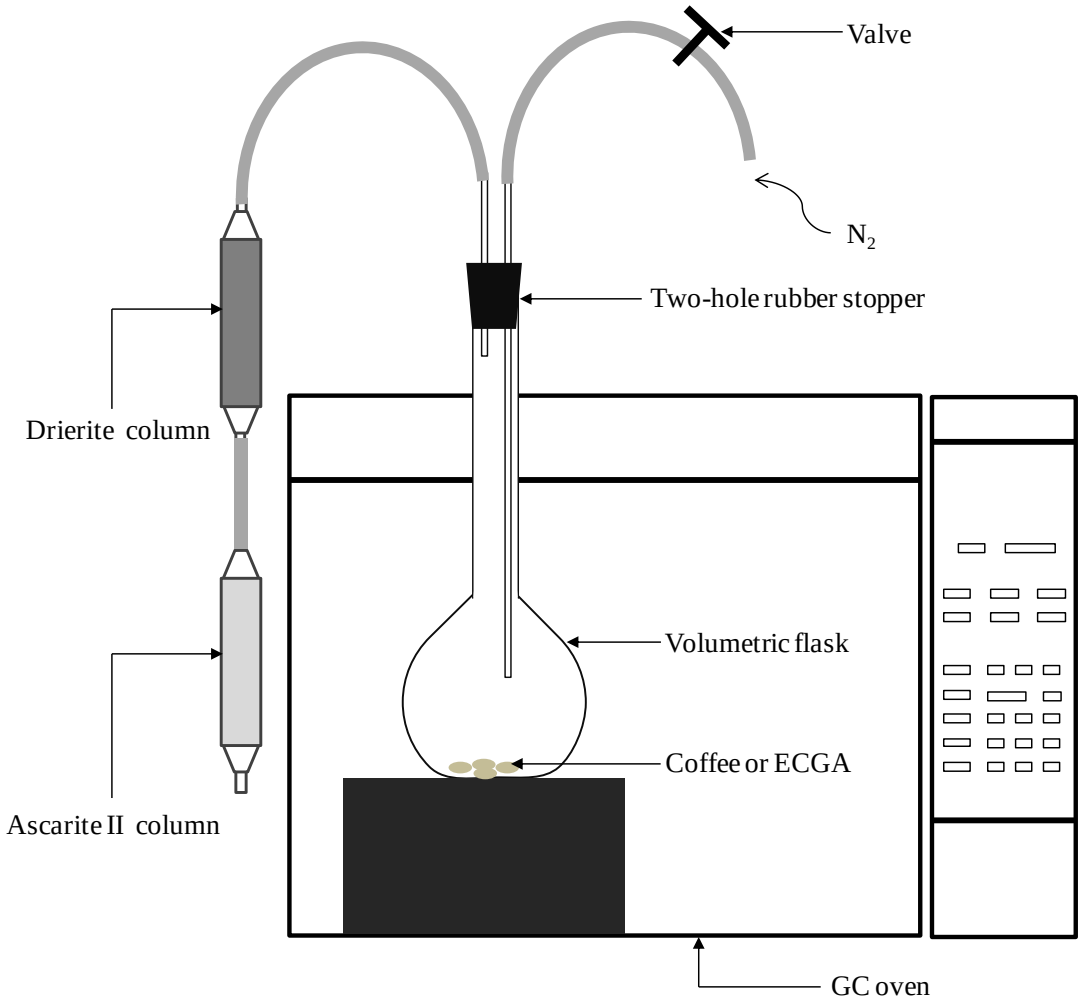

Figure 5.1- Apparatus for determining evolved CO_2 during coffee and pure CGA roasting

5.3 Results and Discussion

5.3.1 Degradation of CGA and formation of CO_2 during coffee roasting

Columbian and Ethiopian green coffee beans were roasted at temperature of 230°C or 250°C for various times to investigate the relationship between CGA degradation and CO_2 formation. The residual CO_2, total CGA, and some other selected physicochemical properties are summarized in Table 5.1. As shown, the maximum roast loss for both Ethiopian and Columbian coffee was ~15%, which corresponds to about medium roast. Moreover, the residual CO_2 contents increased with the extent of roast. Our previous studies showed that this positive relationship was reversed above dark roast due to substantial structural changes caused by the second crack (Wang and Lim 2014). Therefore, roasting was stopped at medium roast in this study. As shown in Table 5.1, as the residual CO_2 content increased, the volume of Columbian coffee increased from 79 to 140 mL per 100 g of green coffee at 230 °C, and from 79 to 150 mL per 100 g at 250 °C. The formation of CO_2 and other volatile compounds during roasting, which results in substantial increase in the internal pressure, is the main reason for expanded bean volume. At equivalent degree of roast, the higher expansion at 250°C than 230°C could be explained by the rapid accumulation of CO_2 at the higher roasting temperature.

A decrease of total CGA content was observed as the roast time increased. For example, at roast loss of around 15%, only ~1% of total CGA was detected for both Ethiopian and Columbian coffees, as compared to the initial contents of 4.7% and 4.0 %, respectively. Concurrently, residual CO_2 content of roasted coffee beans increased, with the amount taking up to ~1.5% of the total bean mass at the maximum roast level in this study.

Plot of total CGA and residual CO_2 content (Figure 5.2), shows strong negative linear correlation (R^2>0.9). These results imply that CGA potentially is a CO_2 precursor.

As compared to the total CGA content, the total polyphenol content measured by Folin-Ciocalteu method was less affected by the roasting. For example, after 12 min roasting at 230°C, the total polyphenol content of Ethiopian and Columbian coffee only changed from 2.5 to 2.2%, and 2.4 to 2.2%, respectively. Since CGA in the major phenolic compounds in coffee, the above observations imply that the phenolic hydroxyl group in CGA mostly remained intact during coffee roasting.

Table 5.1- Physiochemical properties, residual CO_2, total CGA and total polyphenol contents of roasted Ethiopian and Columbian coffee beans

Ethiopian coffee

Temperature	Roasting time (min)	Roast loss (%)	Volume (mL/100g green coffee bean)	Residual CO_2 content (mg/g, wb)	Total CGA (%, 5-CQA)	Total polyphenol (%, gallic acid)
230°C	0	0	75.0 ± 1.4	0	4.7 ± 0.1	2.5 ± 0.5
	1.5	3.5 ± 0.1	96.4 ± 0.2	1.6 ± 0.4	3.5 ± 0.3	2.3 ± 0.2
	3	7.4 ± 0.1	117.8 ± 1.6	4.4 ± 0.2	3.8 ± 0.1	3.0 ± 0.1
	5	10.9 ± 0.1	133.2 ± 1.4	7.8 ± 0.4	2.7 ± 0.1	2.6 ± 0.1
	8	13.2 ± 0.1	139.2 ± 1.8	11.5 ± 0.1	1.6 ± 0.0	2.3 ± 0.1
	12	14.3 ± 0.1	13 9.7 ± 1.1	13.4 ± 0.1	1.2 ± 0.0	2.2 ± 0.1
250°C	0	0	75.0 ± 1.4	0	4.7 ± 0.1	2.5 ± 0.5
	1.5	5.2 ± 0.0	119.0 ± 1.3	2.7 ± 0.1	3.8 ± 0.0	2.9 ± 0.2
	3	11.1 ± 0.1	144.1 ± 0.7	8.0 ± 0.1	2.8 ± 0.2	3.2 ± 0.0
	4.5	13.9 ± 0.3	144.4 ± 3.6	13.0 ± 0.4	1.5 ± 0.0	2.8 ± 0.1
	5.5	15.3 ± 0.1	148.0 ± 2.8	15.7 ± 0.5	1.1 ± 0.1	2.6 ± 0.0

Columbian coffee

Temperature	Roasting time (min)	Roast loss (%)	Volume (ml/100g green coffee bean)	Residual CO_2 content (mg/g, wb)	Total CGA (%, wb)	Total polyphenol (%, gallic acid)
230°C	0	0	79.0 ± 1.8	0	4.0 ± 0.1	2.4 ± 0.1
	1.5	3.5 ± 0.1	102.1 ± 1.3	1.7 ± 0.2	3.9 ± 0.1	2.7 ± 0.0
	3	7.2 ± 0.4	119.7 ± 2.4	3.8 ± 0.2	3.1 ± 0.0	2.8 ± 0.0
	5	10.7 ± 0.0	129.9 ± 2.4	7.6 ± 0.1	2.2 ± 0.1	2.5 ± 0.1
	8	12.6 ± 0.1	135.9 ± 2.5	11.0 ± 0.1	1.6 ± 0.1	2.5 ± 0.1
	12	13.7 ± 0.2	139.9 ± 4.4	13.0 ± 0.2	1.0 ± 0.0	2.0 ± 0.1
250°C	0	0	79.0 ± 1.8	0	4.0 ± 0.1	2.4 ± 0.1
	1.5	5.1 ± 0.1	123.7 ± 2.9	3.3 ± 0.1	3.4 ± 0.1	2.6 ± 0.0
	3	10.7 ± 0.2	143.9 ± 1.1	8.1 ± 0.0	2.5 ± 0.0	2.9 ± 0.0
	4.5	13.4 ± 0.2	149.8 ± 1.0	13.5 ± 0.4	1.5 ± 0.1	2.5 ± 0.0
	5.5	14.1 ± 0.1	149.2 ± 3.7	14.6 ± 0.5	1.2 ± 0.0	2.4 ± 0.0

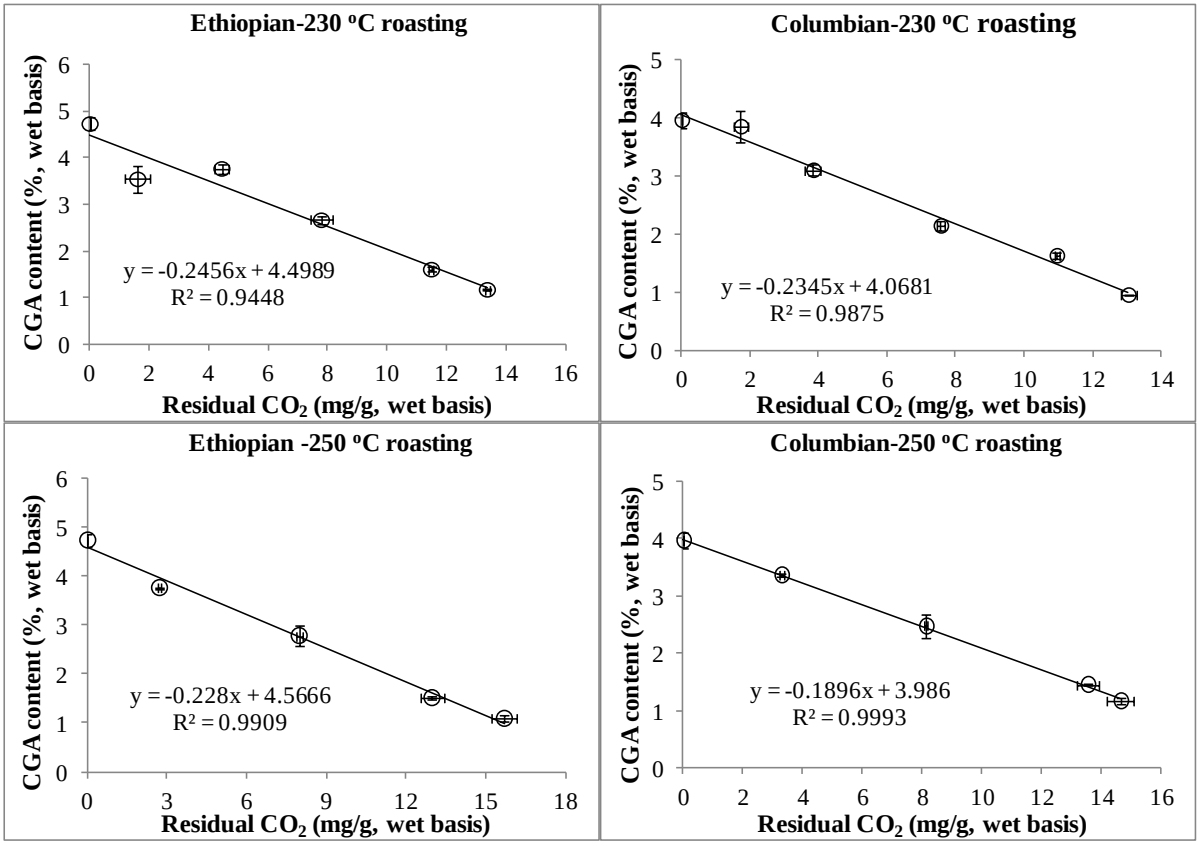

Figure 5.2- Plot of residual CO_2 and total CGA content in roasted coffee, showing strong negative linear correlation.

5.3.2 Thermal degradation of pure CGA under coffee roasting temperatures

Studies in Section 5.3.1 indicated that considerable amount of CGA was degraded during roasting. However, the degradation mechanism remained unclear. To investigate the possible pathway involved during the CGA degradation, the thermal degradation properties of pure CGA under coffee roasting temperatures was studied.

During the thermal treatment in this study, it was observed that the CGA first melted upon heating at around 207 °C, followed by the formation of bubbles as heating continued to progress. In addition, the bubble size was found to grow with the increasing of temperature. This phenomena are consistent with other CGA pyrolysis studies reported in the literature

(Sharma et al. 2000; Sharma, Fisher, and Hajaligol 2002). The weight loss behaviour of CGA under different temperatures is depicted in Figure 5.3, showing that at the same heating time weight loss increased with the increasing of temperature. After 15 min treatment, about 8.2, 10.5, 13.1, and 16.4% of CGA was lost at 210, 230, 250 and 270°C respectively. The semi-log plot shows that weight loss data can be well fitted with logarithmic equation ($R^2 > 0.97$). The slopes of fitted lines were subjected to the Arrhenius plot and activation energy was calculated as 25 kJ/mol (Figure 5.4). This value is significantly lower than that determined by Sharma et al. (2002), who reported an activation energy of 79 kJ/mol based on weight loss for CGA pyrolysis in an inert (non-oxidative) condition at temperature range of 120-750 °C in a tubular reactor. The difference could de due to the different temperature range used and different amount of oxygen involved in the reaction.

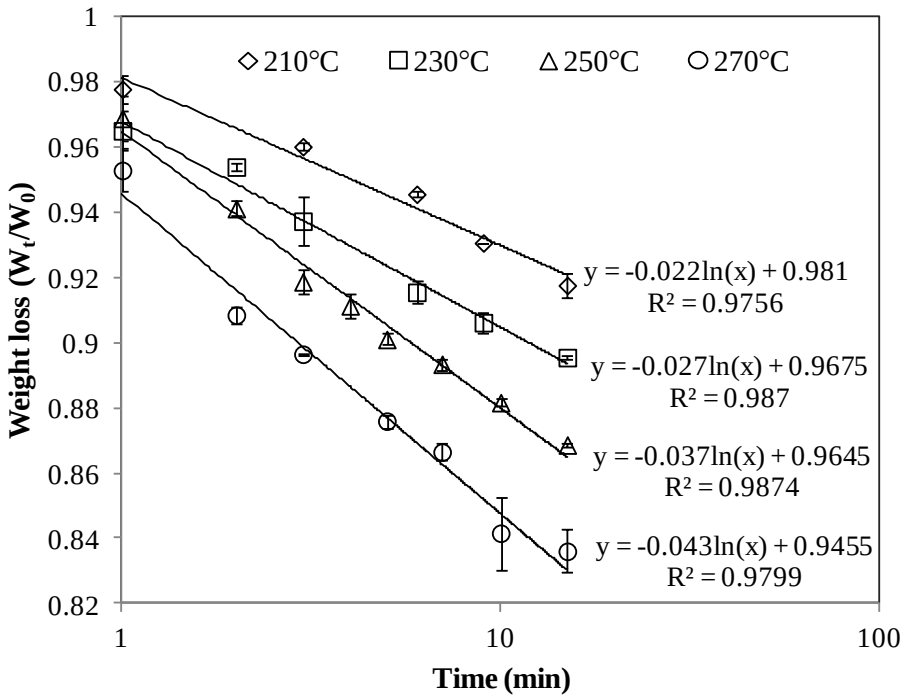

Figure 5.3- Semi-log plot of weight loss kinetics data of CGA in roasting temperature of 210, 230, 250, and 270°C, with the data fitted with logarithmic equation. W_t: weight at roasting time t; W_0: initial weight.

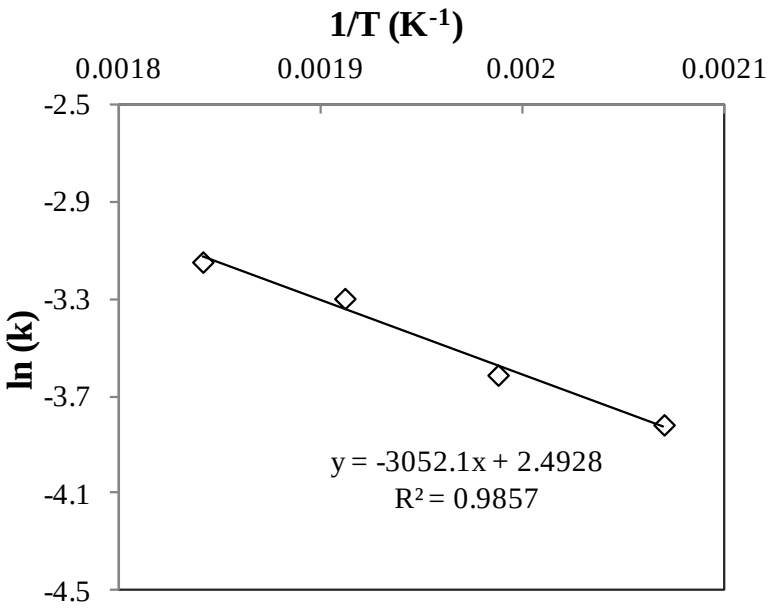

Figure 5.4- Arrhenius plot of weight loss kinetics of CGA heating under coffee roasting temperatures.

The CGA content in the residual chars was evaluated to determine the extent of CGA degradation (Figure 5.5). The results showed rapid degradation of CGA in first two minutes at 270 °C. In comparison, the degradation rates at 250, 230 and 210 °C were lower. Plot of CGA weight loss with degradation ratio indicated their strong correlation. The complete degradation of tested CGA occurred when the weight loss was at ~9 %.

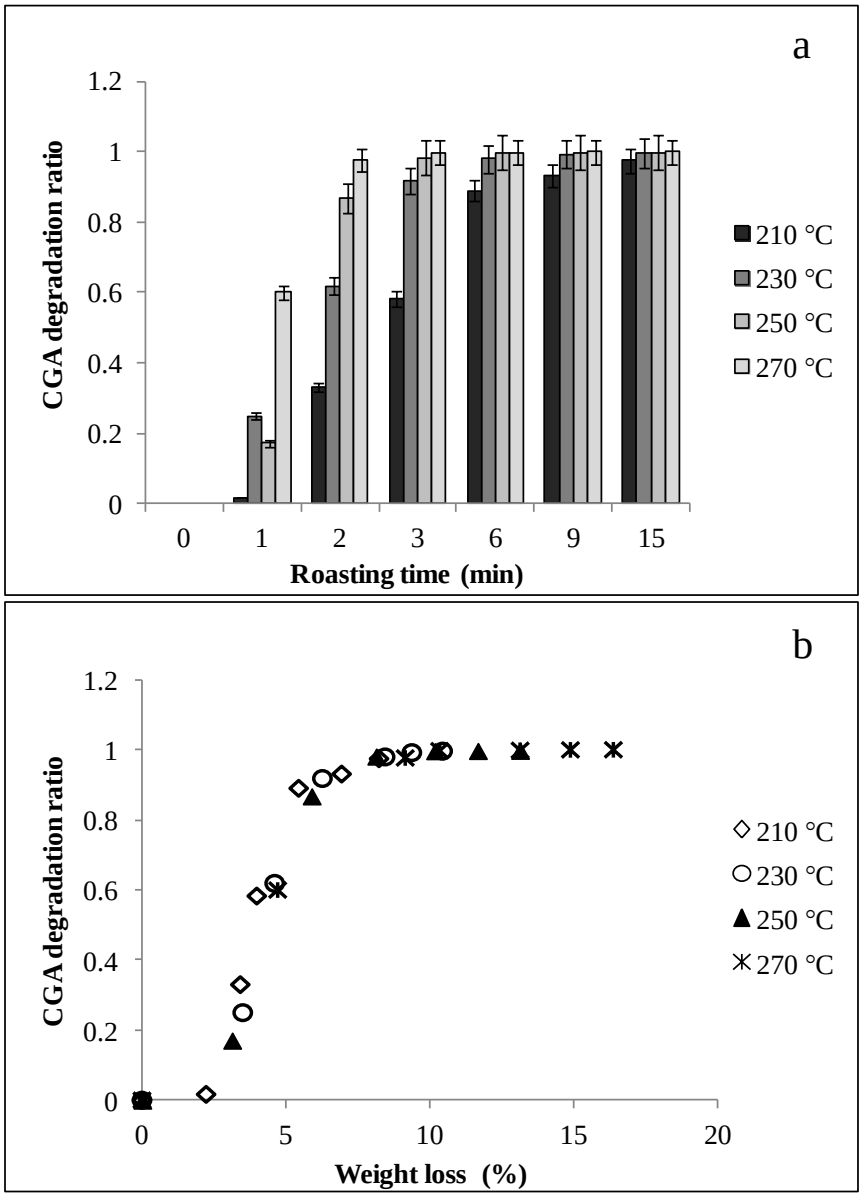

Figure 5.5- CGA degradation ratio under heating temperature of 210, 230, 250, and 270 °C. (a) plot of CGA degradation ratio with roasting time; (b) plot of CGA degradation ratio with roast weight loss.

To investigate the changes in IR active groups of CGA during thermal degradation, FTIR analysis of the residual char was conducted. FTIR spectra analysis of CGA and its two moieties-caffeic acid and quinic acid, allows the identification of CGA's characteristic group. As shown in Figure 5.6, the C=O stretching in quinic acid moiety can be identified by the band at 1681 cm^{-1} wavenumber, while the band at 1639 cm^{-1} wavenumber can be attributed to the C=O stretching for the caffeic acid. The relatively lower C=O vibration wavenumber as compared to those reported in the literature (Lyman et al. 2003; Wang et al. 2009; Wang, Fu, and Lim 2011) indicate that conjugation probably exists among the carbonyl group in CGA. The bands of 1597-1614 cm^{-1} and 1448 cm^{-1} represent the vibration of C=C and the double bond of aromatic ring in the caffeic acid moiety, respectively. The spectral changes in terms of CGA char during heating at temperature of 230°C are depicted in Figure 5.7, showing that considerable changes in the molecular structure of CGA occur. The bands for both hydroxyl (3313 and 3464 cm^{-1}) and carbonyl groups (1681 and 1639cm^{-1}) were progressively become smaller with the increasing of heating time. At 6 min, the C=O absorbance in caffeic acid and quinic acid moiety was basically vanished.

Based on the above results, the CO_2 formation pathway from chlorogenic acid degradation is proposed in Figure 5.8. During coffee roasting, CGA is probably firstly hydrolyzed to quinic acid and the corresponding cinnamic acids. The latter then undergoes decarboxylation to form CO_2 and phenolic volatiles, such as 4-vinylcatechol (Figure 5.8) (Rizzi and Boekley 1993; Clarke and Vitztbum 2001). As for quinic acid, its carbonyl group is more stable than caffeic acid due to the lacking of the C=C bond in the former. However, the vanishing of C=O band as heating progressed indicated that decarboxylation could happen as well (Moon and Shibamoto 2010).

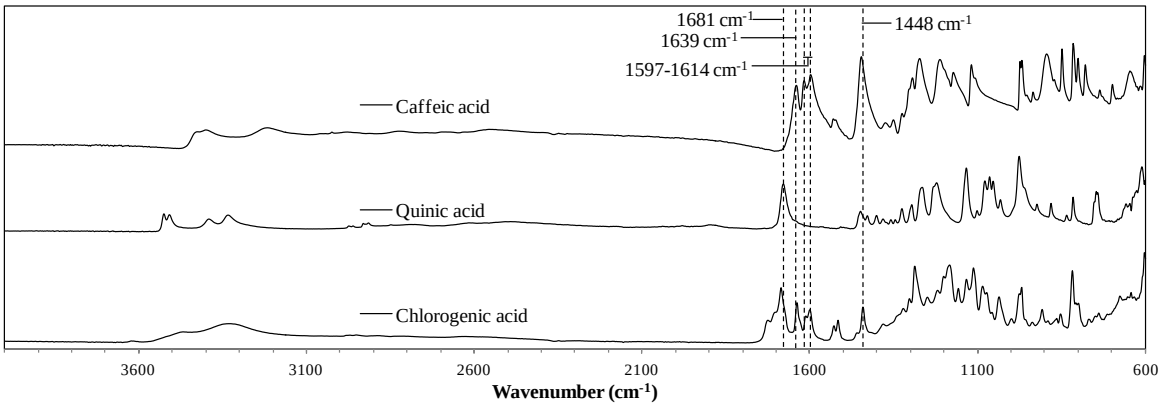

Figure 5.6- FTIR spectra of CGA, caffeic acid and quinic acid, showing wavenumbers of C=O stretching in quinic acid moiety (1681 cm^{-1}) and caffeic acid moiety (1639 cm^{-1}).

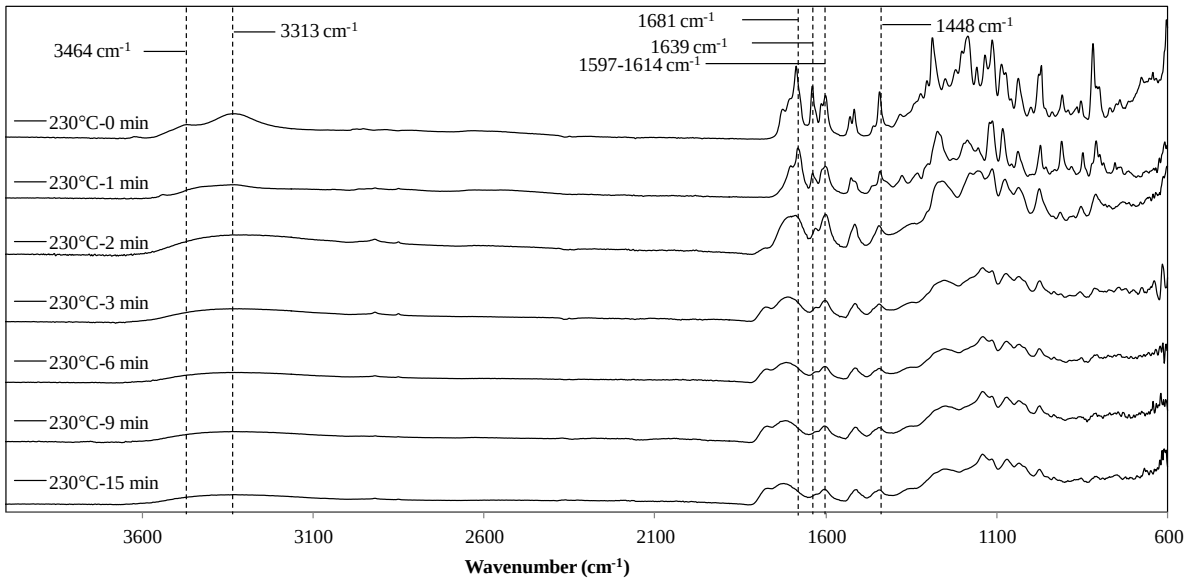

Figure 5.7- FTIR spectra of CGA chars after heating at temperature of 230°C for various times, showing the vanishing of C=O stretching in both quinic acid and caffeic acid moiety.

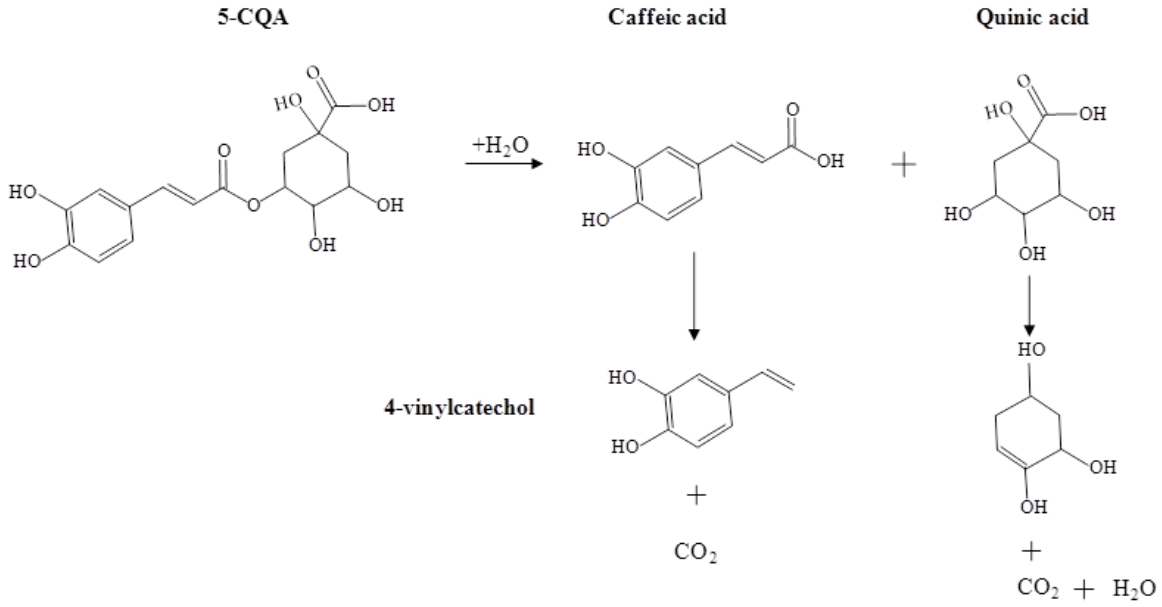

Figure 5.8- The possible CGA degradation mechanism during coffee roasting, taking 5-CQA as an example.

5.3.3 Quantitative analysis of CO_2 formation from CGA, caffeic and quinic acid degradation

In order to test the proposed CO_2 formation mechanism in Figure 5.8, the amount of CO_2 formed during the heating of CGA, caffeic acid and quinic acid was determined by the apparatus as shown in Figure 5.1. The amount of CO_2 generated from CGA heating at 230 °C is shown in Figure 5.9a, showing that about 10 mg of CO_2 was obtained from one gram of CGA. In addition, the amount of CO_2 generated is highly temperature dependent. As shown in Figure 5.9b, more than double of the CO_2 was released at 270 °C compared with 230 °C. The above findings are consistent with those reported by other researchers (Sharma, Fisher, and Hajaligol 2002), where CO_2 has been shown as one of the major volatile compound formed during the pyrolysis of CGA and the CO_2 concentration increased with temperature.

On the basis of the equation from Figure 5.9a, the amount of CO_2 (mg) that could be formed from CGA per gram of Ethiopian green coffee beans at temperature of 230 °C would be:

(1 g× 4.7% × 9.5791) + 0.6024 = 1.1 mg

where 4.7% is the total CGA content in Ethiopian green coffee beans as shown in Table 5.1. Comparing with the residual CO_2 content of roasted Ethiopian coffee in Table 5.1, this calculated value represents less than 10% of the residual CO_2 in the roasted coffee, accounted for a roast loss of ~15%. These results indicate that CGA is a CO_2 precursor, but not the principal one.

To further evaluate the thermal degradation of CGA by products, pure caffeic and quinic acid were heated at 230 °C and their CO_2 produced were monitored. The results indicated around 0.24 g CO_2 was obtained from heating of one gram of caffeic acid, which is equal to ~98% yield of CO_2, assuming the CO_2 formed is derived from decarboxylation mechanism. The caffeic acid degradation is consistent with findings reported by Rizzi and Boekley (1993), who found that cinnamic acids with p-hydroxyl substituent are inclined to decarboxylation degradation upon heating, producing CO_2. On the other hand, no CO_2 was detected from the heating of quinic acid under the same temperature-time conditions. This result suggests that the thermal stability of caffeic and quinic acids are substantially different, and that the degradation of quinic acid may not be through the decarboxylation route. Instead, the quinic acid may form quinide (quinic acid lactone) during heating by losing a water molecule (Clarke and Vitztbum 2001; Farah et al. 2005). The lower yield of CO_2 from CGA degradation as compared to caffeic acid may indicate that the CGA hydrolysis is the limiting step for CO_2 formation from CGA in coffee roasting conditions (Figure 5.8).

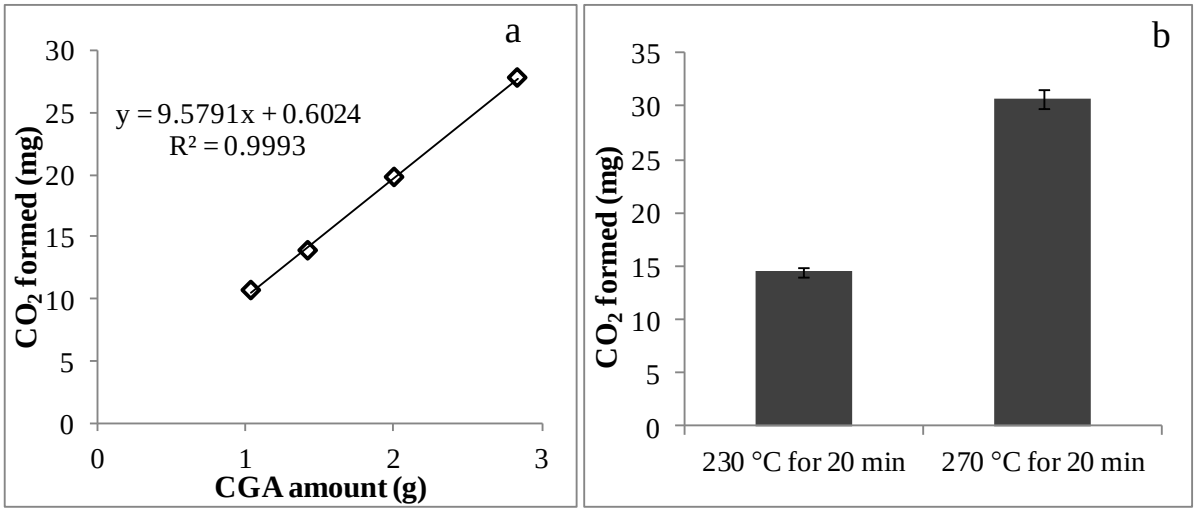

Figure 5.9- Amountof CO_2 formed from CGA heating at 230 °C (a); and the effect of temperature on the obtained CO_2 amount (heating of 1.5 g CGA)(b).

5.3.4 CO_2 formation from CGA spiked green coffee beans

While the model systems discussed above provide some basic understanding on the role of CGA in CO_2 formation, these models are not representative of actual coffee beans consisting of a myriad of components among which complex interactions exist. To better represent the real coffee bean system, "in-bean" experimental techniques were developed to study the role of potential chemical precursors. This approach is based on the use of green coffee beans as "minireactors" to study different reactions. Spiking of untreated green coffee bean with test precursors is one of the approaches of this method. Using this method, Poisson et al. studied the formation pathways of 2-furfurythiol, alkylpyrazines and diketones during coffee roasting (Poisson et al. 2009). The potential of various green bean compounds (chlorogenic acids, caffeine, trigonelline, organic acids, mono-and disaccharides, free amino acids and transition metals) as precursors of thiol-binding sites was investigated by Muller and Hofmann (Muller and Hofmann 2005). In this section, we adopted a similar approach to study the potential precursor compounds of CO_2.

In Section 5.3.3, although we observed low CO_2 yield from heating of the pure CGA, the phenolic compound likely would not exhibit the same properties within the coffee beans, since the existence of many other components in coffee will affect the degradation behaviour. To test the effect of other coffee components on the degradation of CGA, green coffee beans were spiked with CGA. Table 5.2 presents *L*a*b** value for the color developed after roasting of untreated, 0% CGA spiked (control), and 6% CGA spiked green coffee bean at 230 °C for 20 min. To evaluate if the infusion treatment affects the spiking procedure, we measured the *L*a*b** of roasted coffee samples from untreated green coffee and control. Qualitatively, the soaking and drying procedures involved during the spiking process did not result in significant differences in the color development of the control samples as compared with the untreated beans, indicating the validity of the bean model. Next, we evaluated the color of the 6% CGA spiked green coffee beans. Although a darker color was developed on the roasted samples for the spiked beans as compared to the control, the amount of CO_2 formed (residual CO_2 plus those evolved) during roasting were not statistically different ($p>0.05$; Figure 5.10). As shown in Figure 5.10, around 35 mg CO_2 were formed in one gram of green coffee at 230 °C for 20 min, and no significant difference was found between the control and CGA spiked coffee. The above result is consistent with the finding in section 5.3.3 and indicates that CGA is not the major CO_2 precursor.

Table 5.2- Color developed (expressed as *L*a*b** value) after roasting at 230 °C for 20 min

	Untreated green coffee	0 % CGA spiking (control)	6 % CGA spiking
*L**	18.84 ± 0.28	18.31 ± 1.09	17.39 ± 0.51
*a**	5.99 ± 0.15	5.72 ± 0.34	4.72 ± 0.76
*b**	5.76 ± 0.44	5.15 ± 0.52	3.75 ± 0.90

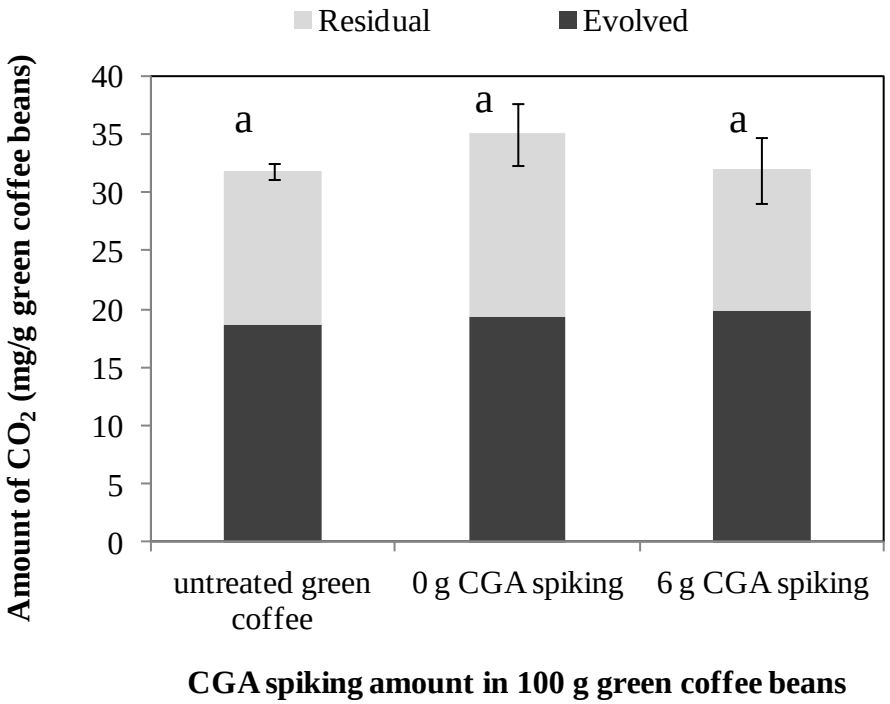

Figure 5.10- Residual CO_2 content and amount of CO_2 evolved during roasting of untreated green coffee, control and 6% CGA spiked coffee at 230 °C for 20 min. Same letter on top of the bar shows there is no significant difference in the total CO_2 formation during roasting.

5.4 Conclusion

Coffee roasting study showed severe degradation of CGA. Moreover, negative linear correlation (R^2>0.9) between residual CO_2 and total CGA content in roasted coffee was observed. The vanishing of carbonyl groups for caffeic acid and quinic acid moieties in FTIR analysis showed that decarboxylation reaction could take place during the CGA thermal degradation under coffee roasting temperature. The above findings indicated CGA as the potential CO_2 precursor in coffee. However, quantification analysis of CO_2 formation during CGA heating at 230 °C obtained only ~8% yield, indicating CGA is a CO_2 precursor but not the principal one. The high yield of CO_2 (>98%) from caffeic acid heating under the same temperature indicated that CGA hydrolysis could be the key rate determining step for CO_2 formation from CGA.

CHAPTER 6 : COMPOSITION OF GREEN COFFEE FRACTIONS AND THEIR CONTRIBUTION TO CO_2 FORMATION DURING ROASTING

6.1 Introduction

The study in Chapter 5 concluded that CGA is a CO_2 precursor but not the principal one, which means that the CGA degradation is not enough to explain the large amount of CO_2 formed during coffee roasting. In addition to CGA degradation, Maillard and Strecker reactions, sugar caramelizttion, as well as thermal degradation of trigonellines, proteins and polysaccharides are also involved during coffee roasting, which could contribute to the formation of CO_2 by various mechanisms.

Strecker degradation has been described as a pathway of CO_2 formation in Maillard series reactions, in which amino acid is degraded by decarboxylation. A number of papers have been published concerning the model reactions of roast aroma formation by treating one or two selected amino acids with sugars under coffee roasting conditions (Baltes and Bochmann 1987a; Baltes and Bochmann 1987b; Baltes and Mevissen 1988; Kunert-kirchhoff and Baltes 1990; Wiiken and Baltes 1990). However, no similar studies regarding CO_2 formation is found in the literature, indicating that there is a lack of knowledge in terms of the contribution of Maillard reactions to CO_2 formation for roasted coffee beans.

In Chapter 5, the hypothesis of "CGA is the principal CO_2 precursor" is rejected. Therefore, further experiments were carried out in the present study in an attempt to elucidate the CO_2 formation in roasted coffee by using the amino acid-sugar model system. In addition, the contribution of various green coffee fractions (namely water insoluble fraction, water

soluble lower molecular fraction, and water soluble higher molecular fraction) to CO_2 formation was elucidated.

6.2 Materials and methods

Columbian (Excelso European Preparation) green coffee were supplied by Mother Parkers Tea & Coffee (Mother Parkers Tea & Coffee Inc., Mississauga, ON, Canada). Sodium hydroxide, tri-sodium citrate, Drierite^{TM} desiccant, Ascarite® II column (sodium hydroxide coated silica gel), glycine, proline, glutamic acid and sucrose were all purchased form Fisher Scientific International Inc. (Ottawa, ON, Canada). CGA was purchased from Changsha Ya Ying Bio-Technology Co., Ltd. (Changsha, Hunan, China).

6.2.1 Coffee roasting and kinetics of CO_2 formation

25 g green coffee beans were subjected to the roasting at 230 °C for various times (5, 10, 15, 20, 25, 30 min) using the apparatus in Figure 5.1. The CO_2 generated during coffee roasting includes the part evolved during roasting and the part trapped in the coffee matrix after roasting. The evolved CO_2 during roasting was determined by the method as described in section 5.2.8, and residual CO_2 was determined using the method in section 3.2.4. Therefore, the CO_2 formation kinetics was obtained. The roast loss, and L^* a^* b^* values of the above roasted coffee samples were measured to indicate the degree of roast using the method described in section 3.2.2 and 3.2.3.

6.2.2 Amino acid-sugar roasting reaction model

Heating experiments were conducted using the apparatus as shown in Figure 5.1. Different combinations of reactants (Table 6.1) were homogenous mixed in volumetric flask for 2-3 min. The flask was then placed in the oven maintained at 230 °C, and heated for 20 min. The CO_2 evolved from the reaction was determined by using the method as described in 5.2.8.

Table 6.1- Low moisture glycine-sucrose roasting reaction model

Reactants	Reactant concentration (mM)													
	1	2	3	4	5	6	7	8	9	10	11	12	13	14
Sucrose	4		8		4	8	4	8	4	8	4	8	4	8
Glycine		4		8	4	8	8	4	4	8	8	4	8	4
CGA									4	8	4	4	8	8

6.2.3 Isolation of green coffee fractions

A sequential fractionation procedure, adapted from De Maria et al. (1994), was used to isolate specific fractions from green coffee (Figure 6.1). In this method, 300 g of ground coffee, with particles size ranging from 1.70-2.38 mm in diameter, was extracted for 15 min with 1 L hot distilled water (80 °C) with the aid of magnetic stir bar. The extraction process was repeated for four times to make sure the complete extraction of water soluble fraction. The insoluble fraction (D) and water soluble fraction (A) were separated by filtration and then freeze-dried. 20 g sample of fraction (A) was dissolved in 25 mL of distilled water (50 °C) and 100 mL 80% ethanol was then added. The mixture was shaken for 30 min and

centrifuged at 100 g for 10 min. The supernatant was collected and the residue was dissolved in water and extracted with ethanol again for two more times. The combined supernatants (fraction B) and residue (fraction C) were freeze-dried separately.

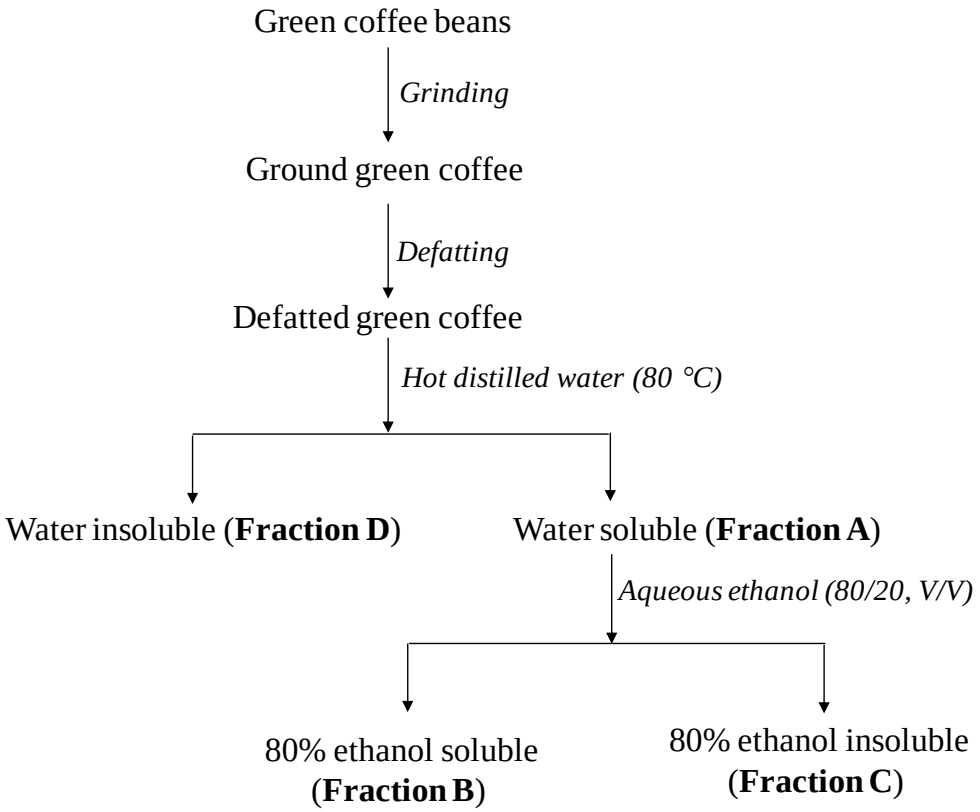

Figure 6.1- Fraction isolation process from green coffee

6.2.4 Roasting of isolated fractions

The freeze-dried isolated green coffee fractions, i.e., water soluble fraction A, water insoluble fraction D, 80% ethanol soluble fraction B, and 80% ethanol insoluble fraction C, were subjected to roasting separately at 230°C for 25 min using the apparatus as illustrated in Figure 5.1. The CO_2 formed during roasting was detected using the same method described in Section 5.2.8. For the water insoluble fraction D, the roasted sample was collected and

subjected to residual CO_2 measurement. The total CO_2 formed from this fraction is the sum of residual CO_2 and CO_2 evolved during roasting.

6.3 Results and discussion

6.3.1 CO_2 formation kinetics during coffee roasting

The amounts of CO_2 formed during coffee roasting at 230 °C, including residual CO_2 and CO_2 evolved, are presented in Figure 6.2. As shown, the amount of CO_2 increased with the increasing of roast time. In agreement with the finding from Chapter 3, the residual CO_2 increased with roasted degree to around dark roast (Table 6.2), thereafter a decrease in residual CO_2 was observed, indicating that roasting behaviours of coffee beans in experimental setup as shown in Figure 5.1 was similar to those in fluidized bed roaster (Figure 3.1). In contrast, the amount of CO_2 evolved increased with the roast degree throughout the entire roasting process. At the maximum roasting time (30 min), around 42 mg of CO_2 was formed from one gram of green coffee beans. Figure 6.2 also indicates that the ratio of the evolved CO_2 to residual CO_2 increased from 0.1 at 5 min to 8.7 as roast time increased from 5 to 30 min, implying that there was a decreasing of CO_2 trapping ability of the coffee beans as roast time increased. This observation can be attributed to the decreasing reactants in coffee that produce CO_2, as well as the increase diffusion loss of the entrapped CO_2 due to the extended exposure to the elevated temperature.

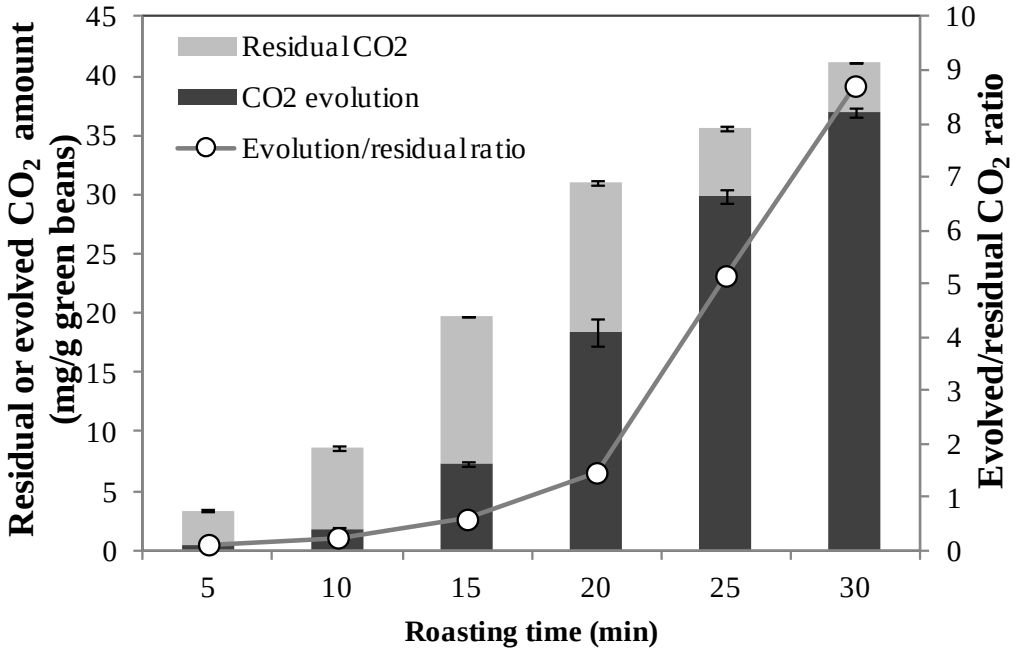

Figure 6.2- CO_2 formation (residual + evolved) and the ratio of evolved to residual CO_2 amount during coffee roasting under roasting temperature of 230 °C by using the apparatus as shown in Figure 5.1.

Table 6.2- Roast loss and *L**, *a**, *b** value of roasted coffee samples (Figure 6.2), indicating the degree of roast.

Roasting time (min)	Roast loss (%)	*L**	*a**	*b**	Degree of roast
5	5.54 ± 0.02	38.87 ± 0.45	10.46 ±1.51	21.22 ± 1.80	Very light
10	9.70 ± 0.24	31.55 ± 0.13	12.29 ± 0.08	20.21 ± 0.10	Light
15	14.30 ± 0.01	21.68 ± 0.35	8.73 ± 0.04	9.92 ± 0.24	Medium-dark
20	17.66 ± 0.04	18.84 ± 0.28	6.00 ± 0.15	5.76 ± 0.44	Very dark
25	20.43 ± 0.04	17.52 ± 0.24	4.73 ± 0.05	4.14 ± 0.16	Very dark
30	22.58 ± 0.01	16.84 ± 0.32	3.77 ± 0.15	2.93 ± 0.48	Very dark

6.3.2 CO_2 formation from heating of amino acid or sugar under coffee roasting conditions

The monosaccharide content is relatively low in green coffee and sucrose is the main low molecular weight carbohydrate (Clarke and Vitztbum 2001). The CO_2 amount formed from heating of sucrose under temperature of 230 °C is shown in Figure 6.3. As shown, ~0.0034 g CO_2 was formed from heating 0.004 mol of sucrose (equal to 1.3692 g) at 230 °C for 20 min. The CO_2 amount doubled when 0.008 mol sucrose (equal to 2.7384g) was used. Given the sucrose content in Arabica green coffee of 6-8.5% (Clarke and Vitztbum 2001), the theoretical amount of CO_2 that would form from sucrose degradation during roasting would be 0.15-0.21 mg per gram of green coffee beans. In comparison with the value in Figure 6.2 (~30 mg/g green coffee at 230 °C for 20 min), it can be concluded that the contribution of sucrose degradation to CO_2 formation in coffee is very minimal.

Figure 6.3 also shows that the CO_2 formation from glycine roasting at 230 °C was limited as well, although the amount was higher than that from sucrose at the same molar mass. About 0.0089 g of CO_2 was formed from heating 0.004 mol of glycine (equal to 0.3003 g). Other amino acids, including glutamic acid and proline, were also tested. At the same molar mass, the CO_2 amount formed from heating of glutamic acid and prolines were less than that from glycine roasting (data not shown). These findings show that the sucrose and the tested amino acids, independently, are not the main precursor for CO_2 formation.

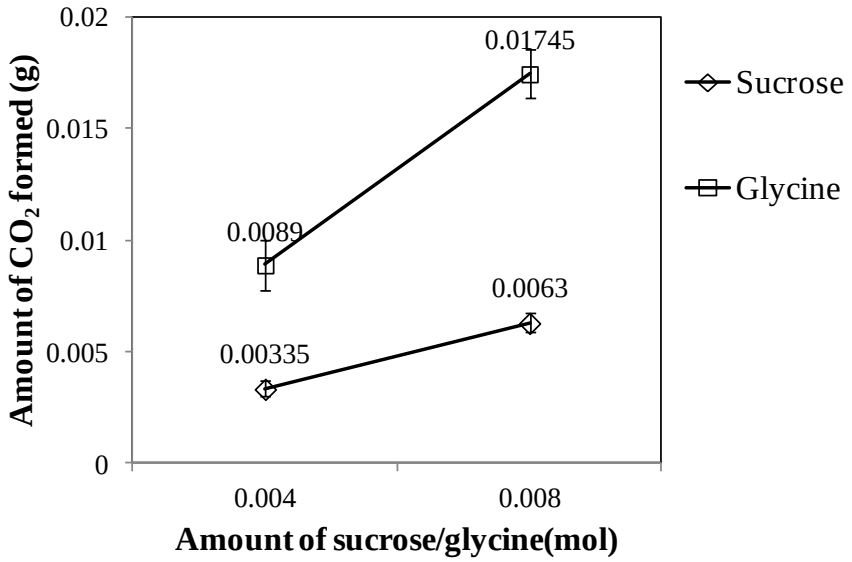

Figure 6.3- Amount of CO_2 formed from heating of sugar or amino acid (glycine) under coffee roasting temperature of 230°C for 20 min.

6.3.3 CO_2 formation from roasting of amino acid-sucrose mixture under coffee roasting conditions

Data in section 6.3.2 show that a minimal amount of CO_2 was formed from the heating of sucrose or amino acid separately. However, when mixture of glycine and sucrose was heated, the Maillard reactions took place and large amount of CO_2 was formed (Figure 6.4). For example, ~0.17 g CO_2 was formed from the roasting of 0.004 mol glycine-sucrose mixture as compared to 0.0124 g CO_2 from the sum of sucrose and glycine roasting separately. If Strecker degradation is the only pathway for CO_2 formation, the theoretical amount of CO_2 formed would be 0.176 g and 0.352 g for 0.004 mol glycine-sucrose mixture and 0.008 mol glycine-sucrose mixture, respectively. These calculated values are comparable with those from the experimental data (0.1719 and 0.3301 g), implying that CO_2 was mainly derived from the glycine structure. However, the amount of CO_2 determined (0.2147 g) from the mixture of 0.008 mol sucrose and 0.004 glycine implies that the CO_2 was also generated

from the sucrose skeleton. Moreover, the amount of CO_2 determined (0.2305 g) from the mixture of 0.004 mol sucrose and 0.008 mol glycine implies that sucrose also plays an important role.

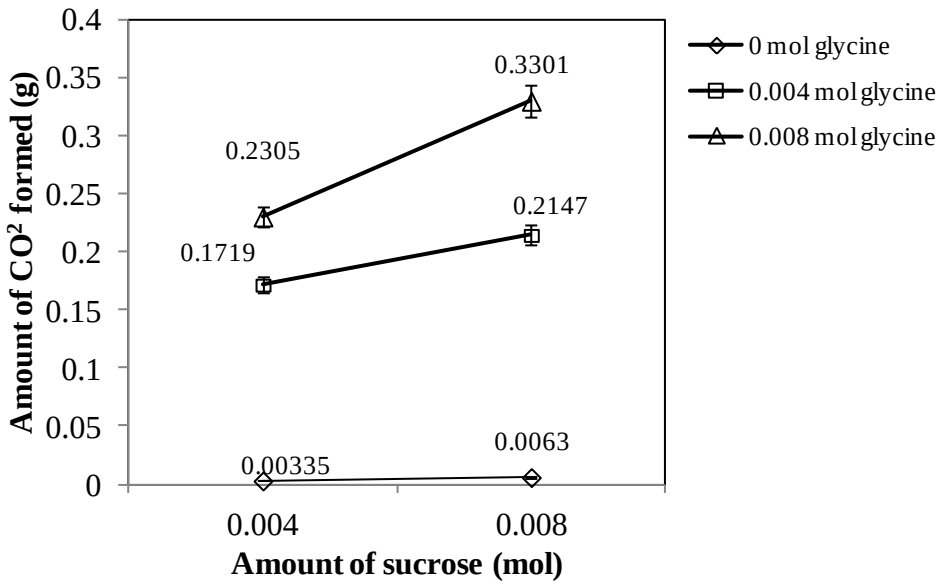

Figure 6.4- Amount of CO_2 formed from roasting of sugar and amino acid (glycine) mixture under coffee roasting temperature of 230 °C for 20 min.

6.3.4 Effect of addition of CGA on CO_2 formation in glycine-sucrose model system

To study the effect of CGA, the phenolic compound was added to the glycine-sucrose model system, and the amounts of CO_2 generated are presented in Figure 6.5. As shown, the addition of CGA decreased the amount of CO_2 formation in the four combinations of model system investigated. This could be explained by the radical scavenging capability of CGA. The suppression behaviours of CGA and other cinnamic acids on the generation of some Maillard flavour compounds, such as pyrazine and Strecker aldehydes, have been reported by previous researches (Wang 2000; Jiang et al. 2009; Jiang and Peterson 2009). The mechanism of CGA's suppression behaviour on Maillard reaction was put forward by Wang (Wang 2000), which attributed to the radical scavenging capability of hydroxycinnamic acids.

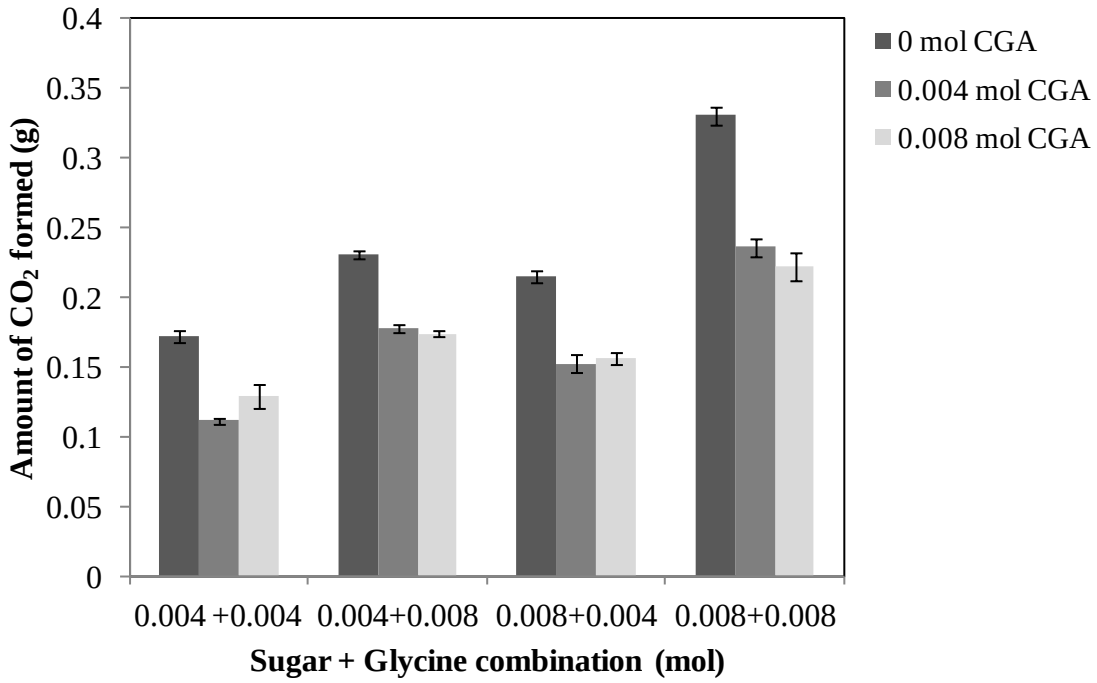

Figure 6.5- Effect of addition of CGA on CO_2 formation in sucrose-glycine Maillard model reaction system.

6.3.5 Fragmentation of green coffee components and their contribution to CO_2 formation

Results in Section 6.3.3 showed that large amount of CO_2 was generated from Maillard reaction under common coffee roasting temperature, implying the importance of free amino acid and sugar for CO_2 generation during coffee roasting. However, the limited contents of free amino acid (0.2-0.8%) and sugar (6-9%) in green coffee beans indicate that there are also some other compounds which could be CO_2 precursors.

To explore other CO_2 precursors, an isolation procedure was adopted to separate the green coffee components into water insoluble fraction, water soluble higher molecular weight fraction, and water soluble low molecular weight fraction, and the contribution of each fraction to CO_2 formation in coffee roasting was investigated. The mass percentage of each

fractions isolated from green coffee is shown in Figure 6.6a and their contributions to the CO_2 formation is presented in Figure 6.6b. As shown, in green coffee, ~68.5% of the material was water insoluble components (fraction D), which mainly included water insoluble proteins and higher molecular weight polysaccharides. The remaining components were water soluble fraction A with 6.3% insoluble in ethanol (fraction C) and 25.2% soluble in ethanol (fraction B). The fraction C mainly contained water soluble proteins and arabinogalactans, while the fraction B consisted of small molecular weight compounds such as sucrose, trigonelline, CGA, amino acids and peptides (De Maria et al. 1994; De Maria et al. 1996). The fractions A, B, C, D obtained from the sequential fractionation procedure were subjected to roasting process at 230 °C for 25 min, and the CO_2 evolved during the process was recorded (Figure 6.6b). As shown, fraction B contributed to around half of the CO_2 formed during the roasting process, while fraction D only contributed to ~20%. CO_2 was also generated from roasting of fraction C, which could be attributed to the reactions between monosaccharide from arabinogalactan degradation with ε-amino group of lysine and the α-amino groups of terminal amino acids in proteins. By comparing the amount of CO_2 generated during coffee roasting to the sum of CO_2 from the roasting of fractions A and D, a unaccounted gap of ~24% of CO_2 from coffee roasting was found. The reason for this unaccounted fraction is unknown, but could be attributed to the interaction between these two fractions.

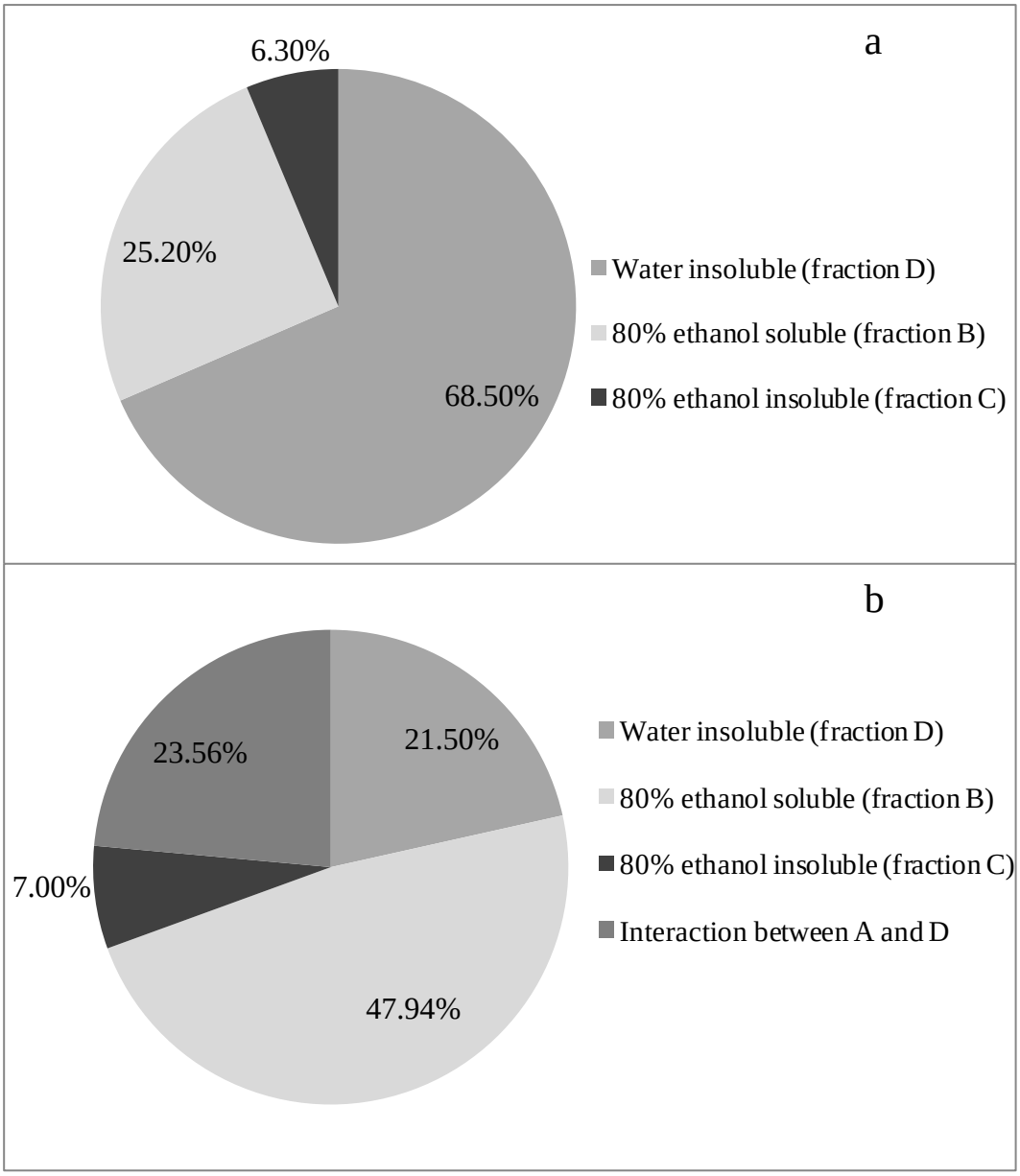

Figure 6.6- Weight distribution of each coffee fraction (a) and their contribution to the amount of CO_2 formation (b).

6.4 Conclusion

This study showed that a large amount of CO_2 was formed from glycine-sucrose roasting model system under coffee roasting conditions, implying the important role of Maillard reactions in CO_2 formation during coffee roasting. Moreover, the addition of CGA

into glycine-sucrose model was found to inhibit the formation of CO_2, due to the radical scavenging capacity of the phenolic compound. The isolation and roasting studies of green coffee fractions showed that CO_2 was generated from various green coffee components, including water insoluble proteins and polysaccharides. Around 50% of CO_2 was formed from thermal reactions of lower molecular weight compounds with this fraction representing ~25% by weight in green coffee. In addition, the sum of CO_2 amount from roasting of those four fractions was found to be lower than the total CO_2 formed during coffee roasting, indicating the existence of unidentified interaction among these fractions.

CHAPTER 7 : CONCLUSION AND RECOMMENDATIONS

This study investigated the CO_2 precursors and CO_2 formation and degassing behaviour as affected by coffee roasting temperature-time conditions, aimed at establishing the fundamental understanding needed to further explore the solution of CO_2 degassing problem in packaging area.

In the first part of the study, the residual CO_2 content as affected by the roasting temperature-time conditions was investigated. Moreover, other physicochemical properties including color, roast loss and volatile compounds, which indicate the degree of roast, were studied as well to explore their relation with residual CO_2. A two-stage behaviour was found for the kinetics of L^* and roast loss with the transition taking place when coffee was roasted to around medium roast. Moreover, significant higher activation energy value was calculated for the second stage. As for the residual CO_2, its content increased with the roasting time until around dark roast and then decreased with further roasting due to the structural changes. Before dark roast, residual CO_2 was found to only depend on the roast degree (expressed as L^* value) and was independent from roasting temperature, which makes L^* an indicator of residual CO_2 content in roasted coffee. Volatile compounds in roasted coffee are very complex and their formation is superimposed by an accelerated decay of some aroma compounds during the final roasting stage. In addition, the profiles of the volatile compounds were highly dependent on the roasting temperature.

In the second section of the study, the CO_2 degassing behaviour as affected by roasting temperature-time conditions was investigated. The CO_2 degassing rate was affected by both roasting temperature and roasting level. High temperature roasted coffee was found to cause significantly higher CO_2 degassing rate as compared to low temperature roasted

coffee. Expectedly, grinding resulted in a loss of large quantity of residual CO_2 depending on the grinding size. CO_2 degassing in ground coffee was significantly faster than in whole beans due to the reduced diffusion distance and large surface to volume ratio. In addition, the increasing of environmental temperature and RH significantly increased the CO_2 degassing rate. Therefore, the roasted coffee conditioning process and degassing valve design should take the roasting temperature-time conditions, coffee grinding size as well as environmental temperature and RH into consideration.

As a major carbonyl containing compound in green coffee bean, CGA was investigated as the principal CO_2 precursor in Chapter 5. Although strong negative correlation between total CGA content and residual CO_2 was found and the disappearance of C=O stretching bands from caffeic acid and quinic acid moiety was observed in the FTIR analyses, quantitative analysis showed that CGA was not the principal CO_2 precursor in coffee. The above conclusion leads to a further study of CO_2 precursors in Chapter 6, where the contributions of various green coffee fractions to the CO_2 formation were investigated. It was found that CO_2 was generated from various green coffee components, including water insoluble proteins and polysaccharides. Around 50% of CO_2 was formed from thermal reactions of lower molecular compounds with this fraction representing ~25% content in green coffee.

Overall, this thesis research has established some fundamental understanding of how CO_2 is formed and degassed, which may serve as a foundation for future research. Based on the results gathered and the phenomena observed during the course of this research, the following recommendations can be made for future studies:

(1) Effect of roasting temperature-time conditions on residual CO_2 content and its degassing behaviour in Robusta roasted coffee. Robusta coffee is an important coffee species

which generally blend with Arabica coffee. Robusta coffee has different chemical compositions, such as higher CGA and caffeine content and lower sugar and oil content than Arabica, which may result in different CO_2 formation and degassing behaviour.

(2) *Effect of roasting conditions on micropores in roasted coffee.* The cell wall porosity test by mercury porosimetry did not reveal any detectable cell wall porosity differences between HTST and LTLT roasted coffee due to the limitation of the technique. Therefore, the pore size below the test range (<3.6 nm) can be tested by gas absorption method which is able to test pore size from 0.55 nm to 350 nm. CO_2 can be used as the gas to obtain the full absorption/desorption isotherm for finely ground coffee. From the isotherm, the pore size distribution and pore volume information will be obtained.

(3) *Effect of roasting and environmental conditions on CO_2 degassing and volatile aroma compounds releasing.* CO_2 degassing study suggested CO_2 degassing is a slow process especially in LTLT roasted whole coffee beans. During this process, the coffee loses quality due to the releasing of volatile aroma compounds and oxidation reactions. Therefore, the effect of CO_2 degassing process on volatile aroma compounds releasing should be evaluated.

CHAPTER 8 : REFERENCES

Ajandouz EH, Tchiakpe LS, Dalle Ore F, Benajiba A, Puigserver A. 2001. Effects of pH on caramelization and Maillard reaction kinetics in fructose-lysine model systems. J. Food Sci. 66:926–931.

Akiyama M, Murakami K, Hirano Y, Ikeda M, Iwatsuki K, Wada A, Tokuno K, Onishi M, Iwabuchi H. 2008. Characterization of headspace aroma compounds of freshly brewed Arabica coffees and studies on a characteristic aroma compound of Ethiopian coffee. J. Food Sci. 73:C335–C346.

Alessandrini L, Romani S, Pinnavaia G, Dalla Rosa M. 2008. Near infrared spectroscopy: an analytical tool to predict coffee roasting degree. Anal. Chim. Acta 625:95–102.

Anderson BA, Shimoni E, Liardon R, Labuza TP. 2003. The diffusion kinetics of carbon dioxide in fresh roasted and ground coffee. J. Food Eng. 59:71–78.

Andrade RDP, Lemus RM, Perez CEC. 2011. Models of sorption isotherms for food: uses and limitations. Vitae 18:325–334.

Anon. Data for calender year commencing-2010-Canada.

Anon. 2011. Coffee Lab: Agtron Test and Degree of Roast. Available from: http://www.coffeeanalysts.com/2011/07/coffee-lab-agtron-test-and-degree-of-roast/

Baggenstoss J, Poisson L, Kaegi R, Perren R, Escher F. 2008. Coffee roasting and aroma formation: application of different time-temperature conditions. J. Agric. Food Chem. 56:5836–5846.

Baggenstoss J, Poisson L, Luethi R, Perren R, Escher F. 2007. Influence of water quench cooling on degassing and aroma stability of roasted coffee. J. Agric. Food Chem. 55:6685–6691.

Bakalis S, Kyritsi A, Karathanos VT, Yanniotis S. 2009. Modeling of rice hydration using finite elements. J. Food Eng. 94:321–325.

Baltes W, Bochmann G. 1987a. Model reactions on roast aroma formation: reaction of serine and threonine with sucrose under the conditions of coffee roasting and identification of new coffee aroma compounds. J. Agric. Food Chem. 35:340–346.

Baltes W, Bochmann G. 1987b. Model reactions on roast aroma formation: mass spectrometric identification of pyrazines from the reaction of serine and threonine with sucrose under the conditions of coffee roasting. Z. Leb. Unters. Forsch. 184:485–493.

Baltes W, Mevissen L. 1988. Model reactions on roast aroma formation: volatile reaction products from the reaction of phenylalanine with glucose during cooking and roasting. Z. Leb. Unters. Forsch. 187:209–214.

Bekedam EK. 2008. Coffee brew melanoidins: structural and functional properties of brown-colored coffee compounds. Wageningen University, Netherlands.

Belitz HD, Grosch W, Schieberle P. 2009. Chapter 21: Coffee, tea, cocoa. In: Food Chemisty. Verlag Berlin Heidelberg: Springer. p. 938–970.

Bell LN. 1996. Kinetics of non-enzymatic browning in amorphous solid systems : distinguishing the effects of water activity and the glass transition. Methodology 28:591–597.

Bemiller JN, Huber KC. 2008. Chapter 3: Carbohydrates. In: Damodaran S, Parkin KL, Fennema OR, editors. Food Chemistry. Fourth. Boca Raton: CRC Press. p. 101–102.

Berger RG. 2007. Flavours and Fragrances: Chemistry, Bioprocessing and Sustainability. New York: Springer.

Bhattacharya S. 1996. kinetics on colour changes in rice due to parboiling. J. Food Eng. 29:99–106.

Bicchi CP, Panero OM, Pellegrino GM, Vanni AC. 1997. Characterization of roasted coffee and coffee beverages by solid phase microextraction-gas chromatography and principal component analysis. J. Agric. Food Chem. 45:4680–4686.

Van Boekel MAJS. 2006. Formation of flavour compounds in the Maillard reaction. Biotechnol. Adv. 24:230–233.

Buffo RA, Cardelli-Freire C. 2004. Coffee flavour: an overview. Flavour Fragr. J. 19:99–104.

Campa C, Doulbeau S, Dussert S, Hamon S, Noirot M. 2005. Qualitative relationship between caffeine and chlorogenic acid contents among wild species. Food Chem. 93:135–139.

Cardelli C, Labuza TP. 2001. Application of Weibull hazard analysis to the determination of the shelf life of roasted and ground coffee. Leb. u.-Technol. 34:273–278.

Casal S, Oliveira MB, Ferreira MA. 2000. HPLC / diode-array applied to the thermal degradation of trigonelline, nicotinic acid and caffeine in coffee. Food Chem. 68:481–485.

Clarke RJ, Macrae R. 1987. Coffee Volume 2: Technology. New York: Elsevier Applied Science.

Clarke RJ, Vitztbum OJ. 2001. Coffee: Recent Development. Oxford: Blackwell Science.

Clifford MN, Kazi T. 1987. The influence of coffee bean maturity on the content of chlorogenic acids, caffeine and trigonelline. Food Chem. 26:59–69.

Corzo O, Bracho N, Pereira A, Vásquez A. 2008. Weibull distribution for modeling air drying of coroba slices. LWT - Food Sci. Technol. 41:2023–2028.

Craig ID, Parker R, Rigby NM, Cairns P, Ring SG. 2001. Maillard reaction kinetics in model preservation systems in the vicinity of the glass transition: experiment and theory. J. Agric. Food Chem. 49:4706–4712.

Cunningham SE, McMinn WAM, Magee TRA, Richardson PS. 2007. Modelling water absorption of pasta during soaking. J. Food Eng. 82:600–607.

Cussler EL. 2009. Diffusion: Mass Transfer in Fluid systems. 3rd ed. New York: Cambrige University Press.

Czerny M, Mayer F, Grosch W. 1999. Sensory study on the character impact odorants of roasted arabica coffee. J. Agric. Food Chem. 47:695–699.

D'Amelio N, Fontanive L, Uggeri F, Suggi-Liverani F, Navarini L. 2009. NMR reinvestigation of the caffeine-chlorogenate complex in cqueous solution and in coffee brews. Food Biophys. 4:321–330.

Datta AK. 2007. Porous media approaches to studying simultaneous heat and mass transfer in food processes. I: Problem formulations. J. Food Eng. 80:80–95.

Davis AP, Govaerts R, Bridson DM, Stoffelen P. 2006. An annotated taxonomic conspectus of the genus Coffea (Rubiaceae). Bot. J. Linn. Soc. 152:465–512.

Dorfner R, Ferge T, Yeretzian C, Kettrup A, Zimmermann R. 2004. Laser mass spectrometry as on-line sensor for industrial process analysis: process control of coffee roasting. Anal. Chem. 76:1386–1402.

Dutra ER, Oliveira LS, Franca AS, Ferrza VP, Afonso RJCF. 2001. A preliminary study on the feasibility of using the composition of coffee roasting exhaust gas for the determination of the degree of roast. J. Food Eng. 47:241–246.

Farah A, Donangelo CM. 2006. Phenolic compounds in coffee. Brazilian J. Plant Physiol. 18:23–36.

Farah A, de Paulis T, Trugo LC, Martin PR. 2005. Effect of roasting on the formation of chlorogenic acid lactones in coffee. J. Agric. Food Chem. 53:1505–1513.

Fen C-S, Liang W, Hsiesh P, Huang Y. 2011. Knudsen and molecular diffusion coefficients for gas transport in unconsolidated porous media. Soil Sci. Soc. Am. J. 75:456–467.

Fischer M, Reimann S, Trovato V, Redgwell RJ. 2001. Polysaccharides of green Arabica and Robusta coffee beans. Carbohydr. Res. 330:93–101.

Franca AS, Oliveira LS, Oliveira RCS, Agresti PCM, Augusti R. 2009. A preliminary evaluation of the effect of processing temperature on coffee roasting degree assessment. J. Food Eng. 92:345–352.

Geiger R, Perren R, Kuenzli R, Escher F. 2005. Carbon dioxide evolution and moisture evaporation during roasting of coffee beans. Food Eng. Phys. Prop. 70:124–130.

Gennadios A, Weller CL. 1994. Moisture adsorption by grain protein films. Am. Soc. Agric. Eng. 37:535–539.

Goneli ALD, Corrêa PC, Oliveira GHH, Afonso Júnior PC. 2013. Water sorption properties of coffee fruits, pulped and green coffee. LWT-Food Sci. Technol. 50:386–391.

Grosch W. 1998. Flavour of coffee. A review. Nahrung 42:344–350.

Hayakawa K, Matas JT, Hwang MP. 1978. Moisture soprtion isotherms of coffee products. J. Food Sci. 43:1026–1027.

Higdon J V., Frei B. 2006. Coffee and health: a review of recent human research. Crit. Rev. Food Sci. Nutr. 46:101–123.

Hodge JE. 1953. Chemisty of brownig reaction in model system. J. Agric. Food Chem. 1:928–943.

Illy A, Viani R. 1995. Espresso Coffee: the Chemistry of Quality. San Diego: Elsevier Academic Press.

Illy A, Viani R. 2005. Espresso Coffee-the Science of Quality. Second. San Diego: Elsevier Academic Press.

Jiang D, Chiaro C, Maddali P, Prabhu KS, Peterson DG. 2009. Identification of hydroxycinnamic acid-maillard reaction products in low-moisture baking model systems. J. Agric. Food Chem. 57:9932–9943.

Jiang D, Peterson DG. 2009. Role of hydroxycinnamic acids in food flavor: a brief overview. Phytochem. Rev. 9:187–193.

Kast W, Hohenthanner CR. 2000. Mass transfer within the gas-phase of porous media. Int. J. Heat Mass Transf. 43:807–823.

Koca N, Burdurlu HS, Karadeniz F. 2007. Kinetics of colour changes in dehydrated carrots. J. Food Eng. 78:449–455.

Kolling-Speer I, Strohschneider S, Speer K. 1999. Determination of free diterpenes in green and roasted coffees. J. High Resolut. Chromatogr. 22:43–46.

Kunert-kirchhoff J, Baltes W. 1990. Model reactions on roast aroma formation: specific products of phenylalanine after cooking L-phenylalanine with D-glucose in a laboratory autoclave. Z. Leb. Unters. Forsch. 190:9–13.

Ky C-L, Louarn J, Dussert S, Guyot B, Hamon S, Noirot M. 2001. Caffeine, trigonelline, chlorogenic acids and sucrose diversity in wild Coffea arabica L. and C. canephora P. accessions. Food Chem. 75:223–230.

Ky C-L, Noirot M, Hamon S. 1997. Comparison of five purification methods for chlorogenic acids in green coffee beans (Coffea sp.). J. Agric. Food Chem. 45:786–790.

Lievonen SM, Laaksonen TJ, Roos YH. 1998. Glass transition and reaction rates : nonenzymatic browning in glassy and liquid systems. J. Agric. Food Chem. 46:2778–2784.

Lyman DJ, Benck R, Dell S, Merle S, Murray-Wijelath J. 2003. FTIR-ATR analysis of brewed coffee: effect of roasting conditions. J. Agric. Food Chem. 51:3268–3272.

Malek K, Coppens M-O. 2003. Knudsen self- and Fickian diffusion in rough nanoporous media. J. Chem. Phys. 119:2801–2811.

Marabi A, Livings S, Jacobson M, Saguy IS. 2003. Normalized Weibull distribution for modeling rehydration of food particulates. Eur. Food Res. Technol. 217:311–318.

Marabi A, Saguy IS. 2004. Effect of porosity on rehydration of dry food particulates. J. Sci. Food Agric. 84:1105–1110.

Marcone MF. 2004. Composition and properties of Indonesian palm civet coffee (Kopi Luwak) and Ethiopian civet coffee. Food Res. Int. 37:901–912.

De Maria CAB, Trugo LC, Moreira RFA, Werneck CC. 1994. Composition of green coffee fractions and their contribution to the volatile profile formed during roasting. Food Chem. 50:141–145.

De Maria CAB, Trugo LC, Neto FRA, Moreira RFA, Alviano CS. 1996. Composition of green coffee water-soluble fractions and identification of volatiles formed during roasting. Food Chem. 55:203–207.

Martins SIFS, Jongen WMF, Boekel MAJS Van. 2001. A review of Maillard reaction in food and implications to kinetic modelling. Trends Food Sci. Technol. 11:364–373.

Maskan M. 2001. Kinetics of colour change of kiwifruits during hot air and microwave drying. J. Food Eng. 48:169–175.

Mayer F, Czerny M, Grosch W. 1999. Influence of provenance and roast degree on the composition of potent odorants in Arabica coffees. Eur. Food Res. Technol. 209:242–250.

Mayer F, Czerny M, Grosch W. 2000. Sensory study of the character impact aroma compounds of a coffee beverage. Eur. Food Res. Technol. 211:272–276.

Mazzafera P, Silvarolla MB. 2010. Caffeine content variation in single green Arabica coffee seeds. Seed Sci. Res. 20:163–167.

Medved I, Cerny R. 2011. Surface diffusion in porous media: A critical review. Microporous Mesoporous Mater. 142:405–422.

Meisami-sal E, Rafiee S, Keyhani A, Tabatabaeefar A. 2010. Determination of suitable thin layer drying curve model for apple slices (variety-Golab). Plant Omi. J. 3:103–108.

Menges HO, Ertekin C. 2006. Mathematical modeling of thin layer drying of Golden apples. J. Food Eng. 77:119–125.

Merwe V Der, Carbo- NALAC, Bradbury AGW, Halliday DJ. 1990. Chemical Structures of Green Coffee Bean Polysaccharides. J. Agric. Food Chem. 38:389–392.

Mondello L, Casilli A, Tranchida PQ, Dugo P, Costa R, Festa S, Dugo G. 2004. Comprehensive multidimensional GC for the characterization of roasted coffee beans. J. Sep. Sci. 27:442–450.

Montavon P, Mauron A-F, Duruz E. 2003. Changes in green coffee protein profiles during roasting. J. Agric. Food Chem. 51:2335–2343.

Moon J-K, Shibamoto T. 2009. Role of roasting conditions in the profile of volatile flavor chemicals formed from coffee beans. J. Agric. Food Chem. 57:5823–5831.

Moon J-K, Shibamoto T. 2010. Formation of volatile chemicals from thermal degradation of less volatile coffee components: quinic acid, caffeic acid, and chlorogenic acid. J. Agric. Food Chem. 58:5465–5470.

Muller C, Hofmann T. 2005. Screening of raw coffee for thiol binding site precursors using "in bean" model roasting experiments. J. Agric. Food Chem. 53:2623–2629.

Munro LJ, Curioni A, Andreoni W, Yeretzian C, Watzke H. 2003. The elusiveness of coffee aroma: new insights from a non-empirical approach. J. Agric. Food Chem. 51:3092–3096.

Mwithiga G, Jindal VK. 2003. Physical changes during coffee roasting in rotary conduction-type heating units. J. Food Process Eng. 26:543–558.

Nalawade SP, Picchioni F, Marsman JH, Janssen LPBM. 2006. The FT-IR studies of the interactions of CO2 and polymers having different chain groups. J. Supercrit. Fluids 36:236–244.

Nehring UP, Maier HG. 1992. Indirect determination of the degree of roast in coffee. Eur. Food Res. Technol. 195:39–42.

Nunes FM, Coimbra MA. 2002. Chemical characterization of galactomannans and arabinogalactans from two Arabica coffee infusions as affected by the degaree of roast. J. Agric. Food Chem. 50:1429–1434.

Nunes FM, Domingues MR, Coimbra MA. 2005. Arabinosyl and glucosyl residues as structural features of acetylated galactomannans from green and roasted coffee infusions. Carbohydr. Res. 340:1689–1698.

Oosterveld A, Coenen GJ, Vermeulen NCB, Voragen AGJ, Schols HA. 2004. Structural features of acetylated galactomannans from green Coffea arabica beans. Carbohydr. Polym. 58:427–434.

Ortola MD, Londono L, Gutierrez CL, Chiralt A. 1998. Influence of roasting temperature on physicochemical properties of different coffees. Food Sci. Technol. Int. 4:59–66.

Özdemir M. 2000. Kinetics of color changes of hazelnuts during roasting. J. Food Eng. 44:31–38.

Perko T, Marko E. 2011. Solubility and diffusivity of CO2 in natural methyl cellulose and sodium carboxymethyl cellulose. J. Chem. Eng. Data 56:4040–4044.

Perrone D, Farah A, Donangelo CM, de Paulis T, Martin PR. 2008. Comprehensive analysis of major and minor chlorogenic acids and lactones in economically relevant Brazilian coffee cultivars. Food Chem. 106:859–867.

Perrone D, Farah A, Donangelo CM. 2012. Influence of coffee roasting on the incorporation of phenolic compounds into melanoidins and their relationship with antioxidant activity of the brew. J. Agric. Food Chem. 60:4265–4275.

Pittia P, Nicoli MC, Sacchetti G. 2007. Effect of moisture and water activity on textural properties of raw and roasted coffee beans. J. Texture Stud. 38:116–134.

Poisson L, Schmalzried F, Davidek T, Blank I, Kerler J. 2009. Study on the role of precursors in coffee flavor formation using in-bean experiments. J. Agric. Food Chem.:9923–9931.

Redgwell R, Fischer M. 2006. Coffee carbohydrates. Brazilian J. Plant Physiol. 18:165–174.

Redgwell RJ, Trovato V, Curti D, Fischer M. 2002. Effect of roasting on degradation and structural features of polysaccharides in Arabica coffee beans. Carbohydr. Res. 337:421–431.

Reh CT, Gerber A, Prodolliet J, Vuataz G. 2006. Water content determination in green coffee – Method comparison to study specificity and accuracy. Food Chem. 96:423–430.

Ribeiro JS, Augusto F, Salva TJG, Thomaziello R a, Ferreira MMC. 2009. Prediction of sensory properties of Brazilian Arabica roasted coffees by headspace solid phase microextraction-gas chromatography and partial least squares. Anal. Chim. Actahimica acta 634:172–179.

Rizzi GP, Boekley LJ. 1993. Flavor chemistry based on the thermally-induced decarboxylation of p-hydroxylcinnamic acids. In: Food Flavors, Ingredients and Composition. Amsterdam, Netherlands: Elsevier Science Publishers. p. 663–670.

Rocculi P, Sacchetti G, Venturi L, Cremonini M, Dalla Rosa M, Pittia P. 2011. Role of water state and mobility on the antiplasticization of green and roasted coffee beans. J. Agric. Food Chem. 59:8265–8271.

Rouquerol J, Avnir D, Fairbridge CW, Everett DH, Haynes JH, Pernicone N, Ramsay JDF, Sing KSW, Unger K k. 1994. Recommendation for the characterization of porous solids. 66:1739–1758.

Sacchetti G, Dimattia C, Pittia P, Mastrocola D. 2009. Effect of roasting degree, equivalent thermal effect and coffee type on the radical scavenging activity of coffee brews and their phenolic fraction. J. Food Eng. 90:74–80.

Saguy IS, Marabi A, Wallach R. 2005. New approach to model rehydration of dry food particulates utilizing principles of liquid transport in porous media. Trends Food Sci. Technol. 16:495–506.

Sahoo KP, Kasera PK, Mohammed S. 2012. Secondary metabolites produced during different seasons in some arid medicinal plants. J. plant Sci. Res. 2:650–652.

Saleeb FZ. 1975. Adsorption of carbon dioxide on roast and ground coffees. In: Proceedings of the 7th ASIC colloquium. Paris, France: ASIC. p. 335–339.

Samaniego-Esguerra CM, Boag IF, Robertson GL. 1991. Comparison of regression methods for fitting the GAB model to the moisture isotherms of some dried fruit and vegetables. J. Food Eng. 13:115–133.

Schenker S, Handschin S, Frey B, Perren R, Escher F. 2000. Pore structure of coffee beans affected by roasting conditions. Food Eng. Phys. Prop. 65:452–457.

Schenker S, Heinemann C, Huber R, Pompizzi R, Perren R, Escher F. 2002. Impact of roasting conditions on the formation of aroma compounds in coffee beans. Food Eng. Phys. Prop. 67:60–66.

Schenker S. 2000. Investigation of the Hot Air Roasting of Coffee Beans. Swiss Federal Institute of Technology.

Schmidt K. 2006. The art and science of roasting. Present. NCA Fall Educ. Conf.

Semmelroch P, Grosch W. 1995. Analysis of roasted coffee powders and brews by gas chromatography-olfactometry of headspace samples. LWT - Food Sci. Technol. 28:310–313.

Semmelroch P, Grosch W. 1996. Studies on character impact odorants of coffee brews. J. Agric. Food Chem. 44:537–543.

Semmelroch P, Laskawy G, Blank I, Grosch W. 1995. Determination of potent odourants in roasted coffee by stable isotope dilution assays. Flavour Fragr. J. 10:1–7.

Sharma RK, Fisher TS, Hajaligol MR. 2002. Effect of reaction conditions on pyrolysis of chlorogenic acid. J. Anal. Appl. Pyrolysis 62:281–296.

Sharma RK, Hajaligol MR, Smith PAM, Wooten JB, Baliga V. 2000. Characterization of char from pyrolysis of chlorogenic acid. Energy and Fuels 14:1083–1093.

Shimoni E, Labuza TP. 2000. Degassing kinetics and sorption equilibrium of carbon dioxide in fresh roasted and ground coffee. J. Food Process Eng. 23:419–436.

Sikorski ZE, Pokorny J, Damodaran S. 2008. Chaper 14: Physical and chemical interactions of components in food systems. In: Damodaran S, Parkin KL, Fennema OR, editors. Food Chemistry. Fourth. Boca Raton: CRC Press. p. 866.

Small LE, Horrel RS. 1993. High yield coffee technology. In: Proceedings of the 15th ASIC Colloquium. Montpellier: ASIC, Paris, France. p. 719–726.

Speer K, Kölling-Speer I. 2006. The lipid fraction of the coffee bean. Brazilian J. Plant Physiol. 18:201–216.

Stadtman FH, Chichester CO, Mackinney G. 1952. Carbon dioxide production in the browning reaction. J. Am. Chem. Soc. 74:1951–1953.

Stennert A, Maier HG. 1996. Trigonelline in coffee. Eur. Food Res. Technol. 202:45–47.

Summa CA, de la Calle B, Brohee M, Stadler RH, Anklam E. 2007. Impact of the roasting degree of coffee on the in vitro radical scavenging capacity and content of acrylamide. LWT - Food Sci. Technol. 40:1849–1854.

Thom E. 2007. The Effect of chlorogenic acid enriched coffee on glucose absorption in healthy volunteers and its effect on body mass when used long-term in overweight and obese people. J. Int. Med. Res. 35:900–908.

Timmermann EO. 2003. Multilayer sorption parameters: BET or GAB values? Colloids Surfaces A Physicochem. Eng. Asp. 220:235–260.

Trugo LC, Macrae R. 1984. A study of the effect of roasting on the chlorogenic acid composition of coffee using HPLC. Food Chem. 15:219–227.

Tsami E, Katsioti M. 2000. Drying kinetics for some fruits: predicting of porosity and color during dehydration. Dry. Technol. 18:1559–1581.

Vignoli JA, Bassoli DG, Benassi MT. 2011. Antioxidant activity, polyphenols, caffeine and melanoidins in soluble coffee: The influence of processing conditions and raw material. Food Chem. 124:863–868.

Wang J, Jun S, Bittenbender HC, Gautz L, Li QX. 2009. Fourier transform infrared spectroscopy for Kona coffee authentication. J. Food Sci. 74:385–391.

Wang N, Fu Y, Lim L-T. 2011. Feasibility study on chemometric discrimination of roasted Arabica coffees by solvent extraction and Fourier transform infrared spectroscopy. J. Agric. Food Chem. 59:3220–3226.

Wang N, Lim L-T. 2012. Fourier transform infrared and physicochemical analyses of roasted coffee. J. Agric. Food Chem. 60:5446–5453.

Wang X, Lim L-T. 2014. A kinetics and modeling study of coffee roasting under isothermal conditions. Food Bioprocess Technol. 7:621–632.

Wang Y. 2000. Effects of naturally occurring phenolic compounds on the formation of Maillard Aroma. Rutgers State University.

Webb SW. 2006. Gas transport mecahnisms. In: Ho CK, Webb SW, editors. Gas Transport in Porous Media. Dordrecht, Netherlands: Springer. p. 5–27.

Welty JR., Wicks CE., Wilson RE., Rorrer GL. 2008. Fundamental of momentus, heat and mass transfer. 5th ed. Hoboken: John Wiley and Sons.

Wiiken C, Baltes W. 1990. Model reaction on roast aroma formation: Formation of pyrrole-2, 5-diones by roasting of aspartic acid and asparagine. Z. Leb. Unters. Forsch. 191:116–118.

Wintgens JN. 2004a. Data on Coffee. In: Wintgens JN, editor. Coffee: Growing, Processing, Sustainable Production. Wintgens: Wiley-VCH. p. 1–976.

Wintgens JN. 2004b. The coffee plant. In: Wintgens JN, editor. Coffee: Growing, Processing, Sustainable Production. Weinheim: Wiley-VCH. p. 1–976.

Yeretzian C, Jordan A, Badoud R, Lindinger W. 2002. From the green bean to the cup of coffee: investigating coffee roasting by on-line monitoring of volatiles. Eur. Food Res. Technol. 214:92–104.

CHAPTER 9 : APPENDIX

220 °C

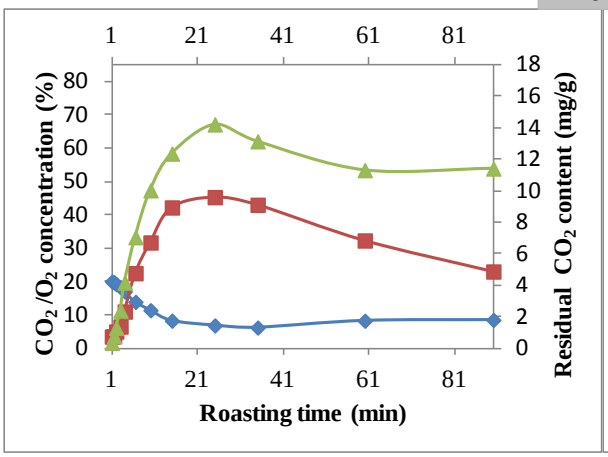

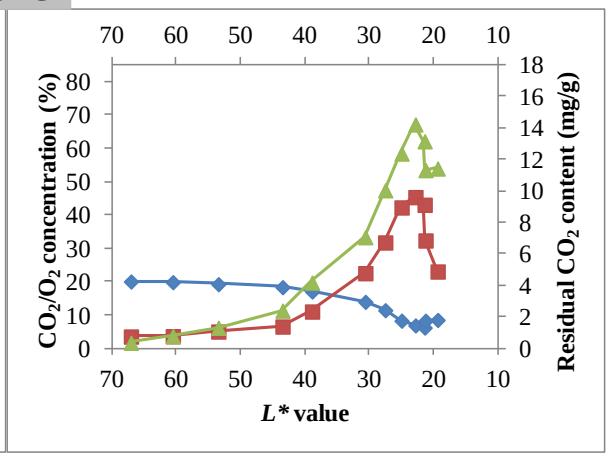

230 °C

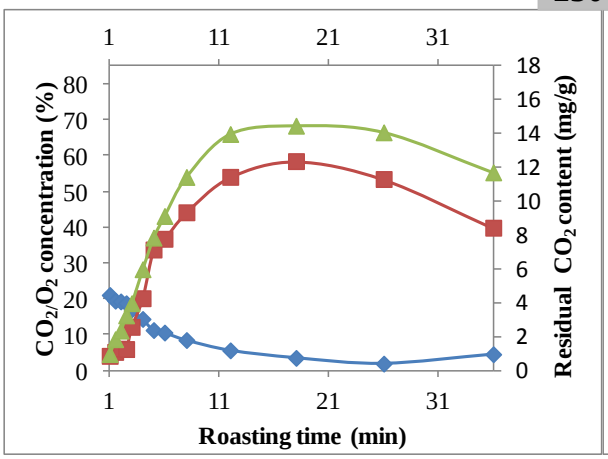

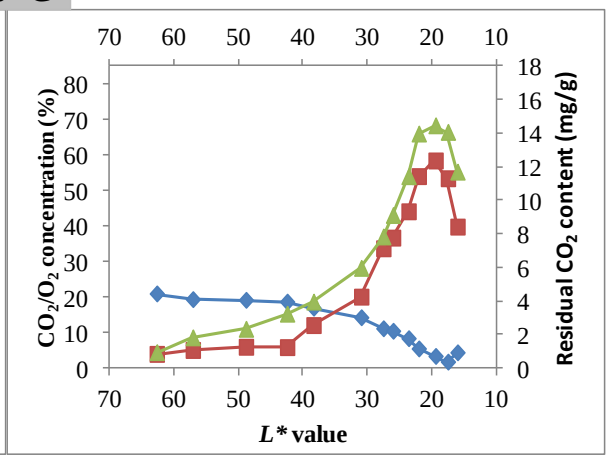

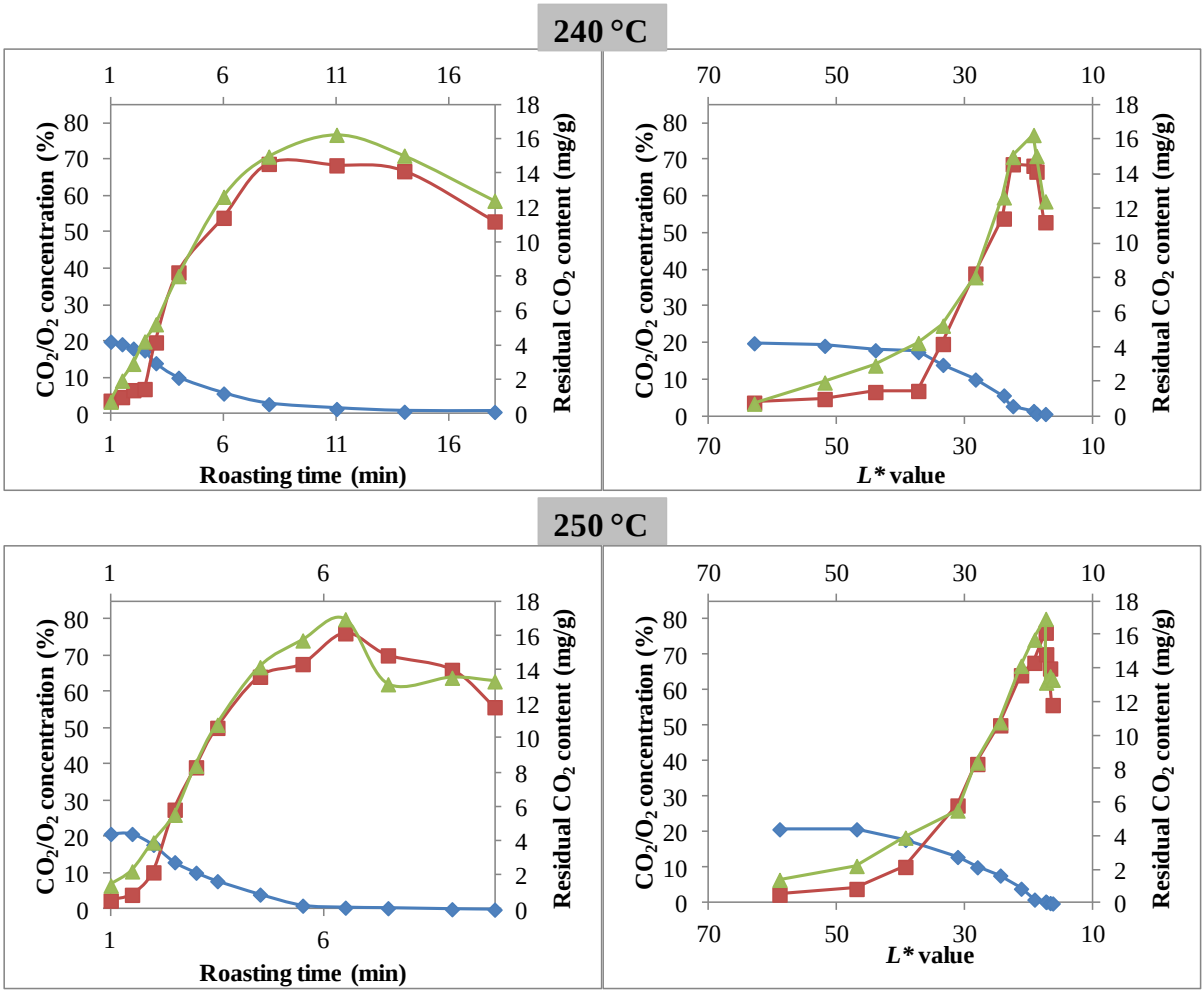

Figure 9.1- The residual CO_2 content in roasted coffee beans from various roasting temperature-time combinations and their headspace CO_2 and O_2 concentration after packaging. The packing condition is 5 grams of roasted coffee beans was packaged in 12 ml glass amber vial with septum containing lid. The headspace CO_2 and O_2 concentration was determined by a headspace gas analyzer (Gaspace Advance Micro, Illinois Instruments, IL USA) after one week storage. The residual CO_2 content and headspace O_2 and CO_2 consternation was plotted with both roasting time and *L** value of the tested coffee beans. The green, red and blue lines represents the residual CO_2 content, headspace CO_2 concentration and headspace O_2 concentration, respectively.

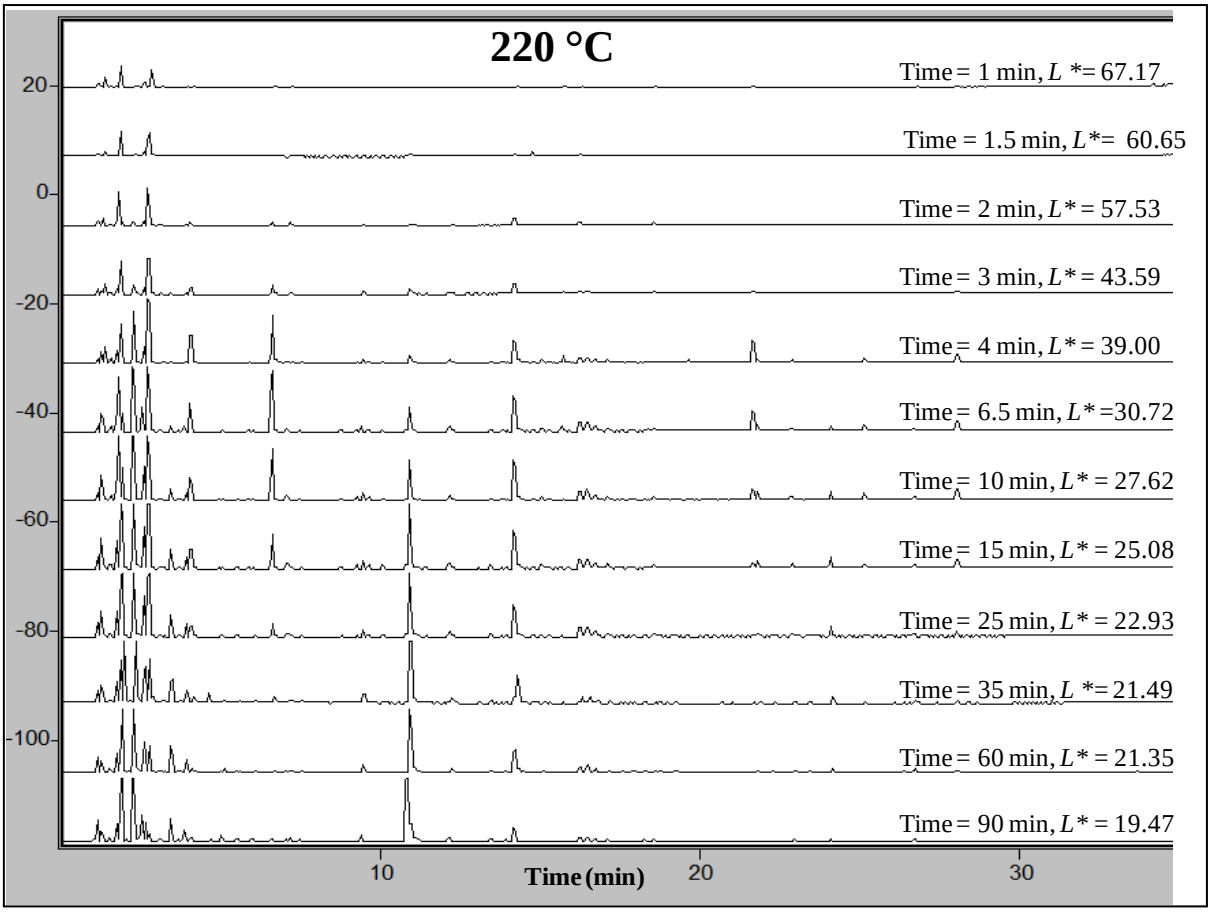
220 °C
Time = 1 min, L *= 67.17
Time = 1.5 min, L*= 60.65
Time = 2 min, L* = 57.53
Time = 3 min, L* = 43.59
Time = 4 min, L* = 39.00
Time = 6.5 min, L* =30.72
Time = 10 min, L* = 27.62
Time = 15 min, L* = 25.08
Time = 25 min, L* = 22.93
Time = 35 min, L *= 21.49
Time = 60 min, L* = 21.35
Time = 90 min, L* = 19.47
20
0
-20
-40
-60
-80
-100
10
20
30
Time (min)

(Continued)

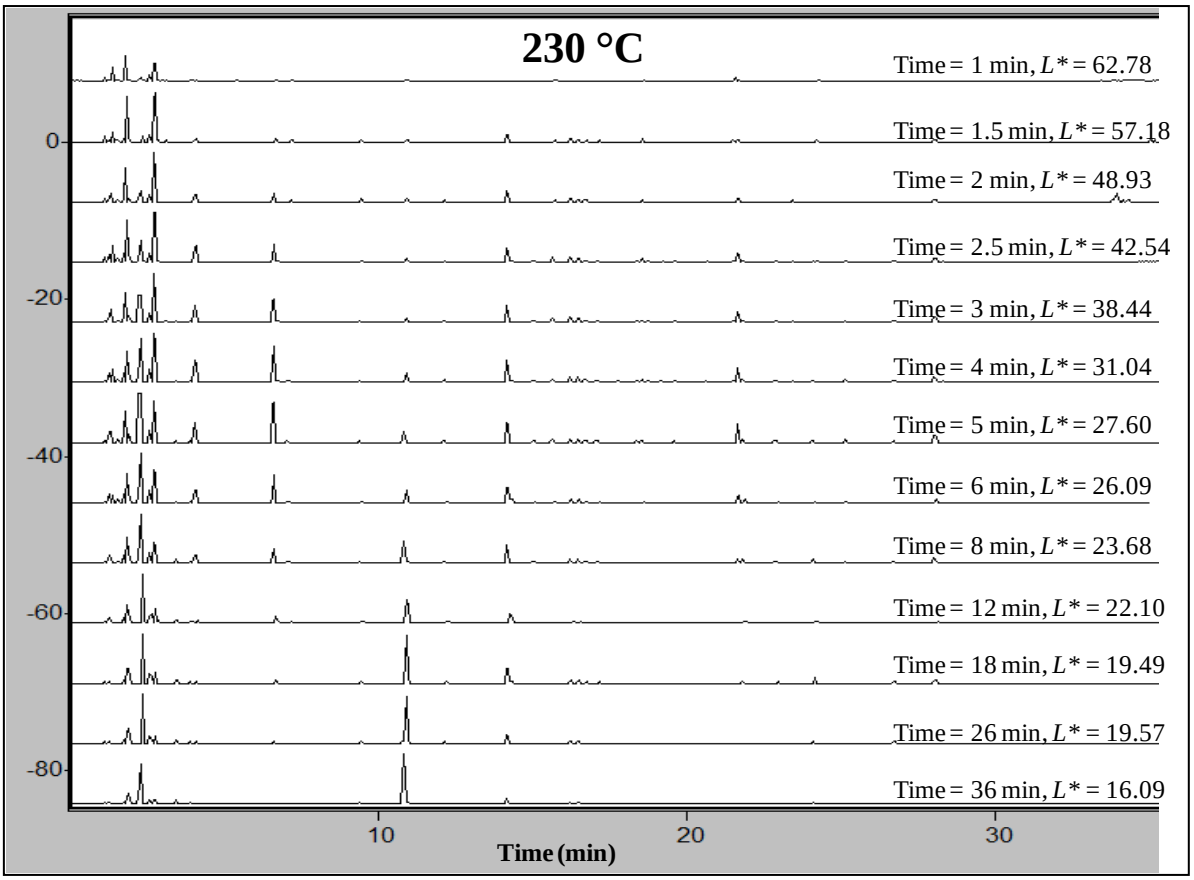
230 °C
Time = 1 min, L* = 62.78
Time = 1.5 min, L* = 57.18
Time = 2 min, L* = 48.93
Time = 2.5 min, L* = 42.54
Time = 3 min, L* = 38.44
Time = 4 min, L* = 31.04
Time = 5 min, L* = 27.60
Time = 6 min, L* = 26.09
Time = 8 min, L* = 23.68
Time = 12 min, L* = 22.10
Time = 18 min, L* = 19.49
Time = 26 min, L* = 19.57
Time = 36 min, L* = 16.09
0
-20
-40
-60
-80
10
20
30
Time (min)

(Continued)

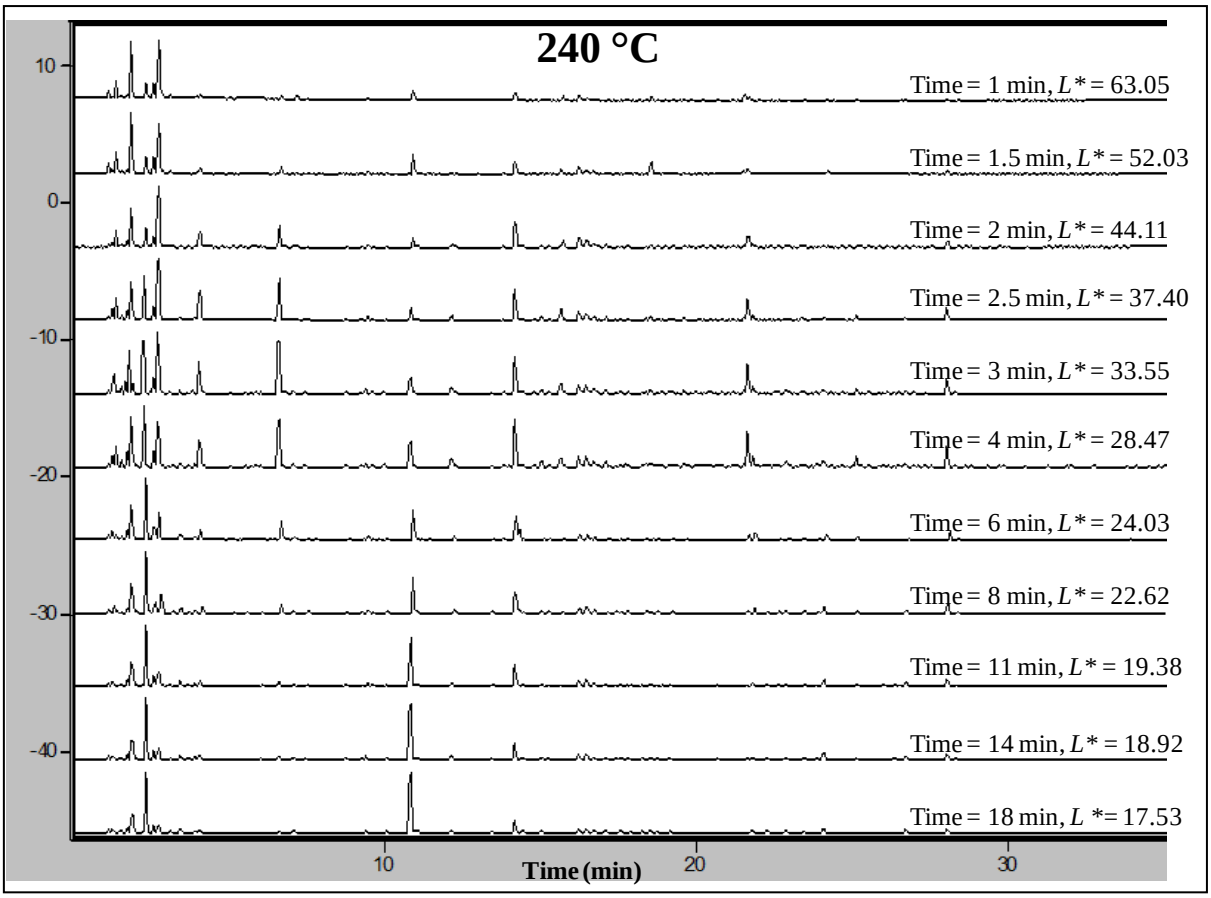
240 °C
Time = 1 min, L* = 63.05
Time = 1.5 min, L* = 52.03
Time = 2 min, L* = 44.11
Time = 2.5 min, L* = 37.40
Time = 3 min, L* = 33.55
Time = 4 min, L* = 28.47
Time = 6 min, L* = 24.03
Time = 8 min, L* = 22.62
Time = 11 min, L* = 19.38
Time = 14 min, L* = 18.92
Time = 18 min, L *= 17.53
10
0
-10
-20
-30
-40
10
20
30
Time (min)

(Continued)

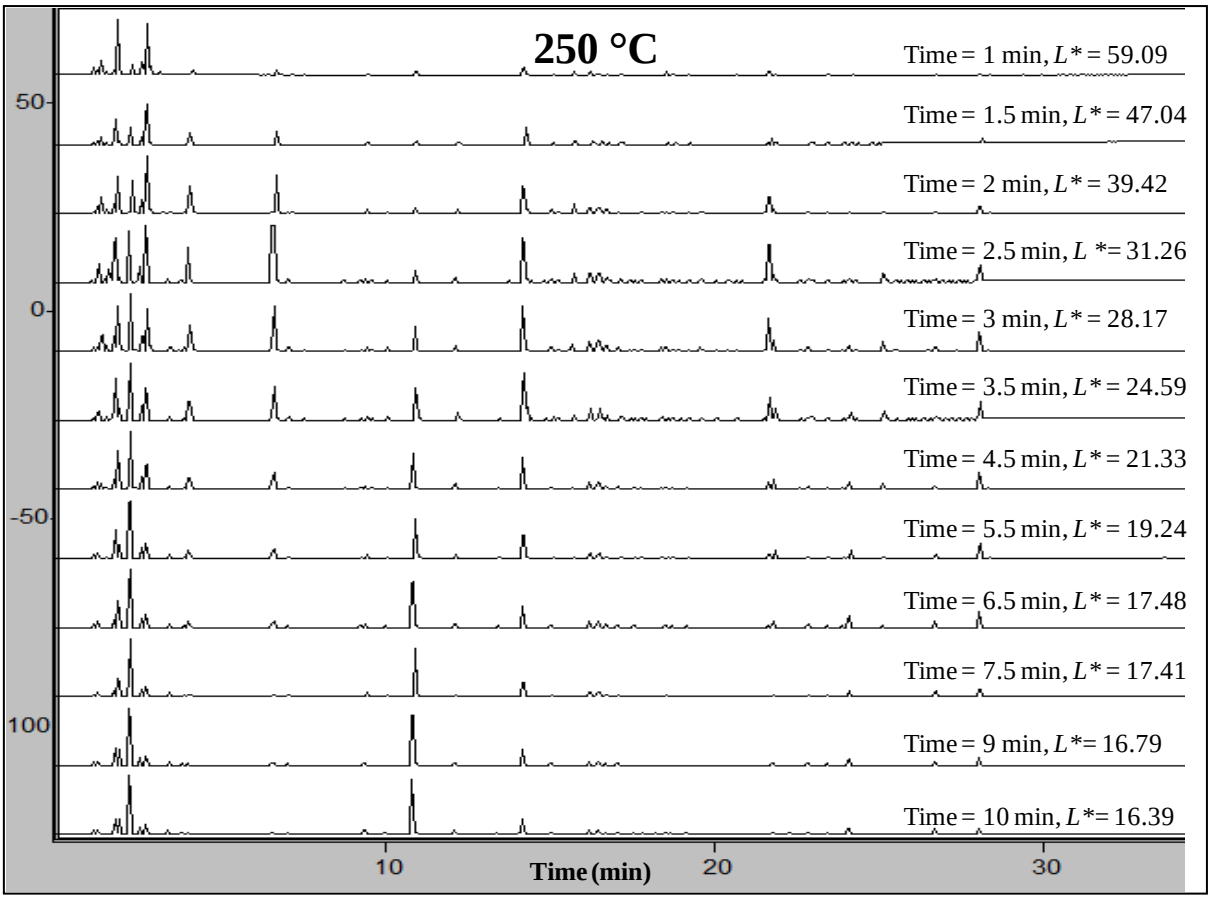

Figure 9.2- Changes of volatile chromatograms (in section 3.3.4) with roasting time at different roasting temperature of 220, 230, 240 and 250 °C, showing the formation of volatiles is superimposed by an accelerated decay of some aroma compounds during the final roasting stage.

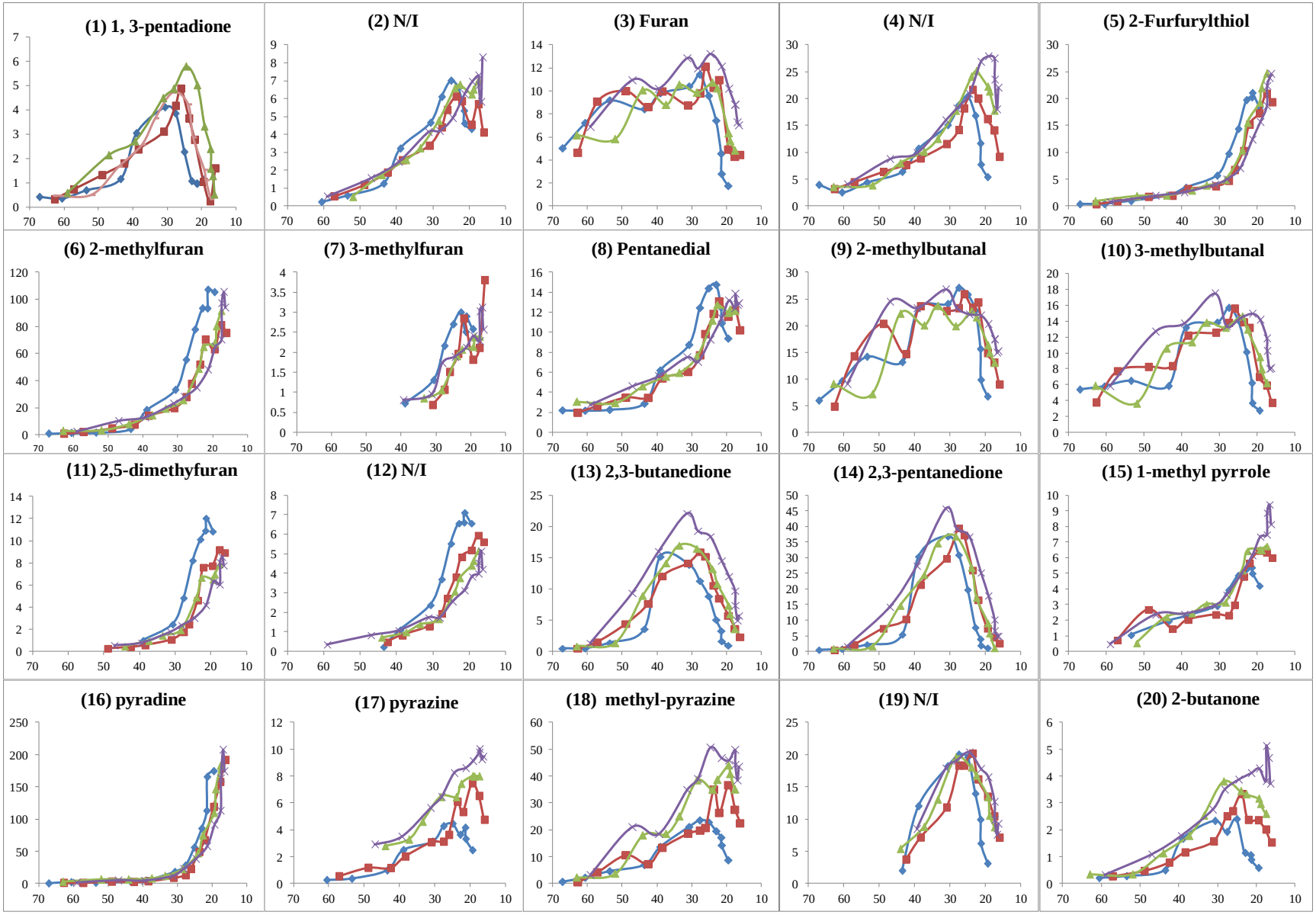
(1) 1, 3-pentadione
(2) N/I
(3) Furan
(4) N/I
(5) 2-Furfurylthiol
(6) 2-methylfuran
(7) 3-methylfuran
(8) Pentanedial
(9) 2-methylbutanal
(10) 3-methylbutanal
(11) 2,5-dimethyfuran
(12) N/I
(13) 2,3-butanedione
(14) 2,3-pentanedione
(15) 1-methyl pyrrole
(16) pyradine
(17) pyrazine
(18) methyl-pyrazine
(19) N/I
(20) 2-butanone

(Continued)

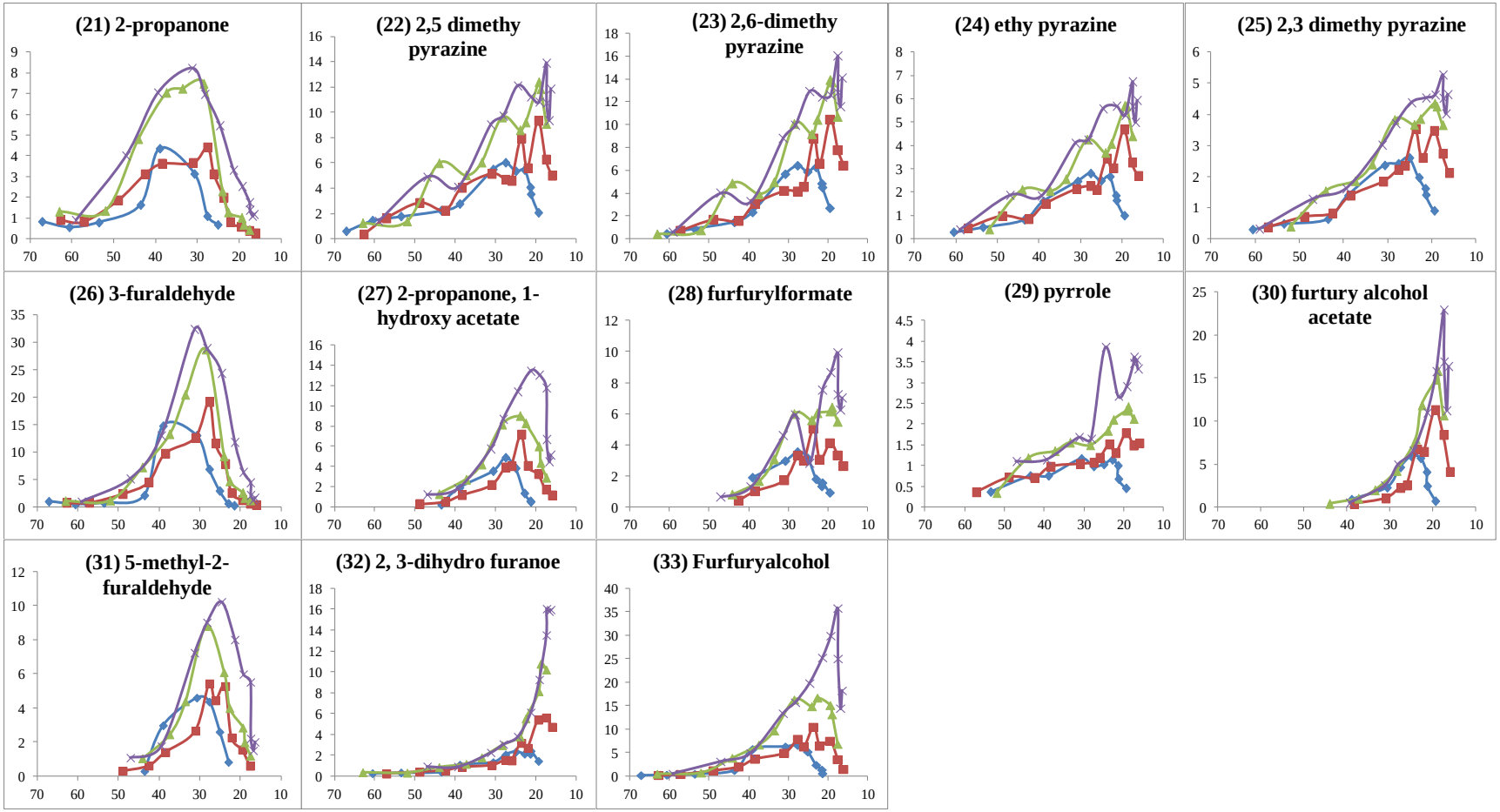

Figure 9.3- Changes of 33 volatile compounds in Table 3.3 during coffee roasting at roasting temperature of 220, 230, 240 and 250 °C. X-axis is the lightness value (*L**) and y-axis is the peak area. Blue, red, green and purple lines represent 220, 230, 240 and 250 °C roasting temperature, respectively.

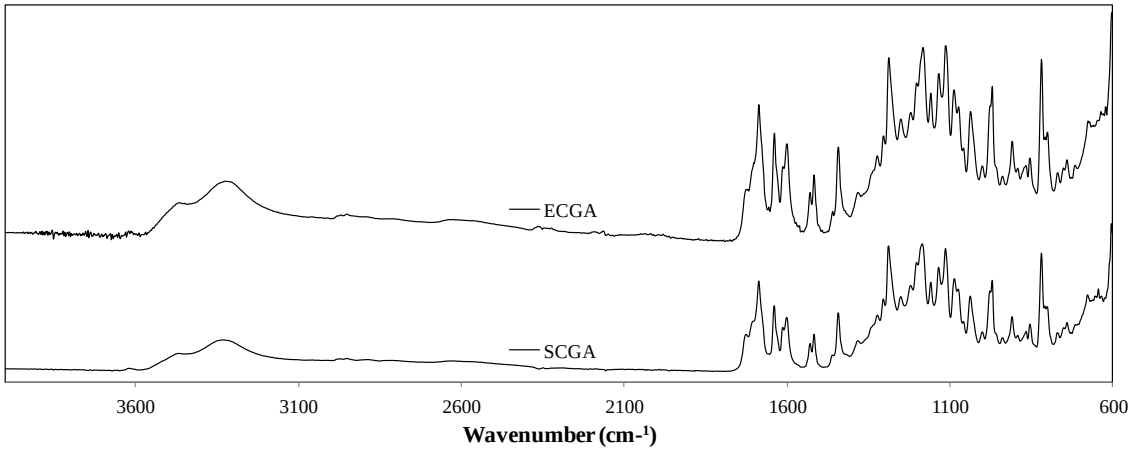

Figure 9.4- FTIR spectra of ECGA and CGA standard.

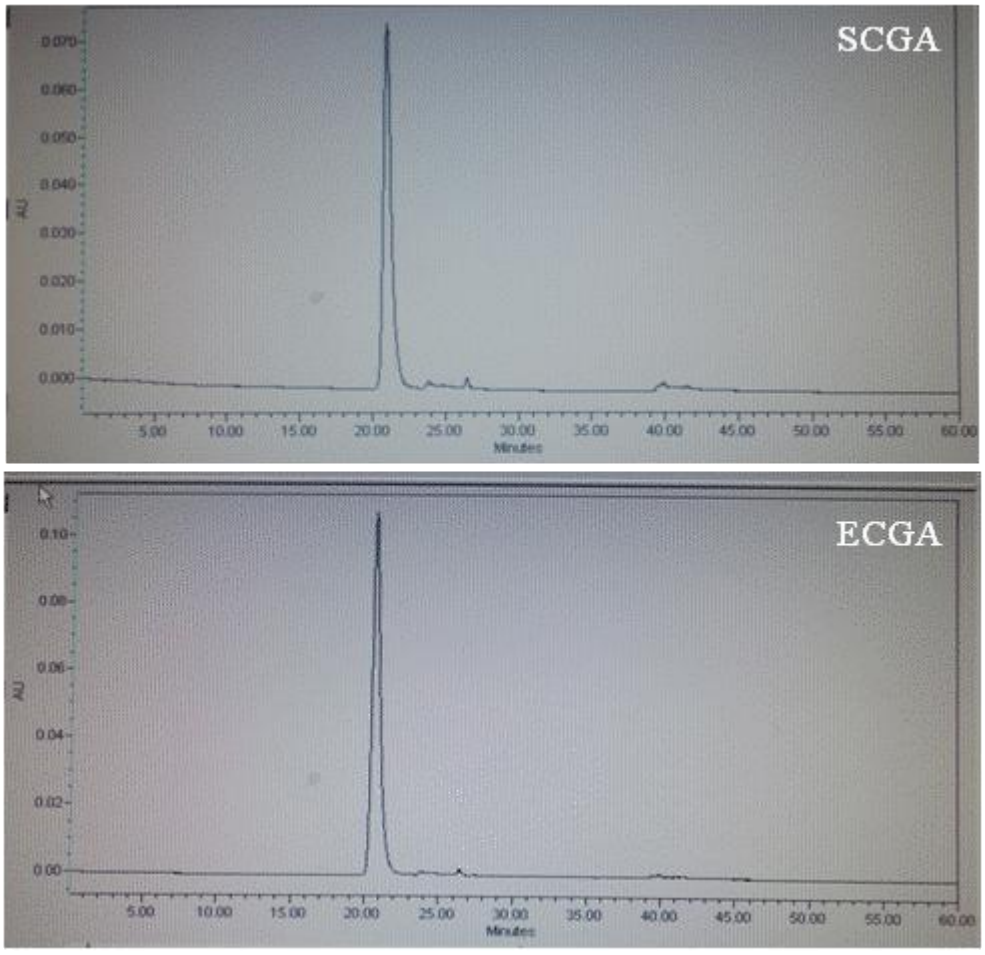

Figure 9.5- HPLC chromatograms of SCGA and ECGA.

Figure 9.6- Original, control and 6% CGA spiked green coffee beans in Chapter 5

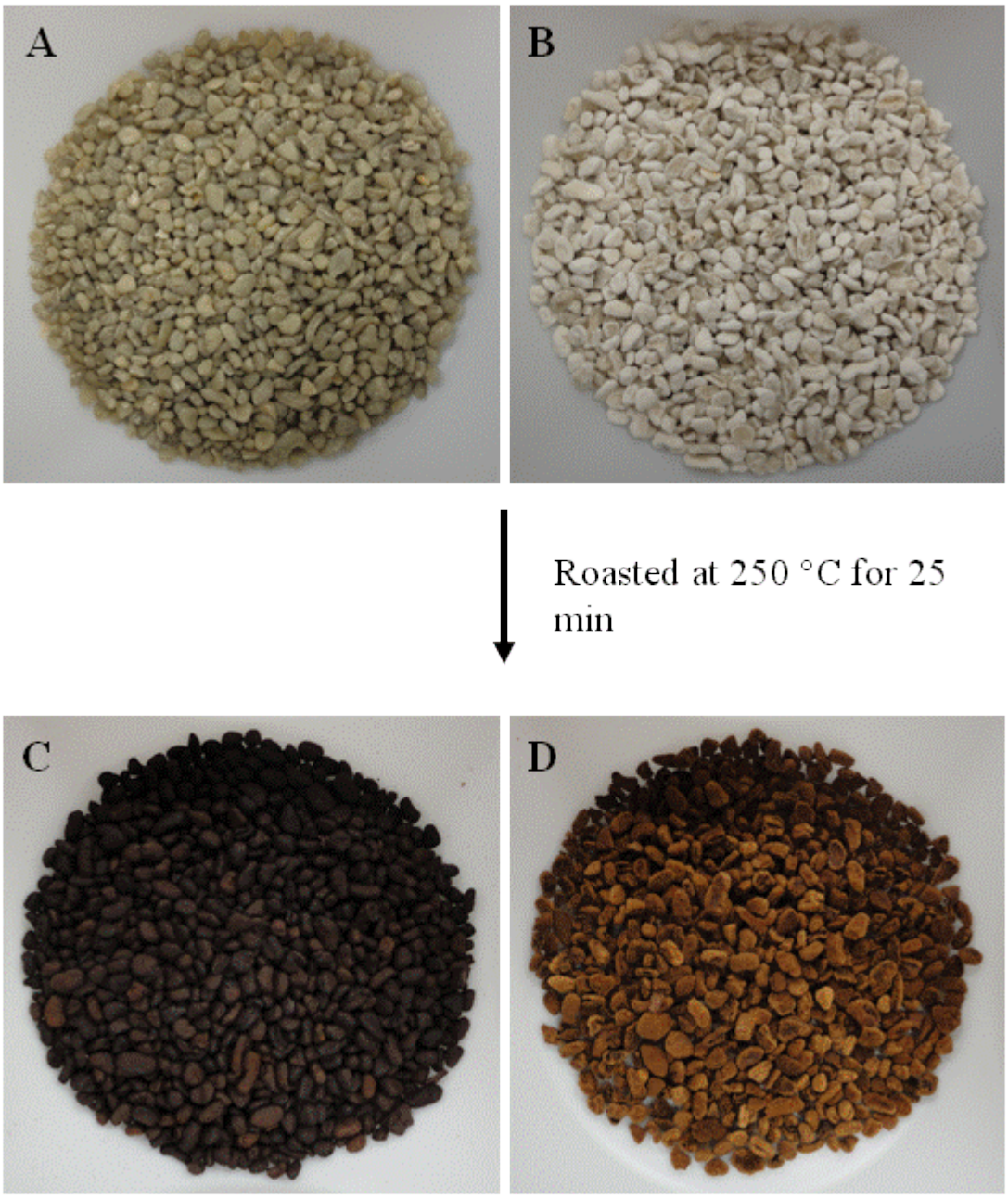

Figure 9.7- (A) Ground coffee for isolation; (B) exhausted ground coffee (Fraction D); (C) roasted coffee from A at 250 °C for 25 min; (D) roasted coffee from B at 250 °C for 25 min.

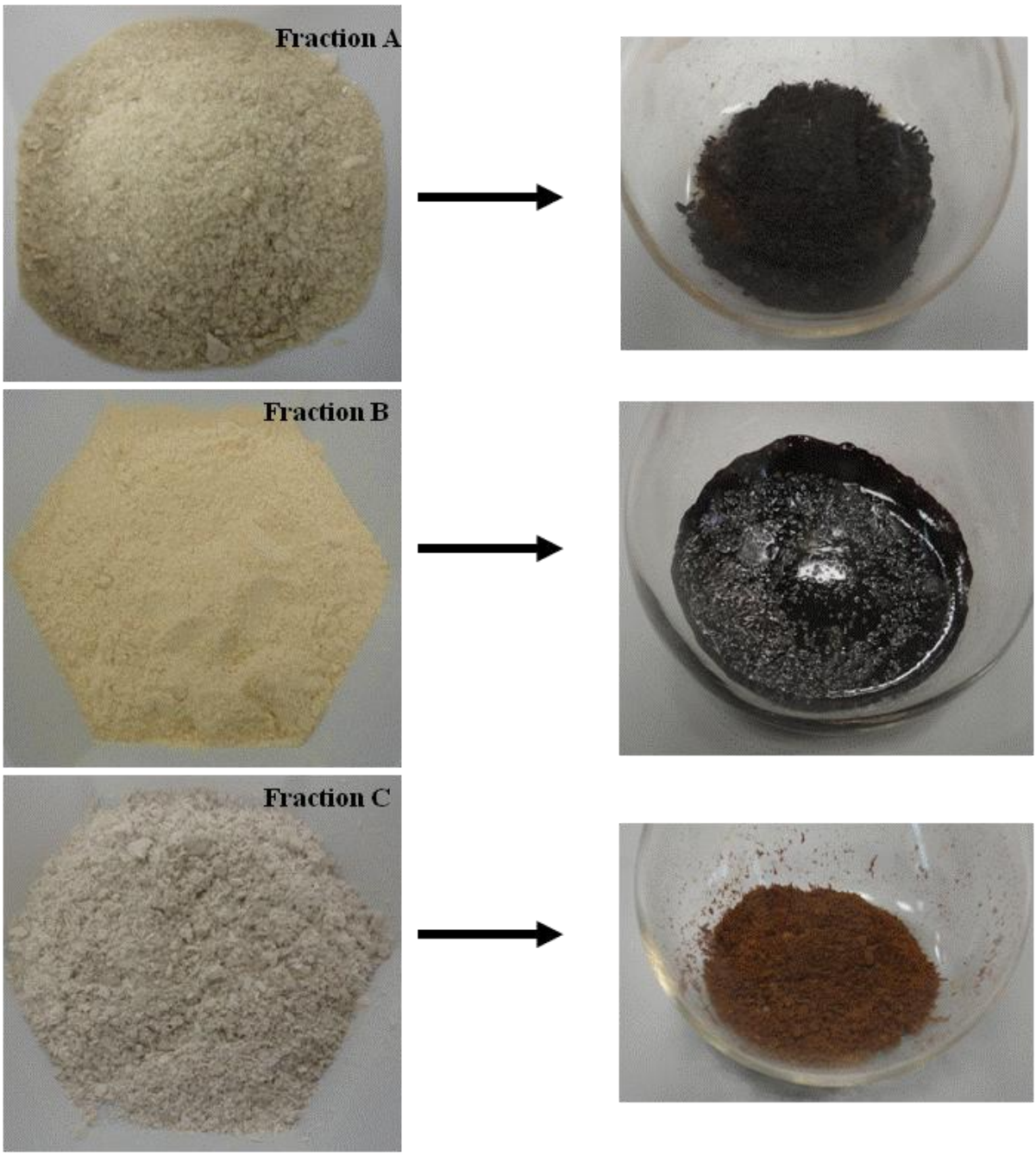

Figure 9.8- Photos of fraction A, B and C, and the corresponding residuals after roasted at 250 °C for 25 min.